Supporting Information

Structure-guided engineering of an aromatic dioxygenase from *Coniochaeta pulveracea* for improved catalysis of lignin-related aromatic olefins

Lei Yu[a,b†], Yunjian Ma[a,b†], Chenhao Feng[a], Frank Hollmann[c], Ren Wei[d], Fanghua Wang[a], Shengjie Guo[a], Bin Wu[a,e]*& Yonghua Wang[a,f]*

[a] School of Food Science and Engineering, South China University of Technology, Guangzhou 510640, China

[b] State Key Laboratory of Advanced Papermaking and Paper-based Materials, South China University of Technology, Guangzhou 510640, China

[c] Department of Biotechnology, Delft University of Technology, van der Maasweg 9, 2629HZ, Delft, The Netherlands

[d] Department of Biotechnology and Enzyme Catalysis, Institute of Biochemistry, University of Greifswald, D-17489 Greifswald, Germany

[e] College of Light Chemical Industry and Materials Engineering, Shunde Polytechnic University, Foshan, 528333, China.

[f] Southern Marine Science and Engineering Guangdong Laboratory (Guangzhou), Guangdong, 511458, China

†Contributed equally to this work

*Corresponding author (BinWu, email: BinWu9070@scut.edu.cn; Yonghua Wang, email: yonghw@scut.edu.cn)

CONTENTS

1. Supporting Figures:

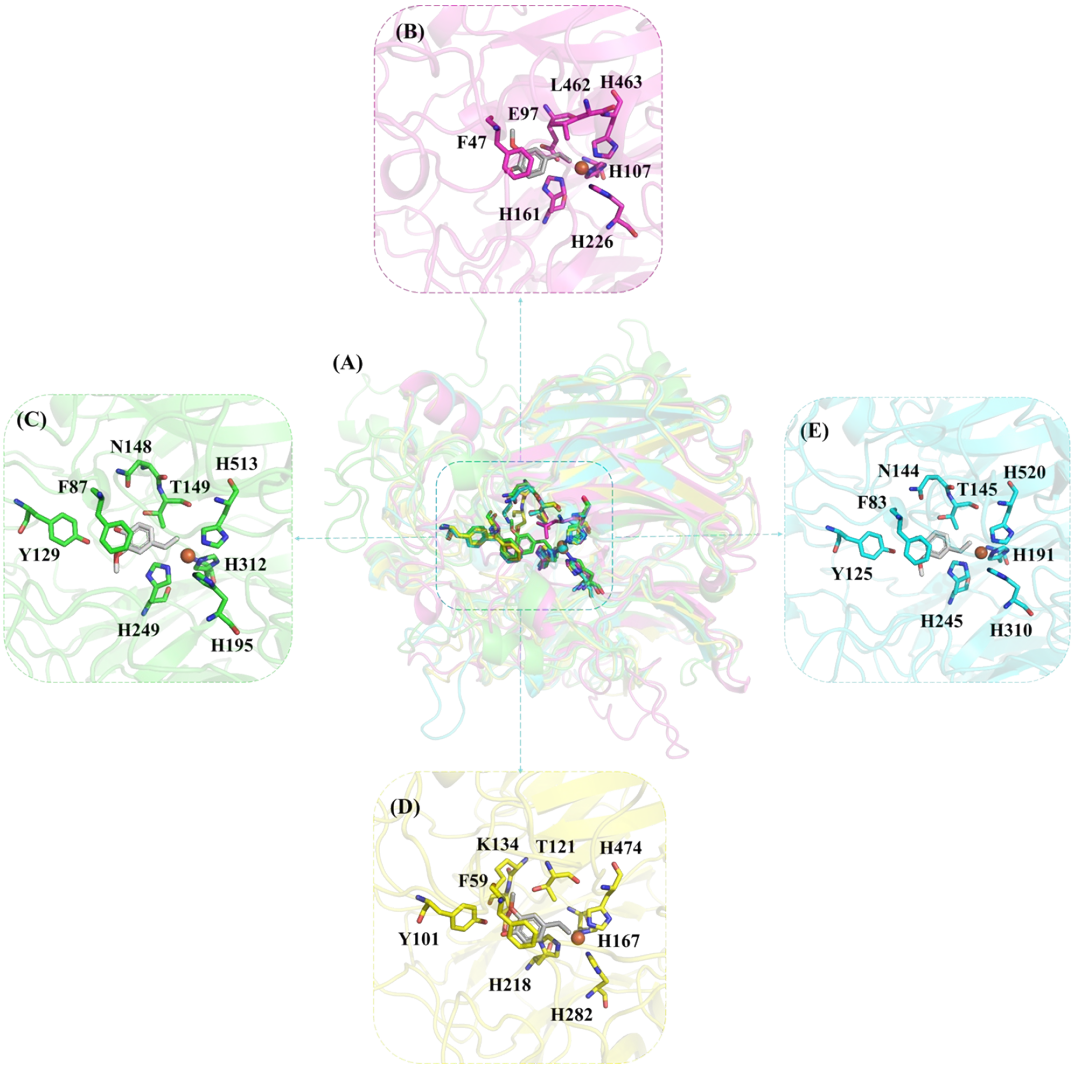

Figure S1. Molecular docking analysis of 4-vinylguaiacol with various ADO enzymes. (A) Structural superposition of the AlphaFold2 models of *Dsp*ADO (pink), *Cpu*ADO (green), *Lsp*ADO (yellow), and *Slo*ADO (cyan). (B-E) Active site pockets of these enzymes, respectively, with interacting residues highlighted as sticks.

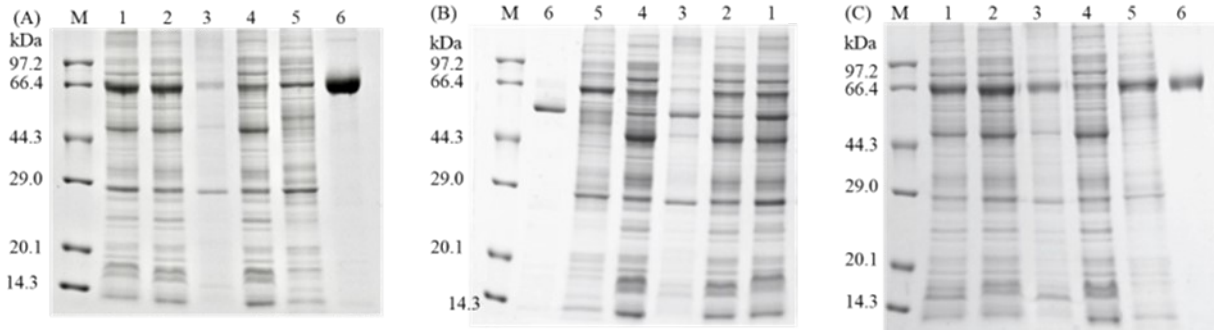

Figure S2. Purification of the recombinant ADOs. (A)-(C) represent the SDS-PAGE gel electrophoresis of the purified

*Tth*ADO, *Lsp*ADO and *Cpu*ADO, respectively. Lane M: protein marker, lane 1: cell extract of recombinant *E.coli* BL21 (DE3) strain, lane 2: supernatant of induced cell lysate, lane 3: induced cell debris, lane 4: Sample of the cell extract after passing through the nickel column; lane 5: Protein sample after impurity removal with 50 mM imidazole; lane 6: Purified ADOs after 200 mM imidazole elution.

(A)

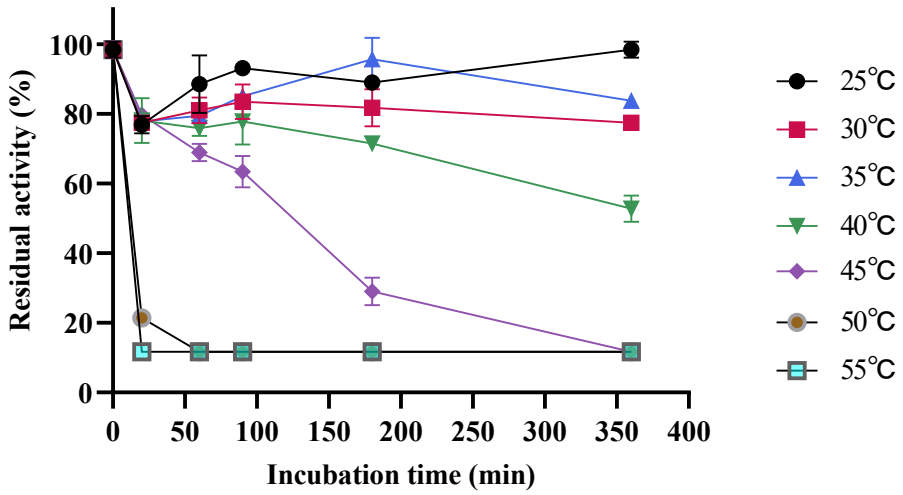

(B)

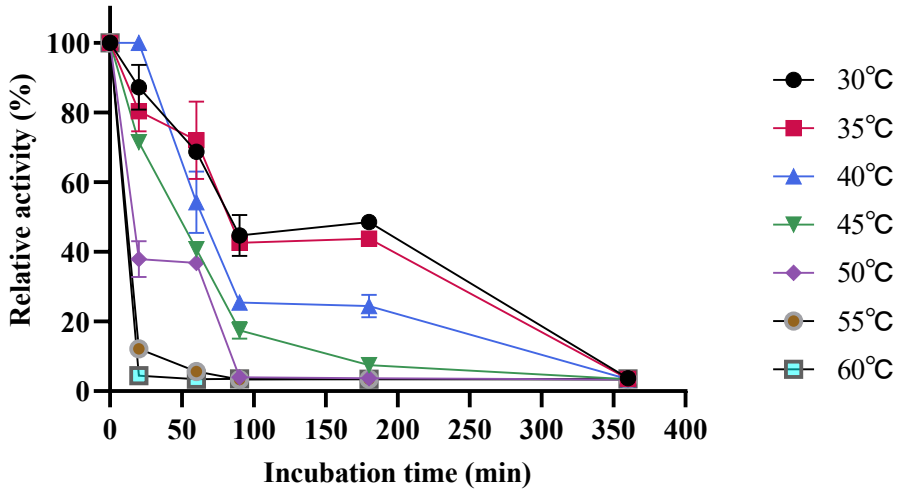

Figure S3. Temperature stability of different ADOs. (A) *Lsp*ADO , (B) *Cpu*ADO . Conditions: c(*Lsp*ADO) = 10 μM, c(*Cpu*ADO) = 2 μM, c(4-vinylguaiacol) = 10 mM (for *Lsp*ADO) and 5 mM (for *Cpu*ADO), t = 20 min (10 min for *Cpu*ADO). Error bars represent the standard deviation of three independent experiments.

(A)

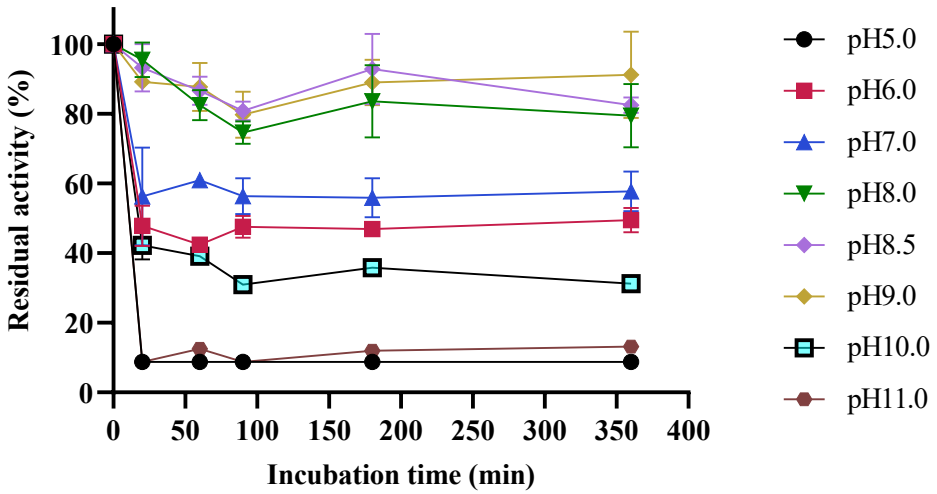

(B)

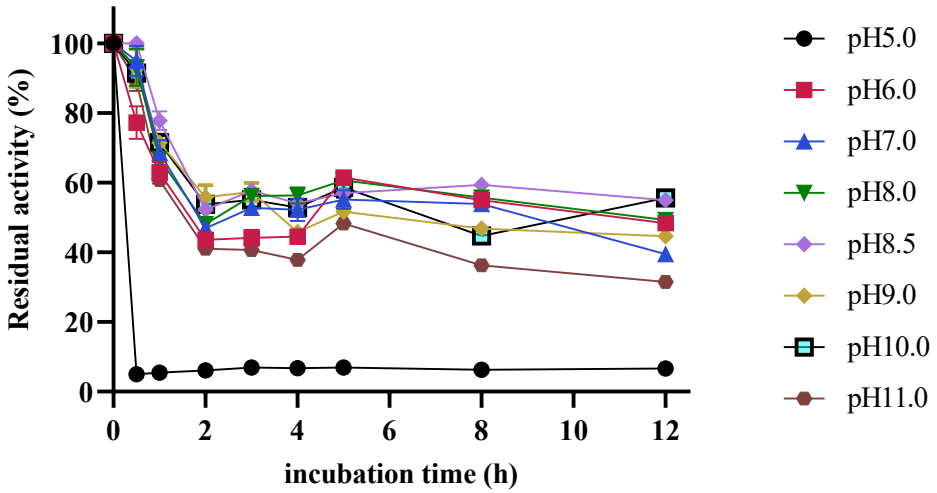

Figure S4. pH stability of different ADOs. (A) *Lsp*ADO, (B) *Cpu*ADO. Conditions: c(*Lsp*ADO) = 10 μM, c(*Cpu*ADO) = 2 μM, c(4-vinylguaiacol) = 10 mM (for *Lsp*ADO) and 5 mM (for *Cpu*ADO), t = 20 min (10 min for *Cpu*ADO). Error bars represent the standard deviation of three independent experiments.

(A)

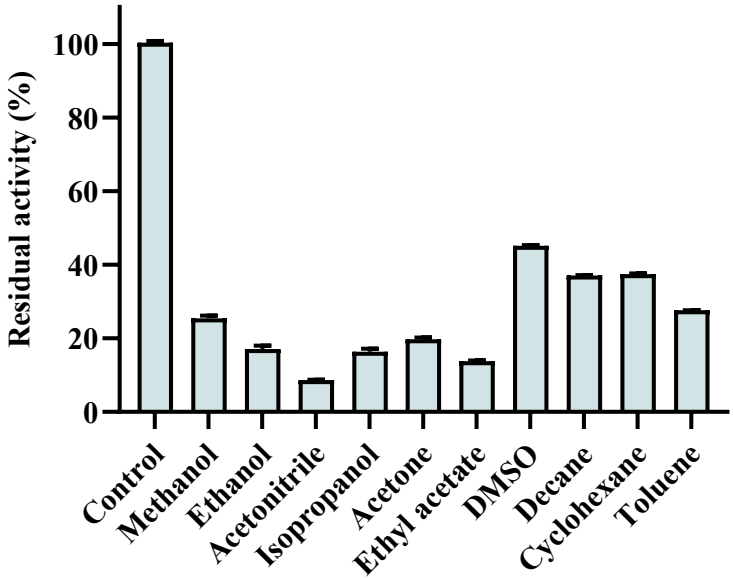

(B)

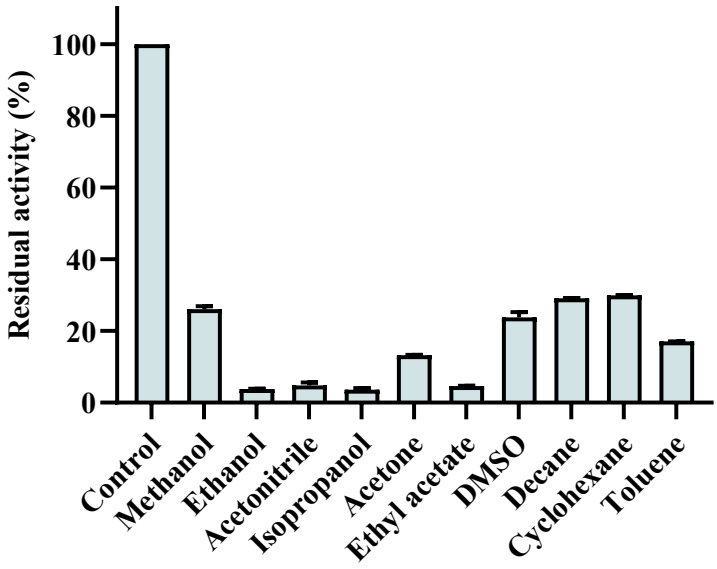

Figure S5. Influence of various hydrophilic and several hydrophobic solvents (30% v/v) on the activity of *Lsp*ADO (A) and *Cpu*ADO (B). Conditions: c(*Lsp*ADO) = 10 μM, c(*Cpu*ADO) = 2 μM, c(4-vinylguaiacol) = 10 mM (for *Lsp*ADO) and 5 mM (for *Cpu*ADO), t = 20 min (10 min for *Cpu*ADO). Error bars represent the standard deviation of three independent experiments.

(A)

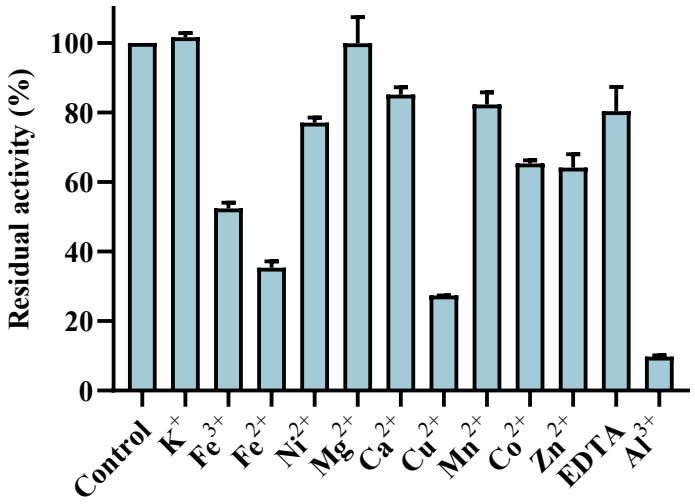

83
84

(B)

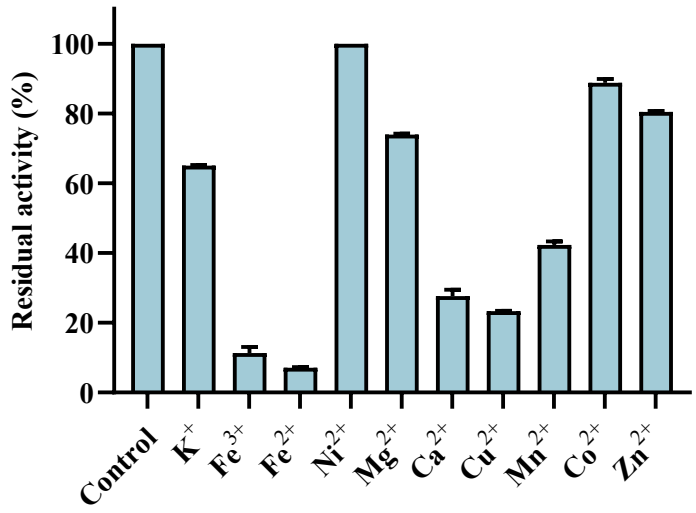

85

86 **Figure S6.** Effect of different metal ions (10 mM) on enzyme activity of *Lsp*ADO (A), *Cpu*ADO (B). Conditions:
87 c(*Lsp*ADO) = 10 μM, c(*Cpu*ADO) = 2 μM, c(4-vinylguaiacol) = 10 mM (for *Lsp*ADO) and 5 mM (for *Cpu*ADO), t
88 = 20 min (10 min for *Cpu*ADO).

89

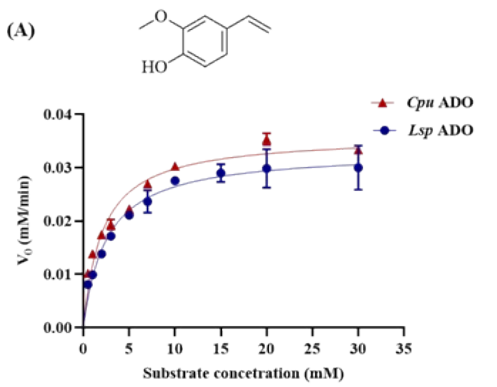

(B)

Table. Kinetic parameters of ADOs towards 4-vinylguaiacol

Enzyme	k_{cat} [s^{-1}]	K_M [mM]	k_{cat}/K_M [$mM^{-1}\ s^{-1}$]
***Lsp*ADO**	0.30 ± 0.001	3.31 ± 0.33	0.09±0.009
***Cpu*ADO**	0.22 ± 0.009	0.84 ± 0.15	0.26±0.003

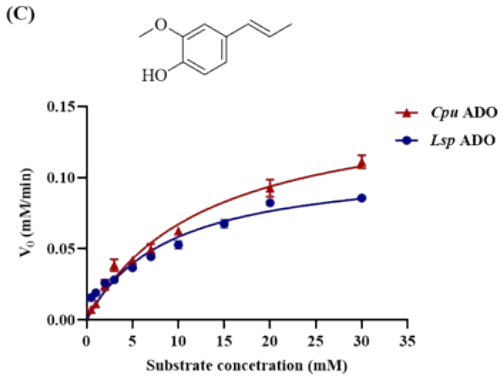

(D)

Table. Kinetic parameters of ADOs towards isoeugenol

Enzyme	k_{cat} [s^{-1}]	K_M [mM]	k_{cat}/K_M [$mM^{-1}\ s^{-1}$]
***Lsp*ADO**	0.92 ± 0.03	8.55 ± 1.24	0.11±0.01
***Cpu*ADO**	1.29 ± 0.14	13.09± 0.31	0.10±0.03

Figure S7. Kinetic curves and parameters of the newly identified ADOs towards 4-vinylguaiacol (A and B) and isoeugenol (C and D) respectively. (Reaction conditions: initial reaction rates were measured at 40℃ in 50 mM phosphate buffer (pH 8.0); the enzyme concentration was 2 μM, the substrate concentrations were varied between 0.5 mM and 30 mM).

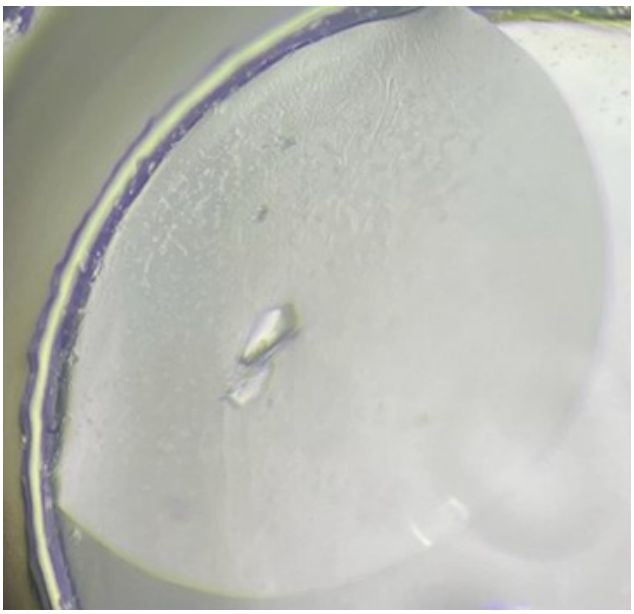

Figure S8. Morphology of *Cpu*ADO protein crystal. (Crystal growth conditions: 0.2M Ammonium sulfate, 0.1M BIS-Tris (pH6.5), 25% w/v Polyethylene glycol 3350)

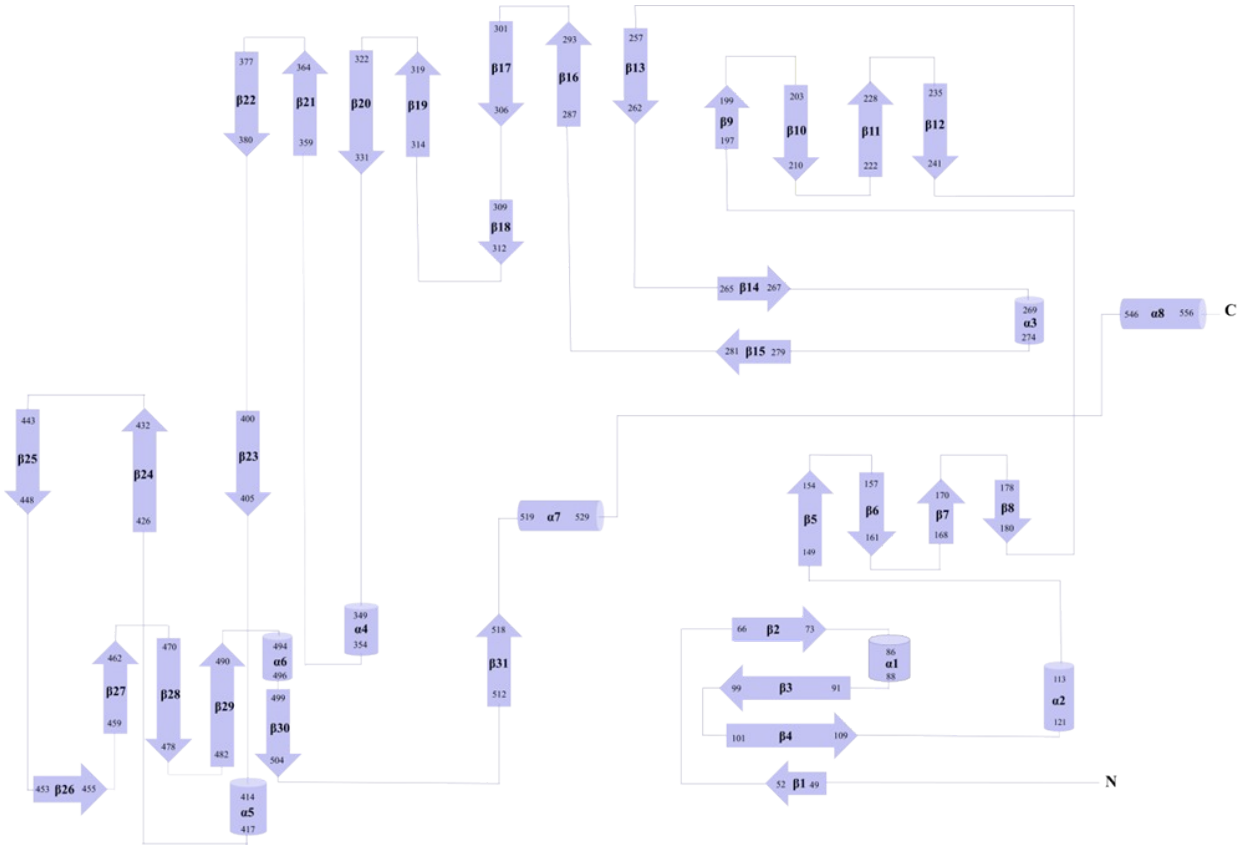

Figure S9. Secondary structure topology diagram of *Cpu*ADO (PDB ID 9LP3), with β-strands and α-helices arranged according to their spatial organization in the crystal structure.

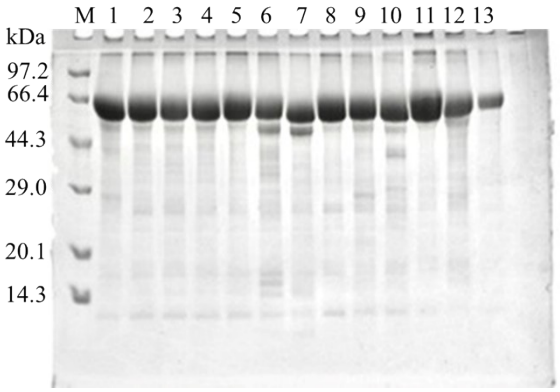

Figure S10. SDS-PAGE analysis of purified alanine mutants. Lane M: protein marker, lane 1: F87A, lane 2: Y129A, lane 3: T149A, lane 4: K162A, lane 5: E163A, lane 6: H195A, lane 7: H249A, lane 8: H312A, lane 9: F336A, lane 10: E385A, lane 11: F386A, lane 12: E457A, lane 13: H513A.

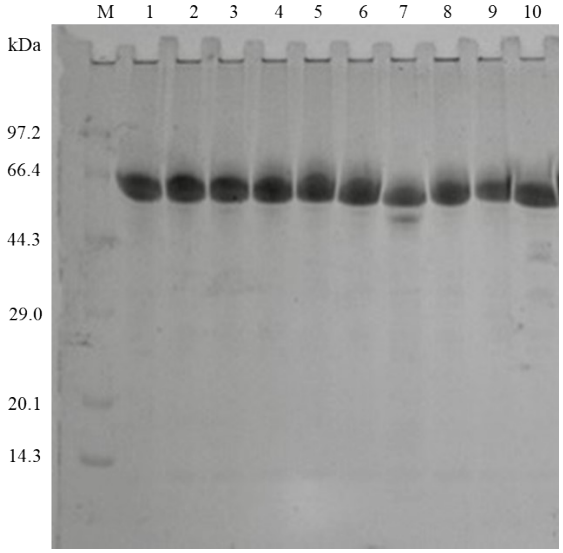

Figure S11. SDS-PAGE analysis of purified structure-guided rationally designed *Cpu*ADO mutants. Lane M: protein marker, lane 1: *Cpu* WT, lane 2: M247R, lane 3: F349V, lane 4: F349L, lane 5: N42A, lane 6: R352K, lane 7: F349W, lane 8: W338F, lane 9: W338D, lane 10: F349V-W338D.

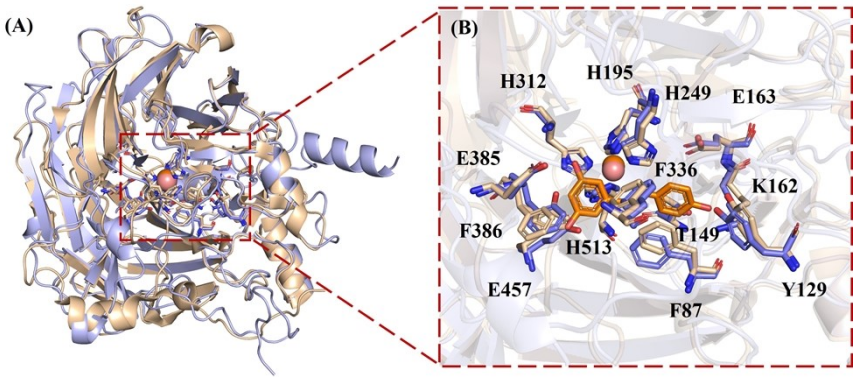

Figure S12. (A) Overall structural alignment of *Cpu*ADO with CAO1 (PDB ID: 5U90); (B) Close-up view of the aligned active site residues. The orange sticks represent the CAO1-bound substrate resveratrol.

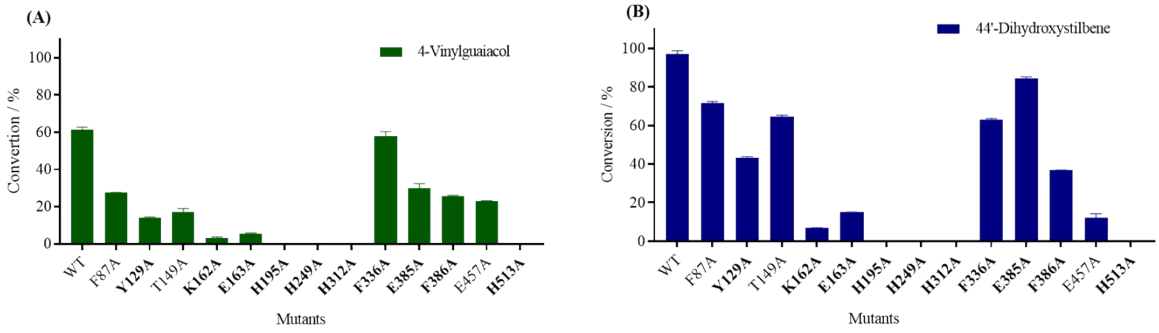

Figure S13. Catalytic Conversion Rates of *Cpu*ADO Alanine Mutants toward 4-vinylguaiacol (A) and 4,4′-Dihydroxystilbene (B)

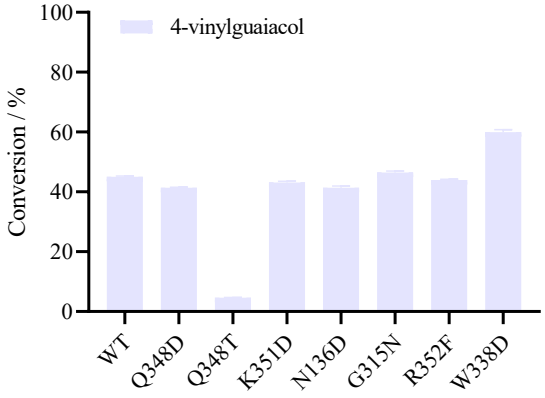

Figure S14. Preliminary screening of *Cpu*ADO variants selected from AI-based zero-shot activity scoring, showing conversion rates toward 4-vinylguaiacol measured using crude enzyme. The top 10 substitutions predicted by the Saprot 650M model are listed in Table S8. Among them, seven variants were successfully expressed and screened experimentally, whereas three failed to express and are therefore not shown. W338D showed the largest improvement in conversion and was subsequently selected for purification and detailed characterization.

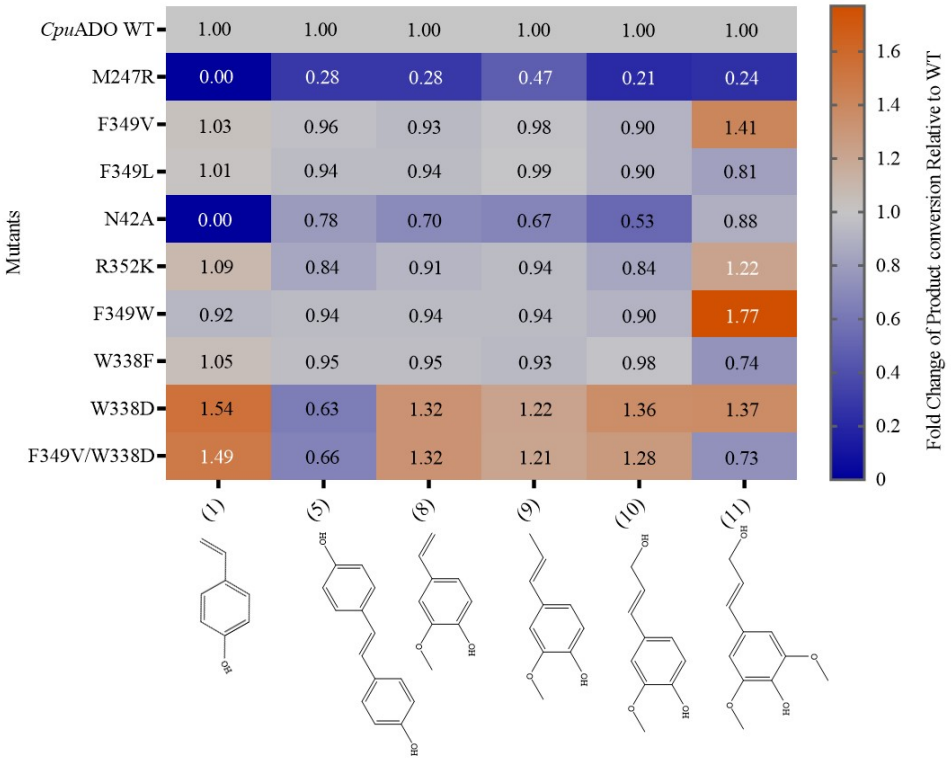

Figure S15. Heatmap of relative product conversion of *Cpu*ADO mutants compared to WT (set as 1.00) for six Lignin-related substrates. Warmer colors indicate increased activity, cooler colors indicate decreased activity.

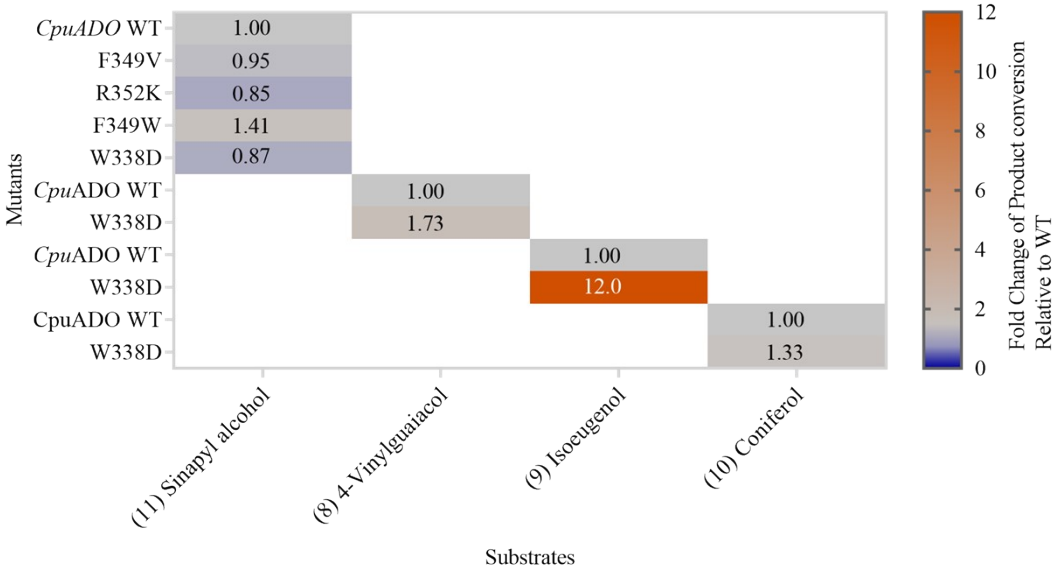

Figure S16. Heatmap of relative catalytic efficiencies (k_{cat}/K_M) of *Cpu*ADO wild-type and mutants toward four Lignin-related substrates (8, 9, 10, and 11), normalised to the corresponding WT values (set as 1.00). Warmer colors indicate increased catalytic efficiency, whereas cooler colors indicate decreased catalytic efficiency.

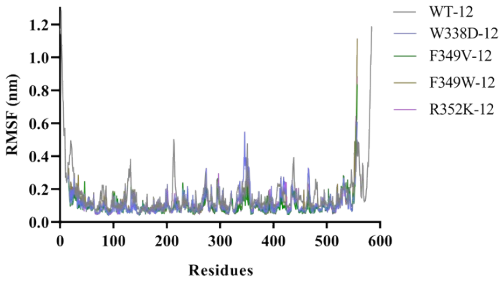

146

147 **Figure S17.** Per-residue backbone RMSF profiles for *Cpu*ADO WT and mutants bound to sinapyl alcohol **(11)**. RMSF
148 values for Cα atoms were calculated from 100 ns MD simulations after alignment on backbone heavy atoms (The
149 overall similarity of the profiles indicates that the mutations do not markedly alter local flexibility).

150

151

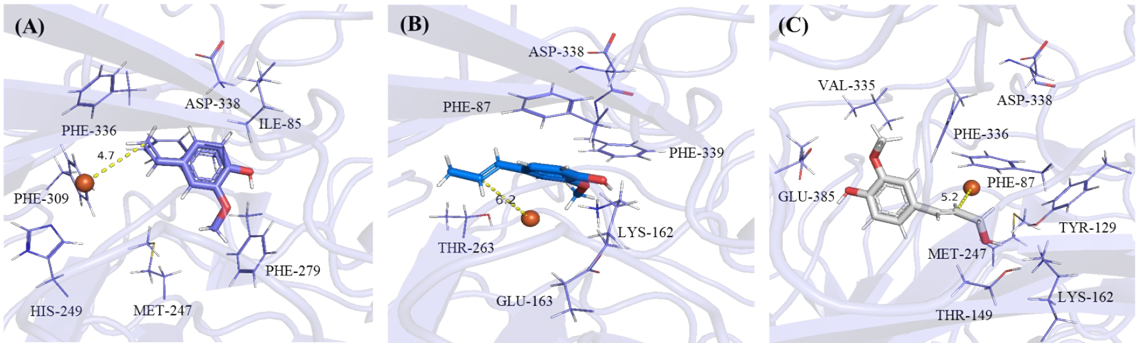

152

153 **Figure S18.** Final Frame Snapshots of W338D Mutants after 100 ns of MD Simulation: W338D-8 (A), W338D-9 (B),
154 and W338D-10 (C).

155

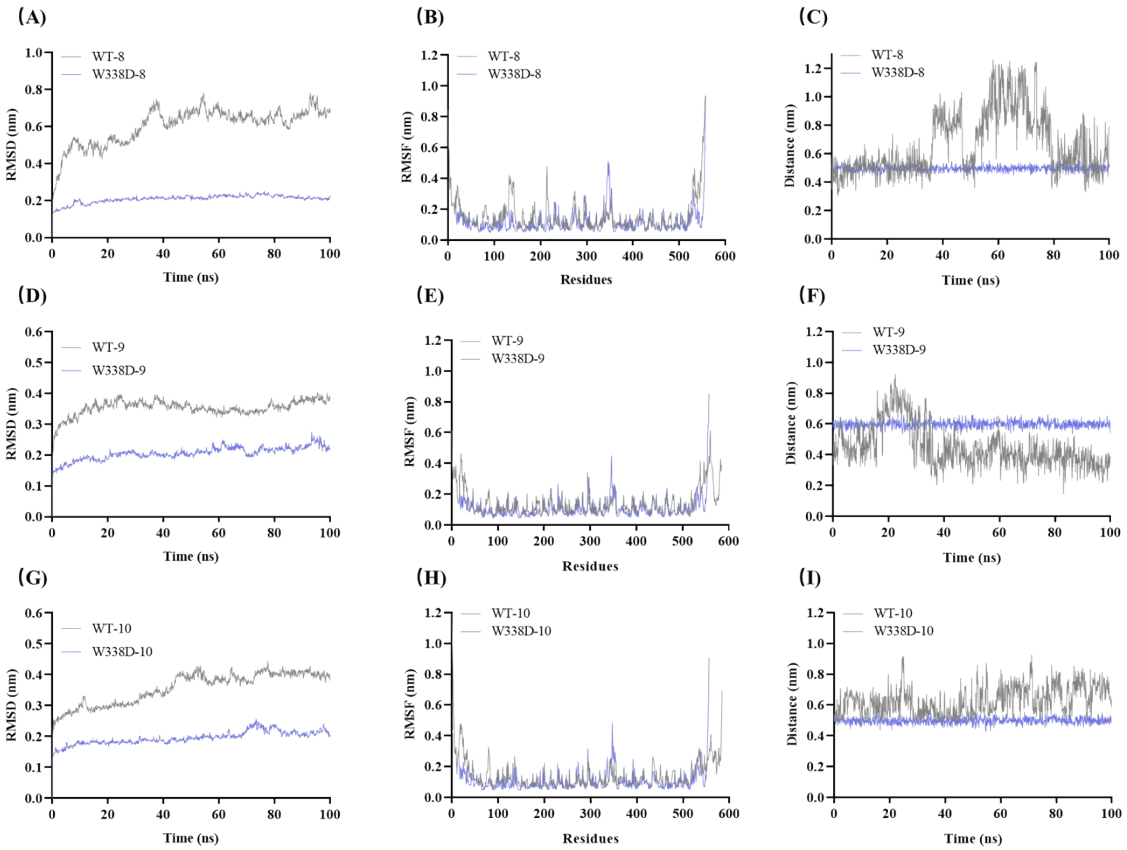

Figure S19. Molecular Dynamics Profiles of *Cpu*ADO Mutants W338D with three different Lignin-related substrates: W338D-8 (4-Vinylguaiacol) (A-C), W338D-9 (Isoeugenol) (D-F), and W338D-10 (Coniferol) (G-I). Root-mean-square deviation (RMSD) profiles of the enzyme backbone over 100ns (A, D, G). Root-mean-square fluctuation (RMSF) of each residue (B, E, H). Time evolution of the distance between Fe^{2+} -C=C bond of the bound substrate (C, F, I).

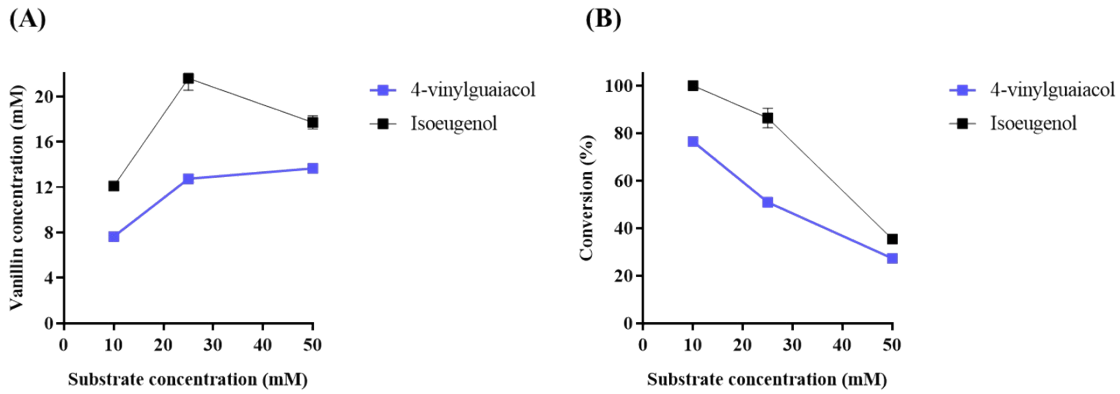

Figure S20. Effect of increased substrate loading on vanillin formation and conversion from 4-vinylguaiacol **(8)** and isoeugenol **(9)** by *Cpu*ADO W338D.

(A) Final vanillin concentrations obtained at substrate concentration of 10, 25, and 50 mM.

(B) Corresponding conversion under the same conditions. Reactions were performed in a 1 mL system with 5% (v/v) DMSO.

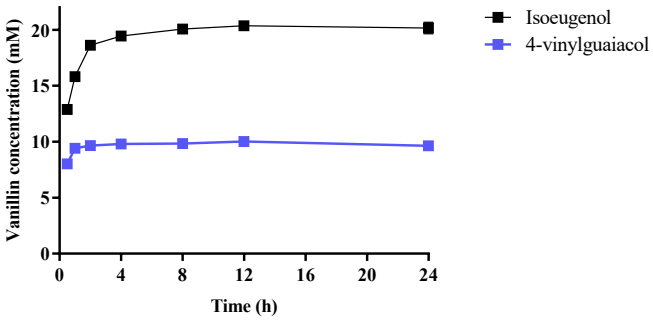

Figure S21. Time-course analysis of vanillin formation from 4-vinylguaiacol **(8)** and isoeugenol **(9)** in 50 mL-scale reactions catalyzed by *Cpu*ADO W338D. Aliquots were withdrawn at 0.5, 1, 2, 4, 8, 12 and 24 h for GC analysis. Reactions were performed at a substrate concentration of 25 mM with 5% (v/v) DMSO.

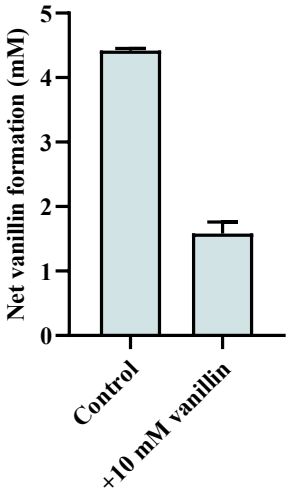

Figure S22. Effect of 2 h pre-incubation with 10 mM vanillin on the subsequent activity of *Cpu*ADO toward 4-vinylguaiacol **(8)**. Net vanillin formation after 30min was compared between the control and vanillin-treated groups. Net vanillin formation was calculated as the difference between product concentrations at 30 min and 0 min.

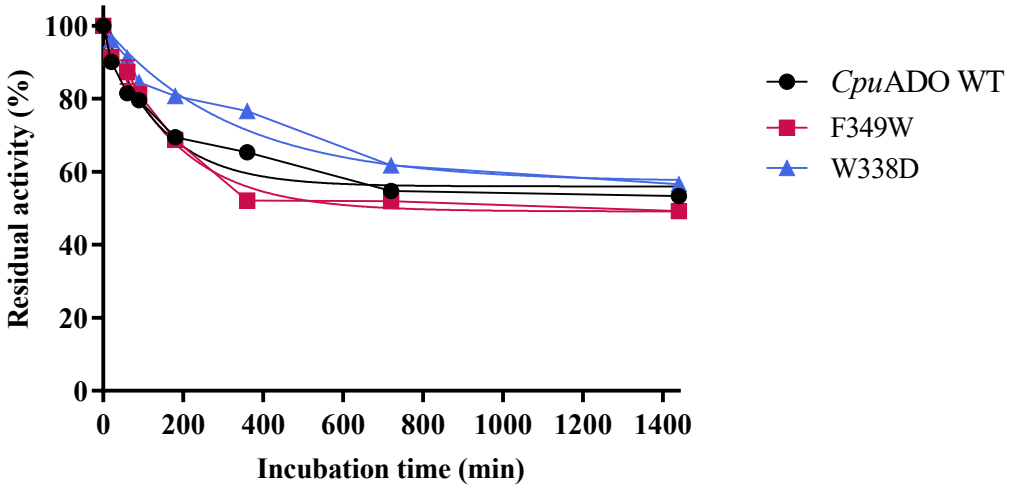

Figure S23. Thermal stability of *Cpu*ADO WT and selected beneficial mutants at 40 °C under the sinapyl alcohol assay conditions. The corresponding fitted apparent half-lives are summarised in Table S10.

2. Supporting Tables:

Table S1. Primers used in alanine mutagenesis and structure-guided, rationally designed mutants of *Cpu*ADO.

Mutants	Forward and reverse primers
F87A	CATTCACGCAAACGGCGATGGTAGCGTG
	CCGTTTGCGTGAATGTCATCTTCAAACATCGGC
Y129A	CGGCCGTGCACGTAACCCGTGGACCGATAACG
	TTACGTGCACGGCCGAACAGGCTACG
T149A	GTCTAACGCAAACGTGTTCTTCTGGCGTGG
	GTCTAACGCAAACGTGTTCTTCTGGCGTGG
E163A	GACCAAAGCAGATGGTCCGCCGTACGCG
	CCATCTGCTTTGGTCGCCAGCAGCATGC
H195A	CACCGCGGCACCGAAATTCGATCCGCGCAC
	TTCGGTGCCGCGGTGAAGGTCGGGCTC
H249A	CATGATTGCAGATTGCGGTCTGTCTGAAAACTGG
	CAATCTGCAATCATGCCCGCGAACGG
H312A	TCACGGTGCAGTGGCGGGCTGCTACGAAAACG
	GCCACTGCACCGTGAAACGCGTTTTCGC
F336A	TAACGTTGCATTCTGGTTTCCGCCGGAC
	CAGAATGCAACGTTACCATCTGCCACGG
E385A	CAACGGTGCATTTAGCCGTATCGATGATCGTTGG
	CTAAATGCACCGTTGGTCGGCCAAAC
F386A	CATGATTGCAGATTGCGGTCTGTCTGAAAACTGG
	CAATCTGCAATCATGCCCGCGAACGG
E457A	CTTCCAGGCACCGACCTTCATCCCGAAAG
	GTCGGTGCCTGGAAGGTGCAGGTCGG
H513A	GGGTCTGGCAGGCAACTGGGTGGACTGG
	TTGCCTGCCAGACCCAGTTTCAGTTTCAGCG
M247R	CGCGGGCCGTATTCATGATTGCGGTCTGTCTG
	TGAATACGGCCCGCGAACGGAGCTTC
F349V	GGGTCAGGTTGCAAAACGTAACAAACTGTCCTCCC
	TTTGCAACCTGACCCTGTTCTTCACCGTCC
F349L	GGGTCAGCTGGCAAAACGTAACAAACTGTCCTCCC
	TTTGCCAGCTGACCCTGTTCTTCACCGTCC
N42A	GAGCATGGCAAAACCGTCCCGTTTCGAAGG
	GGTTTTGCCATGCTCGCGAAAACCGG
R352K	CGCAAAAAAAAACAAACTGTCCTCCCCGACC
	TTGTTTTTTTTTGCGAACTGACCCTGTTC
F349W	GGGTCAGTGGGCAAAACGTAACAAACTGTCCTCCC
	TTTGCCCACTGACCCTGTTCTTCACCGTCC
W338D	TTTCTTCGATTTTCCGCCGGACGGTGAAG
	GGAAAATCGAAGAAAACGTTACCATCTGCCACG

W338F	TTTCTTCTTTTTTCCGCCGGACGGTGAAG	
	GGAAAAAAGAAGAAAACGTTACCATCTGCCACG	
F349V-W338D	TTTCTTCGATTTTCCGCCGGACGGTGAAG	
	GGAAAATCGAAGAAAACGTTACCATCTGCCACG	
F349V-R368K	GTTGCAAAAAAAAACAAACTGTCCTCCCCGACC	
	GTTTGTTTTTTTTTGCAACCTGACCCTGTTC	

Table S2. Primers used for Site-Directed Mutagenesis of *Tth*ADO Based on Structrue-Guided Mutations Identified in *Cpu*ADO.

Enzyme	Mutants	Forward and reverse primers
*Tth*ADO	F335D	TTTCTTCGATTTCCCGCCGGACGACAACATCACC
		GGGAAATCGAAGAAAACGTTACCGTCCGCC
*Tth*ADO	R352K	TGCGAAAAAAAAACCGTCTGAGCTCCCCG
		CGGTTTTTTTTCGCAACACCGTCTGCC

Table S3. List of amino acid sequences of different ADOs

Enzyme name	**amino acid sequence**
Tth ADO	MAHIHDLAPEVSNYSSGRLTPPTPVRFPRTPVFASMNKPCRFEGDVFDLEVS GAIPPDIDGTFFRVQPDHRFPPLFEDDIHFNGDGSVTAIRISGGHADLRQRYV RTERYLLETRARRSLFGRYRNPWTDNESVRGVIRTASNTNVVFWRGALLA MKEDGPPFAMDPVTLETLGRYDFEGQILSPTFTAHPKIDPDTGEMVCFAYE AGGDGSDCSVDVAVWTVDADGKKVEECWYKAPFAGMIHDCGITKNWVV LPLTPIKMDLERMKRGGNKFAWDPSEDQWYGVVPRRGAKSDDIIWFRAD NGFHGHVAGCYELPSGEIVFDLTVADGNVFFFFPPDDNITPPADGVAKRNR LSSPTVRWIFDPKAKKSAIRTEAAGDADIWVADERVKPALTWPTNGEFSRI DDRYVTKPYRHFWQAVVDPTRPYDFEKCGPPAGGLFNCLGHYTWSDQNY HHGHNTGDPSGDGRSNGSAEEATAGKFGLQDVYFAGPTMTFQEPTFIPRQ GAAEGEGYLIALLNHLDELRNDVVIFEARNLGKGPLAVIHLPLKLKLGLHG NWVDSREIEAWRRRRAENGDVGPLRVAKEPLPWQKKFAAAAQNGSNGV
Lsp ADO	MNAFPPLPIYTGFNTPLRMEVDIHDLEVEGQVPEGLDGIFYRVGPDPQYPPR LGNDIYFNGDGMVSAFRFEKGRVDLKCRYARTDKFLLERDARKALFGAYR NPFFDDPAVEGRIRGANTNVVYHAGKLLALKEDSPPLVMDPWTLETRGYY DYEGVLTSETFTAHPKLDPHTGEMIAFGYSAKGIASPDVAYYVIDRDGKIV HEVWFQMPYPCLVHDFGVTRDYVVFPIVPVISSLDFARAGRPTFGWDASK DVYLGVLPRRGSAKDLRWFRTSNLFASHVMNAFNDGTKIHFDTPVAKGN MFPFFPDVTGAPFDPVAATAHVTRWSVDYAGGEGIGFEQLTTLAGEFPRID

	DRYAMEAYRHGYICVSDRSRPYDEKRAGSITGMFINCLGHIDHATGSSDDV YYVGPVSSLQEPAFIPASKDAPEGEGYLVALANRYDEQRSDLLVLDAQRLQ EGPIATIKLPLKLRNGLHGNWVPVEDLPPRPAGA
Cpu ADO	MAHIFDLAPEVSLPDEPIYKDGKLHRPNHVQFPQTPVFASMNKPSRFEGTIL SLEHTGIIPPEINGTFFRVQPDHRFPPMFEDDIHFNGDGSVTAIRIFDGKVDFR QRYVHTERYKAETKARRSLFGRYRNPWTDNESVKGVIRTASNTNVFFWRG MLLATKEDGPPYAMDPVTLETYGRYDFEGQILSPTFTAHPKFDPRTGEMVC FAYETGGDGADCSREVMVWTLDKDGKKVSERWFEAPFAGMIHDCGLSEN WLVLPLTPIKMDLERMKRGGNKFAWDPKEDQVYGLVPRRGDGEVKWFR GENAFHGHVAGCYENAQGHVVIDLTVADGNVFFWFPPDGEEQGQFAKRN KLSSPTHRWILDPSLPNNARITPALVWPTNGEFSRIDDRWTTRKYKHFWLA KVDPSRPYDFAKCGPPAGGLFNCLGHYTWDLDNELATGQEDVYFAGPTCT FQEPTFIPKGDKEGEGWLIALVNHLDVLRNDVVILDAQNLAKGPVCTIHLP LKLKLGLHGNWVDWRDIEDWTKRRQEDGEVGPVQVATEMLPWQKAFWE KEKEKNGNGVEGPNINGTNGANGTNGVNGSSH
Dsp ADO	MAHIFSLAPAVKGYKDGRLTRPGEATTFPQTPVFSGINKPSRLEGDVFDLEV TGTIPKEINATFYRIQPDQRFPPLFEDDVHFNGDGSVTAIRISNGHADFKQRY VQTDRYKAETAARQSLFGRYRNPFTDNESVKGVIRTASNTNITFRRGMLLA SKEDGPPFAMDPVTLETLGRYDFEGQITAPTFTAHPKFDPETGEMICFAYEA GGNGNDGSLDIIMWTIDADGKKTEEAFYKAPFAGMIHDIGVSKNYVVMPL TPIKVNMDRMKRGGEKFAWDPYEDQWYGLVPRRNGKSSDIIWFRADNAF QGHIAGCYENEDGHVVVDLTVADGNVFFWWPPDEELTPIQPDKVTARDKL NSQTTRWILDPKAKTGTRIKPAFVWDINGEFSRIDDRWVTKKYKHFWQARI DPTKPYDFQKCGPPAGGLFNSLGHYTWDSENPLAHGDEDTYFFGPTSTVQ EPSFIPRGEDAAEGEGYLIALVNRLGELRNDVAIFDAQNLAQGPLAVLHLPL ALKLGLHGNFVDHRDIEAWQRRRDAGGDVGPVKIATEPLPWQKELANGA NGSH
Slo ADO	MDESSRLEGDVFDLEVTGTLPADINGTFFRVQPDHRFPPLYEDDIHFNGDGS VTAIRIADGHADFKQRYVRTERYQAETRARKSLFGRYRNPWTDNESILSPT FTAHPKVDPETGEMVCFAYEAGGDGADCSVDVAVWTVDADGKKIEECW YKAPFAGMIHDCGISENYVVLALTPIKMDFERMKRGGNKFAWDPNEDQW YGVVPRRGAKSEDIIWFRADNGFHGHVAGCYELPSGEIVFDLTVADGNVFF FFPPDDNITPPDGVAKRNRLSSPTVRWIFDPKAKKSAIRTPAAGDADVWVA DERSKPVVTWLTNGEFSRIDDRVTTKPYRHFWQAVVDPTRPYDFDKCGPP AGGLFNCLGHYTWSEEHFHTDKPAQNGTNGKSGEEGKFGLEDMYFPGPT MTFQEPTFIPREGGAEGEGYLIALLNHLDQLRNDVVIFDAQNLAKGPLATV HLPLKLKLGLHGNWVDNRDIEAWQRRRGTNGDVGPVQVATEPLPWQKKL AEQNGTGA

Table S4. Comparative kinetic parameters of representative reported ADO/ADO-like enzymes on the common substrates 4-vinylguaiacol (substrate **8**) and isoeugenol (substrate **9**), including *Cpu*ADO WT and selected mutants from this study.

4-Vinylguaiacol (substrate 8)							
Enzyme/variant	Source	k_{cat} [s^{-1}]	K_M [mM]	k_{cat}/K_M [mM^{-1} s^{-1}]	Assay format	Conditions	Reference
*Cpu*ADO WT	*Coniochaeta pulveracea*	0.22 ± 0.01	0.84 ± 0.15	0.26 ± 0.01	Initial-rate	50 mM phosphate buffer, pH 8.0, 40 °C, 2µM enzyme, 0.05-30mM substrate	This work (Figure S7)
*Cpu*ADO W338D	*Coniochaeta pulveracea*	2.22 ± 0.10	4.94 ± 0.68	0.45 ± 0.06	Initial-rate	50 mM phosphate buffer, pH 8.0, 40 °C, 2µM enzyme, 0.05-30mM substrate	This work (Table 2)
Cso2	*Caulobacter segnis* ATCC 21756	NR	4.1	NR	HPLC-based steady-state kinetic assay (Lineweaver-Burk)	50 mM potassium phosphate buffer, pH 7.5, 0.2-1mg/mL enzyme, 0.5-2 mM substrate[l]	25
*Tth*ADO	*Thermothelomyces thermophila*	3.3±0.40	2.73±0.14	1.21±0.16	Initial-rate	50 mM potassium phosphate buffer, pH 7.5, 1.3mg/mL enzyme, 0.5-7 mM substrate	18
*Tt*CCO (ADO)	*Thermothelomyces thermophilus*	0.45	1.42 ± 0.08	0.32	Initial-rate	100 mM PBS, pH 7.0, 0-2 mM substrate	24
*Tt*CCO (M3)	*Thermothelomyces thermophilus*	0.91	0.42 ± 0.035	2.14	Initial-rate	100 mM PBS, pH 7.0, 0-2 mM substrate	24
*Map*ADO	*Moesziomyces aphidis DSM 70725*	361± 12	0.22± 0.05	1640.91±347.17	Endpoint measurement on HPLC	10 mM potassium phosphate buffer, pH 7.4, 0.02-6 mM substrate	27

Table S4. (continued).

Isoeugenol (substrate 9)							
Enzyme/variant	Source	k_{cat} [s^{-1}]	K_M [mM]	k_{cat}/K_M [mM^{-1} s^{-1}]	Assay format	Conditions	Reference
*Cpu*ADO WT	*Coniochaeta pulveracea*	1.29 ± 0.14	13.09 ± 0.31	0.10 ± 0.03	Initial-rate	50 mM phosphate buffer, pH 8.0, 40 ℃, 2μM enzyme, 0.05-30mM substrate	This work (Figure S7)
*Cpu*ADO W338D	*Coniochaeta pulveracea*	3.64 ± 0.27	3.05 ± 0.73	1.20 ± 0.3	Initial-rate	50 mM phosphate buffer, pH 8.0, 40 ℃, 2μM enzyme, 0.05-30mM substrate	This work (Table 2)
Cso2	*Caulobacter segnis* ATCC 217568	NR	0.85	NR	HPLC-based steady-state kinetic assay (Lineweaver-Burk)	50 mM potassium phosphate buffer, pH 7.5, 20℃, 0.2-1mg/mL enzyme, 0.5-2 mM substrate	25
*Tth*ADO	*Thermothelomyces thermophila*	5.28±0.08	2.0±0.14	2.64±0.19	Initial-rate	50 mM potassium phosphate buffer, pH 7.5, 1.3mg/mL enzyme, 0.5-7 mM substrate	18
*Tt*CCO (ADO)	*Thermothelomyces thermophilus*	44	2.24±0.26	19.64±2.32	Initial-rate	100mM PBS buffer, pH 7.0, 30℃, 0-2 mM substrate	24
*Map*ADO	*Moesziomyces aphidis DSM 70725*	238	0.12±0.01	2016.95±222.21	Continuous initial-rate UV-Vis	10 mM potassium phosphate buffer, pH 7.4, 0.05-2 mM substrate	27
*Map*ADO	*Moesziomyces aphidis DSM 70725*	654 ± 2	0.58 ± 0.10	1123.71±198.98	Endpoint measurement on HPLC	10 mM potassium phosphate buffer, pH 7.4, 0.02-6 mM substrate	27

206

207 a Values are reported as given in the original references unless otherwise indicated.

208 b k_{cat} / K_m values were recalculated where necessary and are uniformly expressed in $mM^{-1}\ s^{-1}$ for direct comparison.

209 c Direct comparison across studies should be interpreted with caution because detection methods, enzyme preparation, and reaction conditions differ between reports.

210 d Substrate numbering follows the main manuscript scheme: substrate **8**=4-vinylguaiacol; substrate **9**=Isoeugenol.

211 NR, not reported.

Table S5. Retention times of different substrates and products

	Substrate Name	Structure	Retention time (min)	Product Name	Structure	Retention time (min)
1	4-Vinylphenol	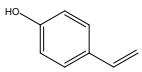	1.7	4-hydroxybenzaldehyde	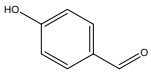	2.542
2	4-Isopropenylphenol	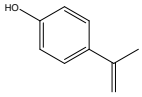	2.139	4-Hydroxyacetophenone	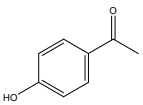	3.219
3	p-Coumaryl alcohol	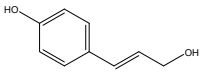	5.008	p-Hydroxybenzaldehyde	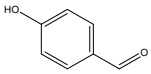	2.542
4	trans-4-Hydroxystilbene	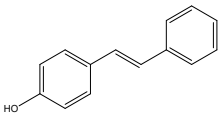	9.261	p-Hydroxybenzaldehyde	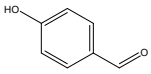	2.542
5	4,4'-Dihydroxystilbene	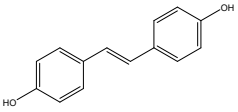	12.936	p-Hydroxybenzaldehyde	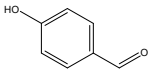	2.542
6	4-(3,5-Dimethoxystyryl)phenol	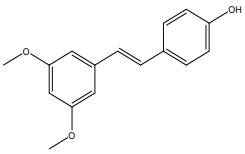	15.504	p-Hydroxybenzaldehyde	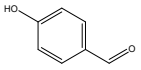	2.542
7	resveratrol	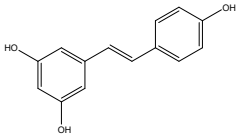	16.923	p-Hydroxybenzaldehyde	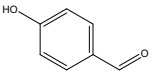	2.542
8	4-vinylguaiacol	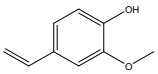	2.294	vanillin	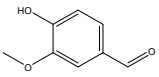	2.94
9	Isoeugenol	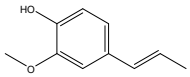	3.349	vanillin	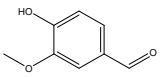	2.94
10	Coniferol	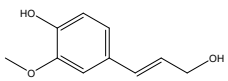	6.204	vanillin	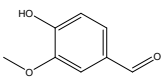	2.94
11	Sinapyl alcohol	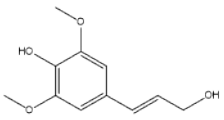	8.702	syringaldehyde	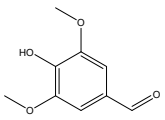	5.41

12	Piceatannol	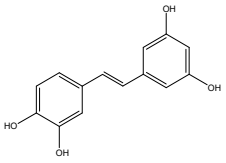	19.12	3,5-Dihydroxybenzaldehyde	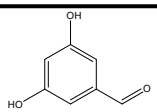	5.068
13	Oxyresveratrol	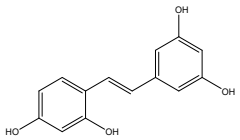	16.84	3,5-Dihydroxybenzaldehyde	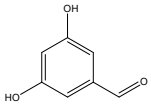	5.068
14	Isorhapontigenin	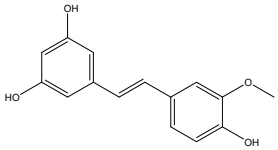	16.05	vanillin	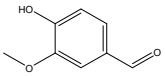	2.94
15	curcumin	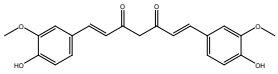	16.7	vanillin	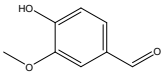	2.94
16	4-Vinylaniline	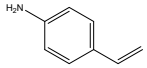	1.848	4-Aminobenzaldehyde	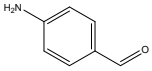	3.069

Table S6. Some substrates that did not produce any products are listed in this table.

No.	Substrate	Retention time (min)	Product	No.	Substrate	Retention time (min)	Product
17	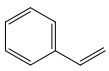	1.068	-	30	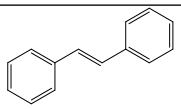	5.93	-
18	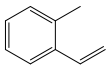	1.188	-	31	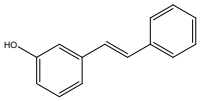	9.152	-
19	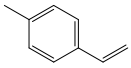	1.189	-	32	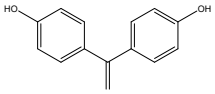	10.325	-
20	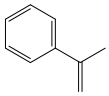	1.163	-	33		1.035	-
21	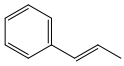	1.233	-	34	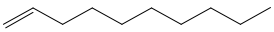	1.159	-
22	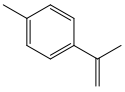	1.353	-	35	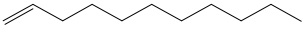	1.33	-
23	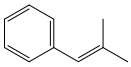	1.34	-	36	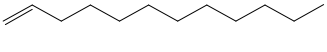	1.615	-
24	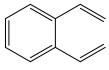	1.42	-	37		2.089	-
25	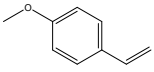	1.525	-	38		2.794	-

26	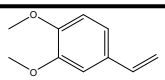	2.612	-	39	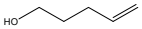	1.048	-
27	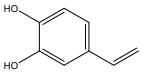	1.031	-	40	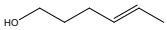	1.033	-
28	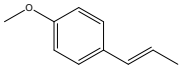	2.119	-	41	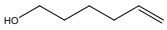	1.031	-
29	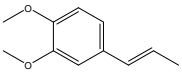	3.746	-	42	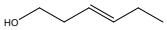	1.041	-

[a]Reaction conditions: 10 μM enzyme, 10 mM substrate (dissolved using 1% DMSO), pH 8.0, 40 °C, 24h.

"-" represents no product generated.

Table S7. Crystallographic data collection and refinement statistics of *Cpu*ADO.

	***Cpu* ADO**
Data collection	
Space group	P 21 21 21
Cell dimensions	
a, *b*, *c* (Å)	66.902, 90.052, 194.065
α, β, γ (°)	90, 90, 90
Resolution (Å)	48.52-2.20 (2.26-2.20)[a]
R_{merge}	0.234 (0.524)
I/s(I)	6.9 (4.0)
$CC_{1/2}$	0.975 (0.908)
Completeness (%)	100.0 (100.0)
Redundancy	8.4 (8.5)
Refinement	
Resolution (Å)	45.03-2.20 (2.28-2.20)
No. reflections	60362
R_{work} / R_{free}[b]	0.1942/0.2395
No. atoms	
Protein	8717
Ligand	0
Water	773
Ion	4
***B* factors**	
Protein	34.42
Ligand	-
Water	33.48
Ion	29.64
R.m.s.deviations	
Bond lengths (Å)	0.007
Bond angles (°)	0.92

Ramachandran favored (%)	94.7
Ramachandran outliers (%)	0.0

[a]Values in parentheses are for the highest-resolution shell.

Table **S8**. Top 10 Mutations Predicted by Saprot 650M Zero-Shot Model for Activity Enhancement of *Cpu*ADO

No.	**Mutation**	Score
1	Q348D	6.52
2	M224G	5.70
3	Q348T	5.38
4	K351D	5.03
5	N136D	5.01
6	G315N	4.89
7	Q348S	4.59
8	R352F	4.44
9	F414E	4.36
10	W338D	4.31

Table S9. Catalytic Conversion Rates of *Tth*ADO Mutants Carrying Structure-Guided Mutations Derived from *Cpu*ADO

Substrates	4-Vinylphenol	4,4'-Dihydroxystilbene	4-vinylguaiacol	Isoeugenol	Coniferol	Sinapyl alcohol
*Tth*ADO WT	27.4±0.12	83.27±1.55	35.74±0.28	62.07±0.79	11.23±0.23	2.68±0.03
F335D	32.03±0.59	96.03±1.16	40.19±1.25	70.76±0.54	15.74±0.1	4.42±0.01
R352K	45.8±0.65	56.16±1.9	49.29±1.65	94.69±0.84	16.92±0.31	3.44±0.06

Table S10. Fitted thermal-stability parameters of *Cpu*ADO WT, F349W, and W338D at 40 °C under the sinapyl alcohol assay conditions.

Variant	Plateau (%)	Apparent half-life (min)	Residual activity at 1440 min (%)
Cpu ADO WT	55.98	99.5	53.3
F349W	49.13	124.0	49.2
W338D	57.24	225.6	56.6

Apparent half-lives were obtained from one-phase decay fitting with a non-zero plateau and therefore describe the fitted decay behaviour under the present assay conditions. Residual activities at 1440 min are experimental values.

Table S11. Simple E-factor breakdown for the 50 mL-scale transformation of isoeugenol to vanillin catalysed by CpuADO W338D.

Component	Mass [g]	E-factor contribution [$kg_{component}\,kg^{-1}_{Product}$]
Product	0.152	-
Non-reacted substrate	0.205	0.35
Enzyme	0.033	0.22
Water	47.5	312.5
Phosphate	0.237	1.8
DMSO	2.53	16.6
HCl	0.08	0.53
Ethyl acetate	6.28	41.3
Total	56.895	374.3

E-factor contributions were calculated from the mass of each input component relative to the mass of vanillin obtained under the current 50 mL-scale reaction conditions. Solvent recycling and wastewater treatment were not considered in this simplified analysis.

Discussion of the E-factor analysis

A simple E-factor analysis of the 50 mL-scale transformation of isoeugenol to vanillin provides an initial indication of the environmental impact of the proposed reaction. In total, 374 kg of waste are generated per kg of vanillin. Of this, 98% is solvent-related (83% water, 11% ethyl acetate, and 4% DMSO). Consequently, further development should focus on reducing wastewater formation, preferably by increasing the substrate concentration. In addition, DMSO should be avoided as a water-miscible co-solvent, as it is likely to complicate product isolation at preparative scale. A potential strategy to address these issues may be the implementation of a fed-batch addition of isoeugenol. The limited aqueous solubility of vanillin may further facilitate product isolation by simple filtration.

With regard to the buffer system, alternatives to non-renewable phosphate should be explored. Given that the overall reaction is pH-neutral, it may even be possible to omit buffering altogether.

The enzyme performance (E-factor contribution of 0.22 kg kg^{-1}) is not critical from an environmental perspective. Nevertheless, a productivity of approximately 4 kg product kg^{-1} enzyme is unlikely to be economically viable. Accordingly, further research should focus on identifying the factors limiting catalytic performance.

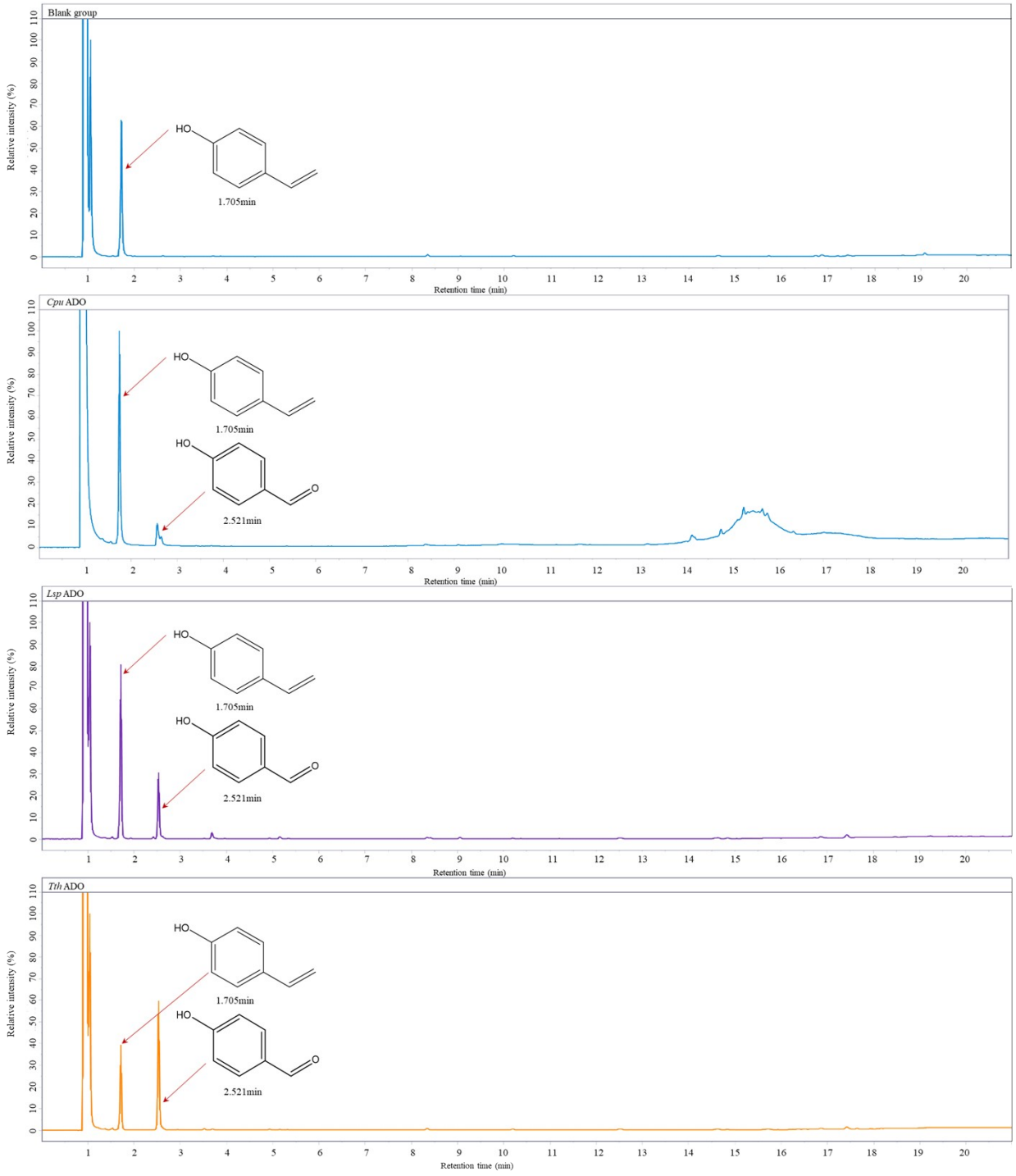

255

256 **Figure S24**-1. Gas chromatography results of the blank control group and different ADOs using 4-vinylphenol as a
257 substrate

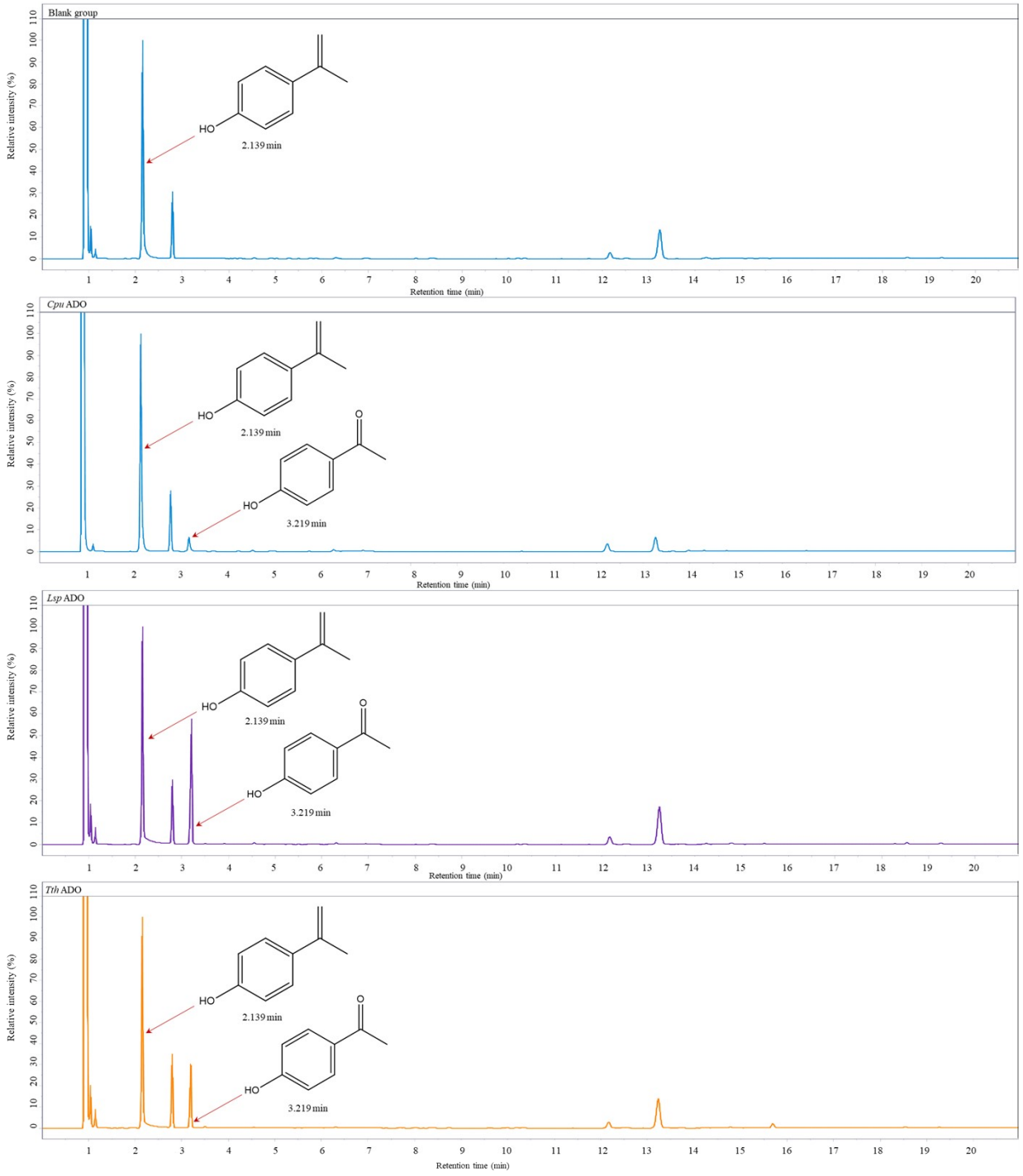

Figure S24-2. Gas chromatography results of the blank control group and different ADOs using isopropenylphenol as substrate

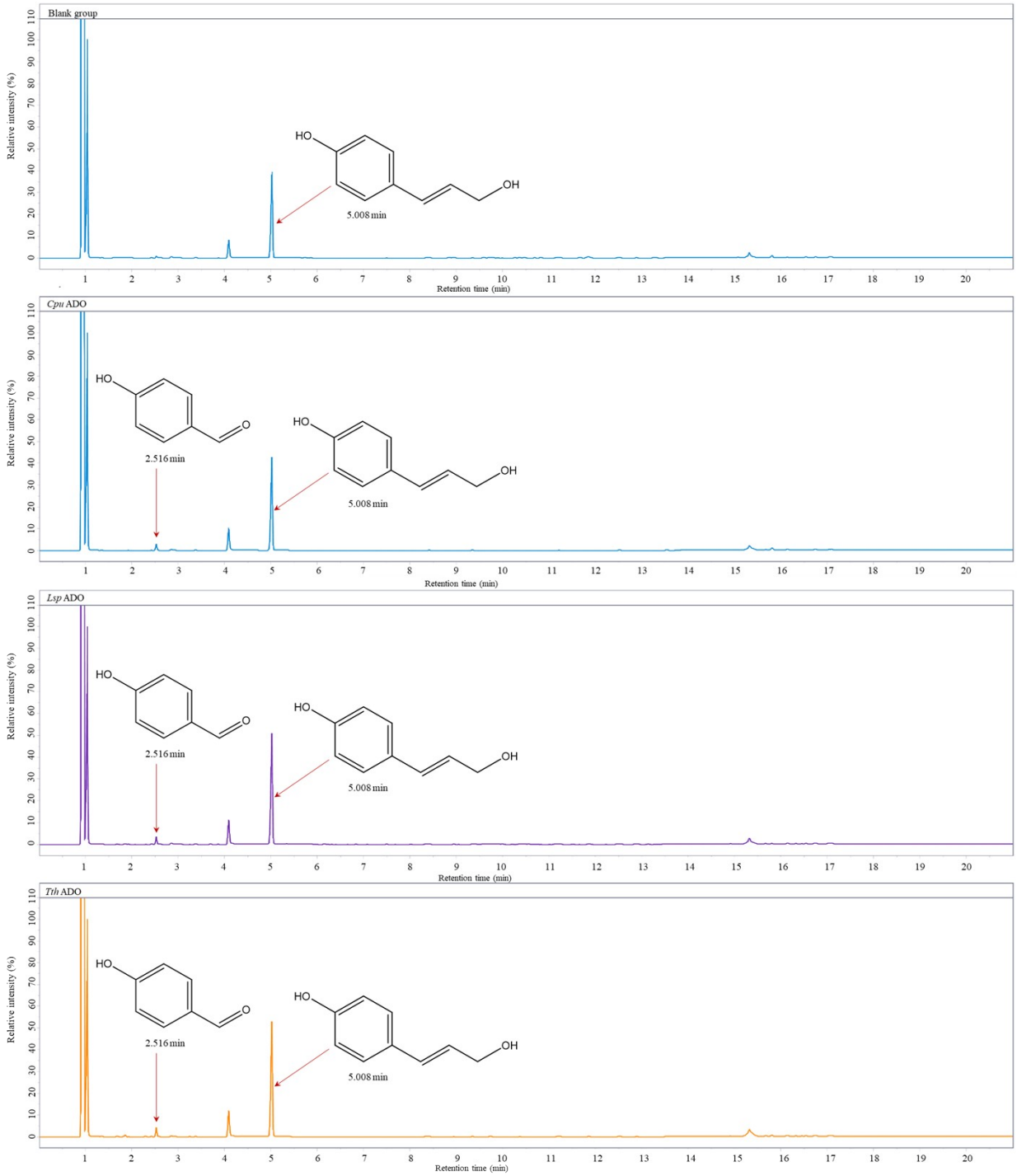

Figure S24-3. Gas chromatography results of the blank control group and different ADOs using *p*-coumaryl alcohol as substrate

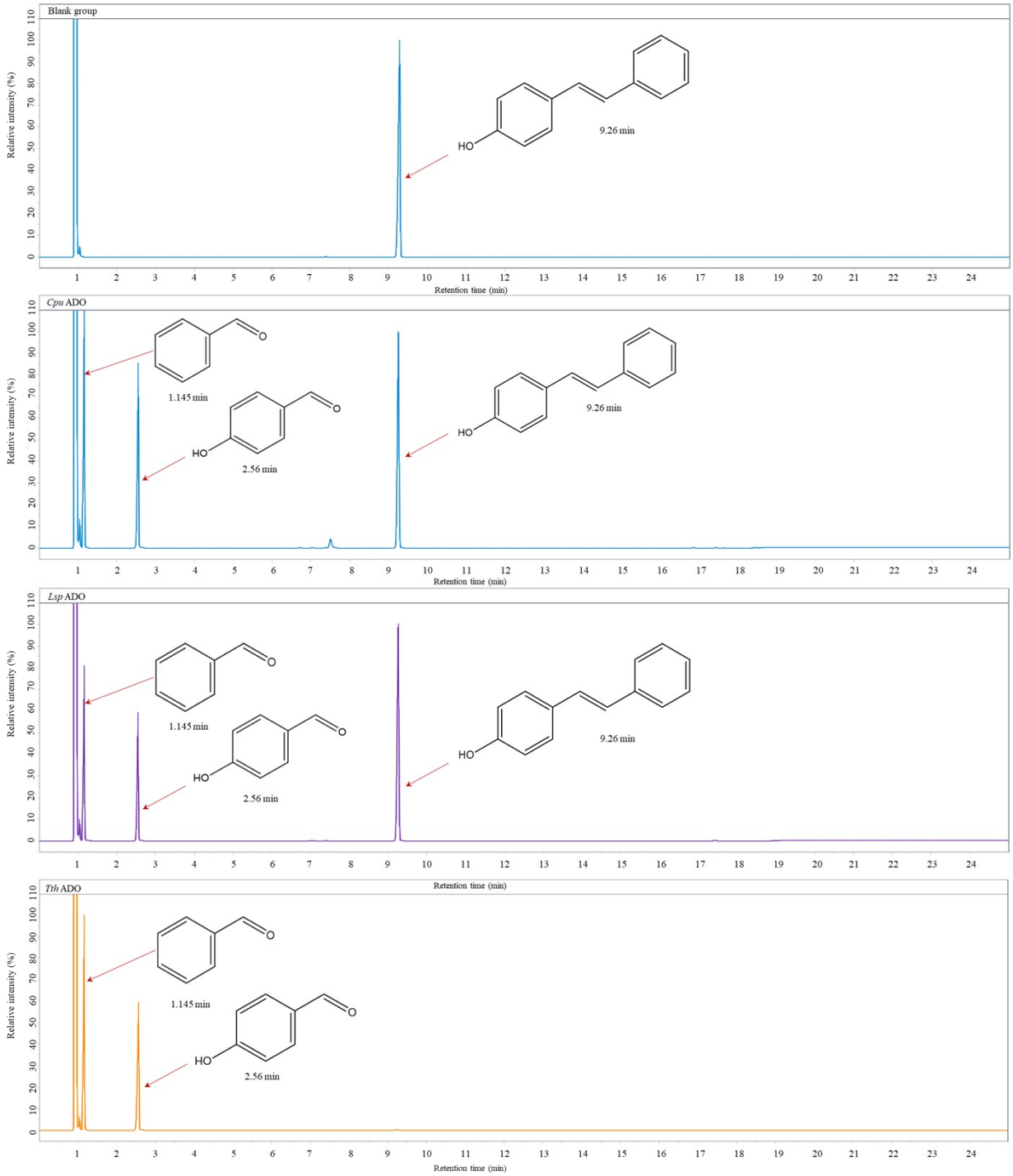

Figure S24-4. Gas chromatography results of the blank control group and different ADOs using *trans*-4-hydroxystilbene as substrate

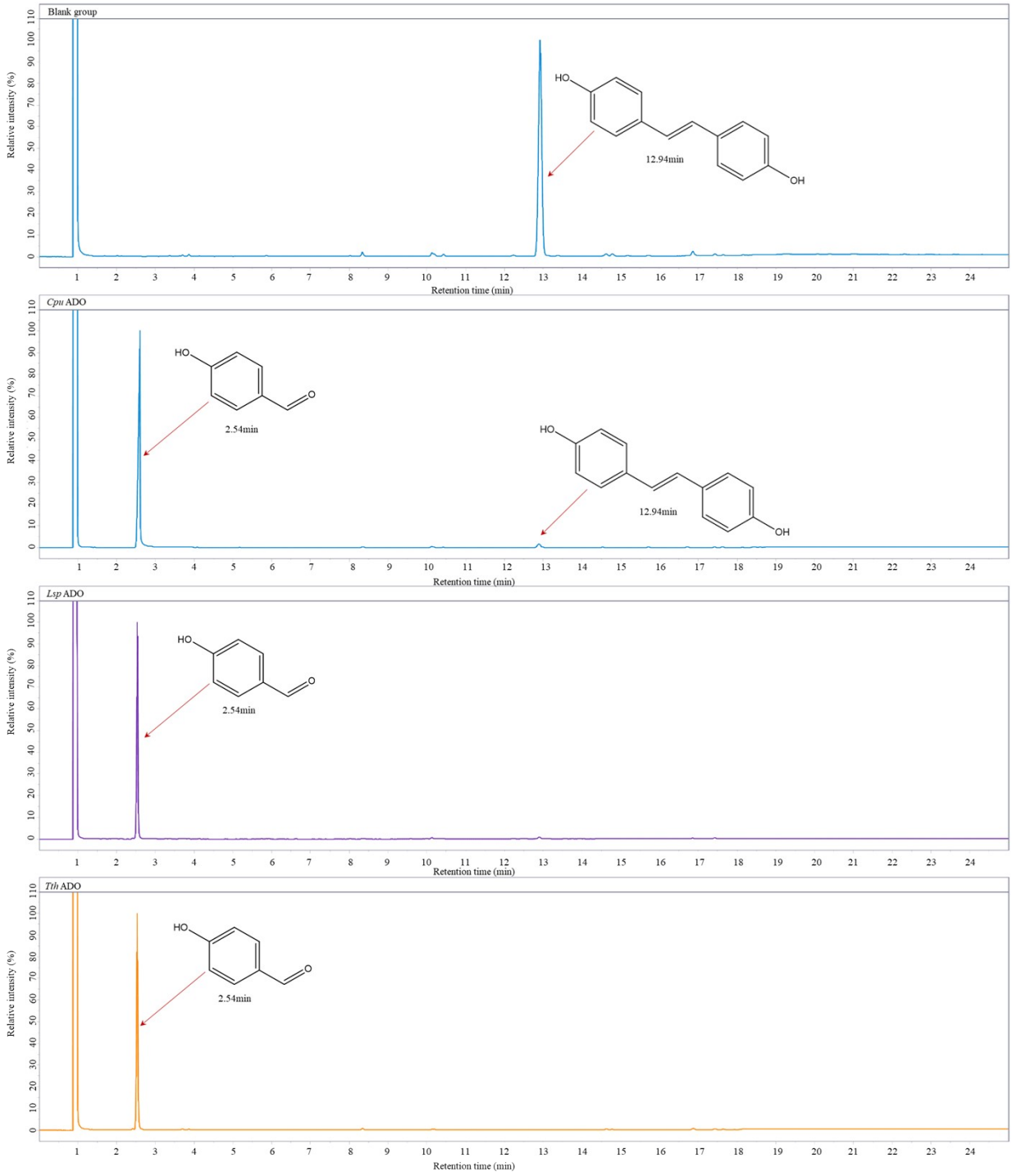

Figure S24-5. Gas chromatography results of the blank control group and different ADOs using 4,4'-dihydroxystilbene as substrate

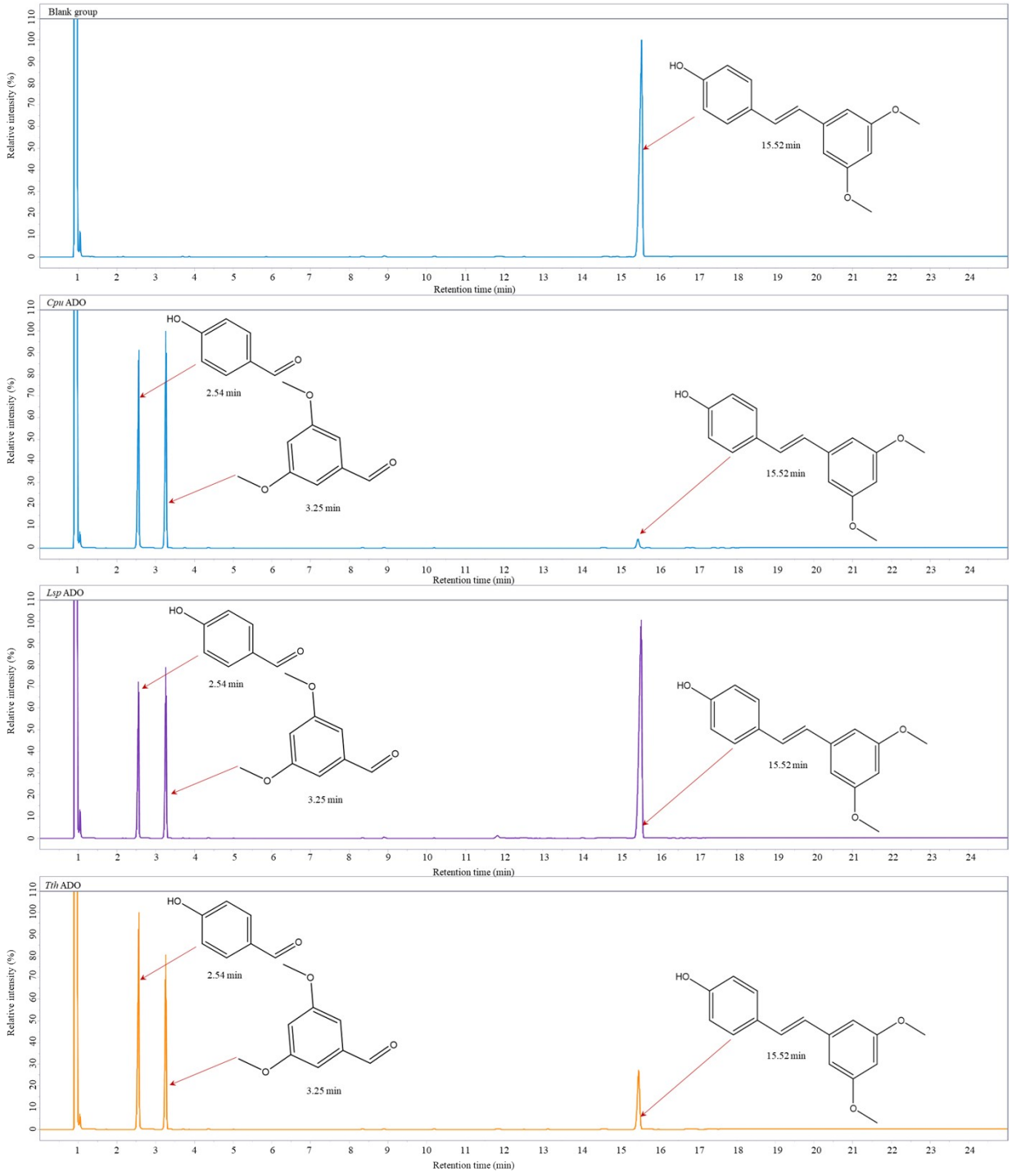

Figure S24-6. Gas chromatography results of the blank control group and different ADOs using 4-(3,5-dimethoxystyryl)phenol as substrate

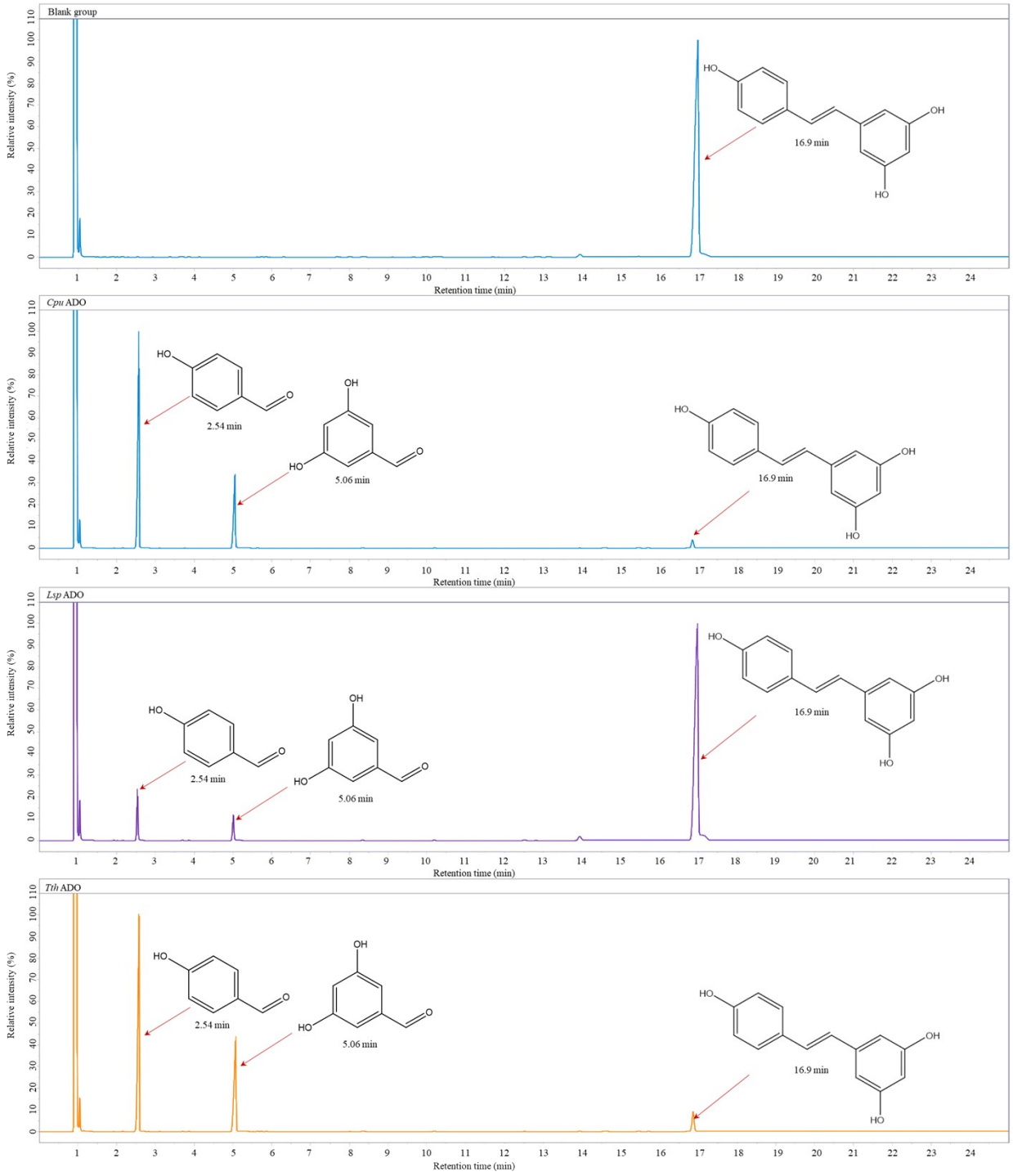

Figure S24-7. Gas chromatography results of the blank control group and different ADOs using resveratrol as substrate

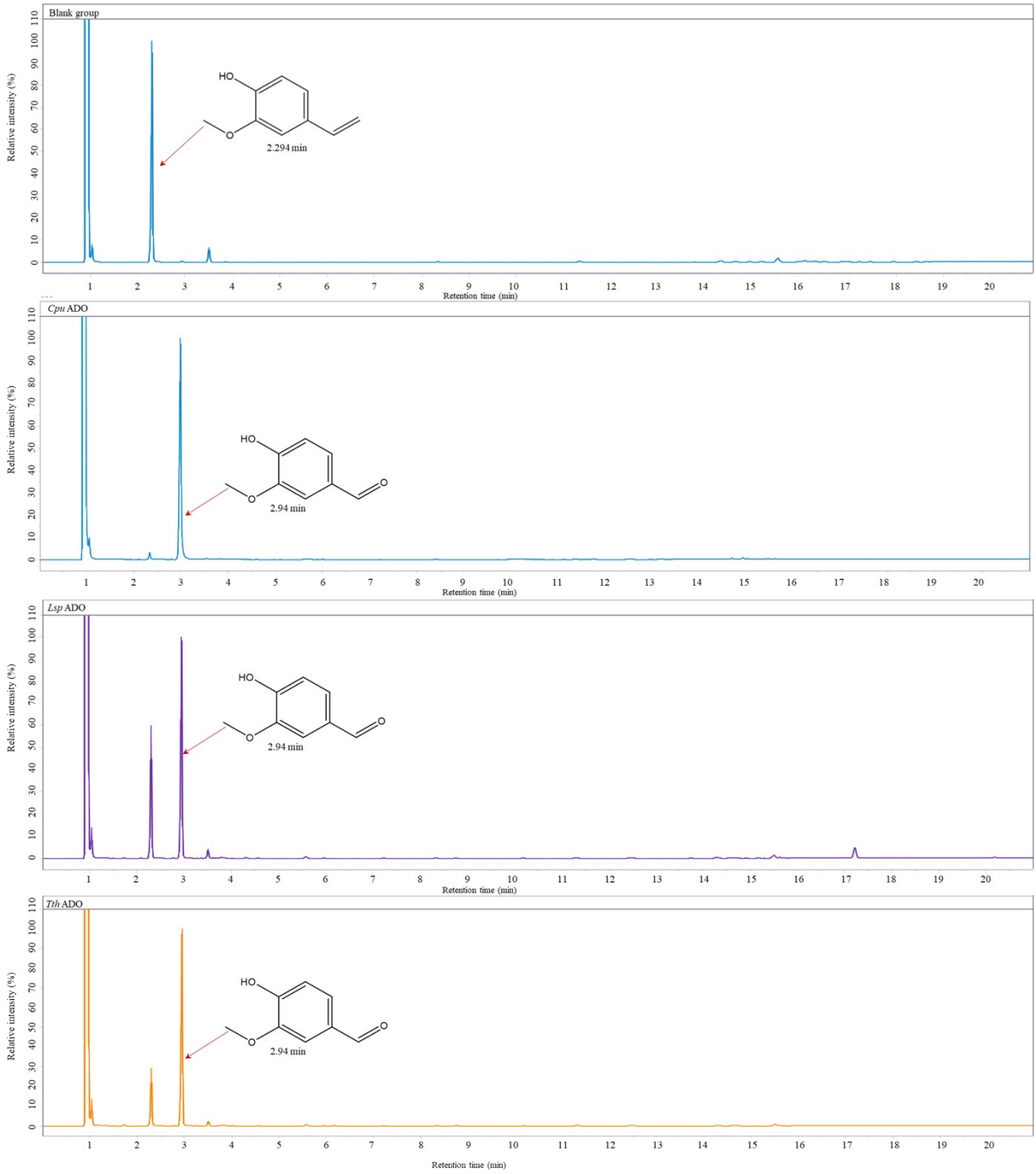

283

284 **Figure S24**-8. Gas chromatography results of the blank control group and different ADOs using 4-vinylguaiacol as
285 substrate

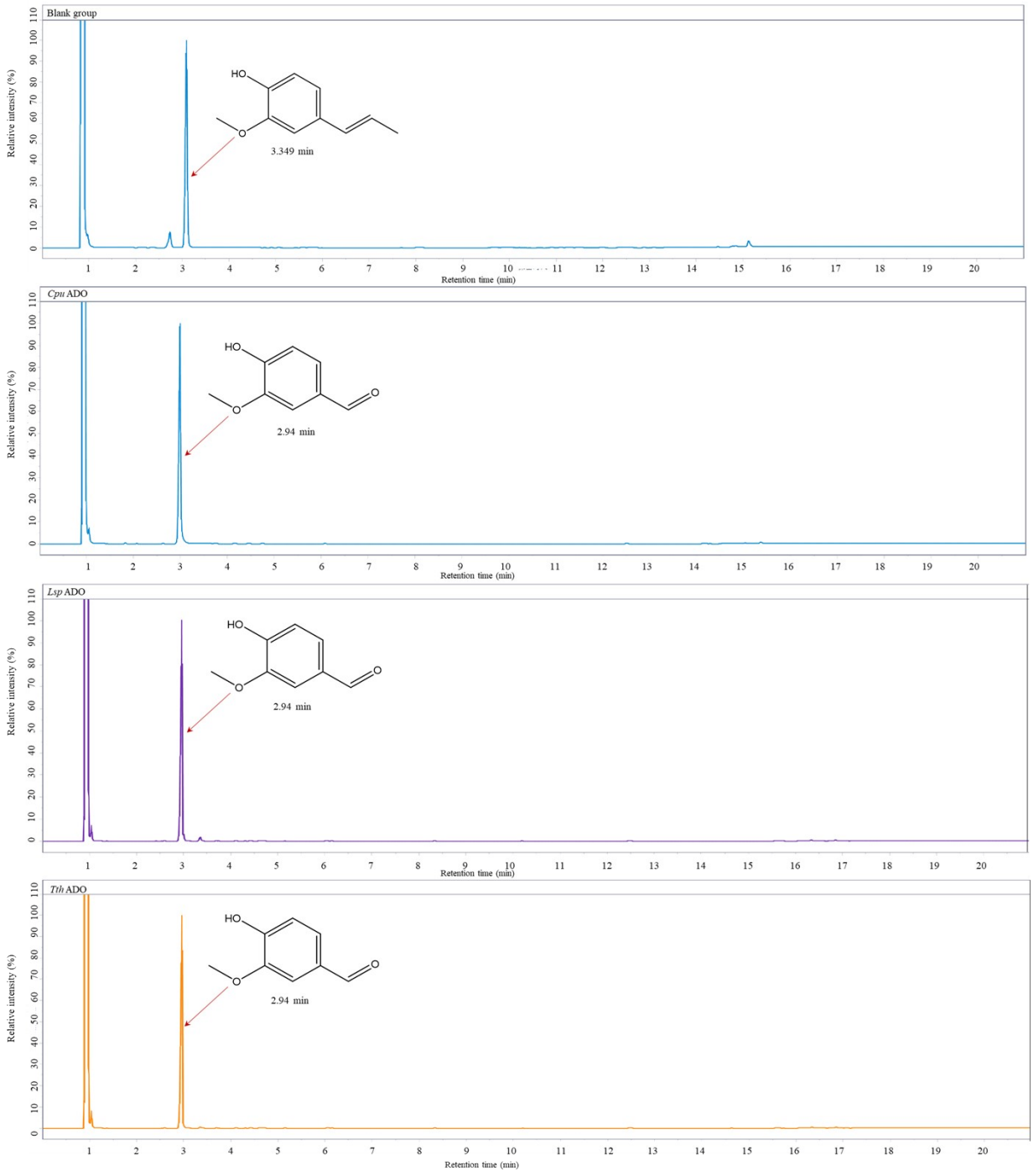

Figure S24-9. Gas chromatography results of the blank control group and different ADOs using isoeugenol as substrate

Figure S24-10. Gas chromatography results of the blank control group and different ADOs using coniferol as substrate

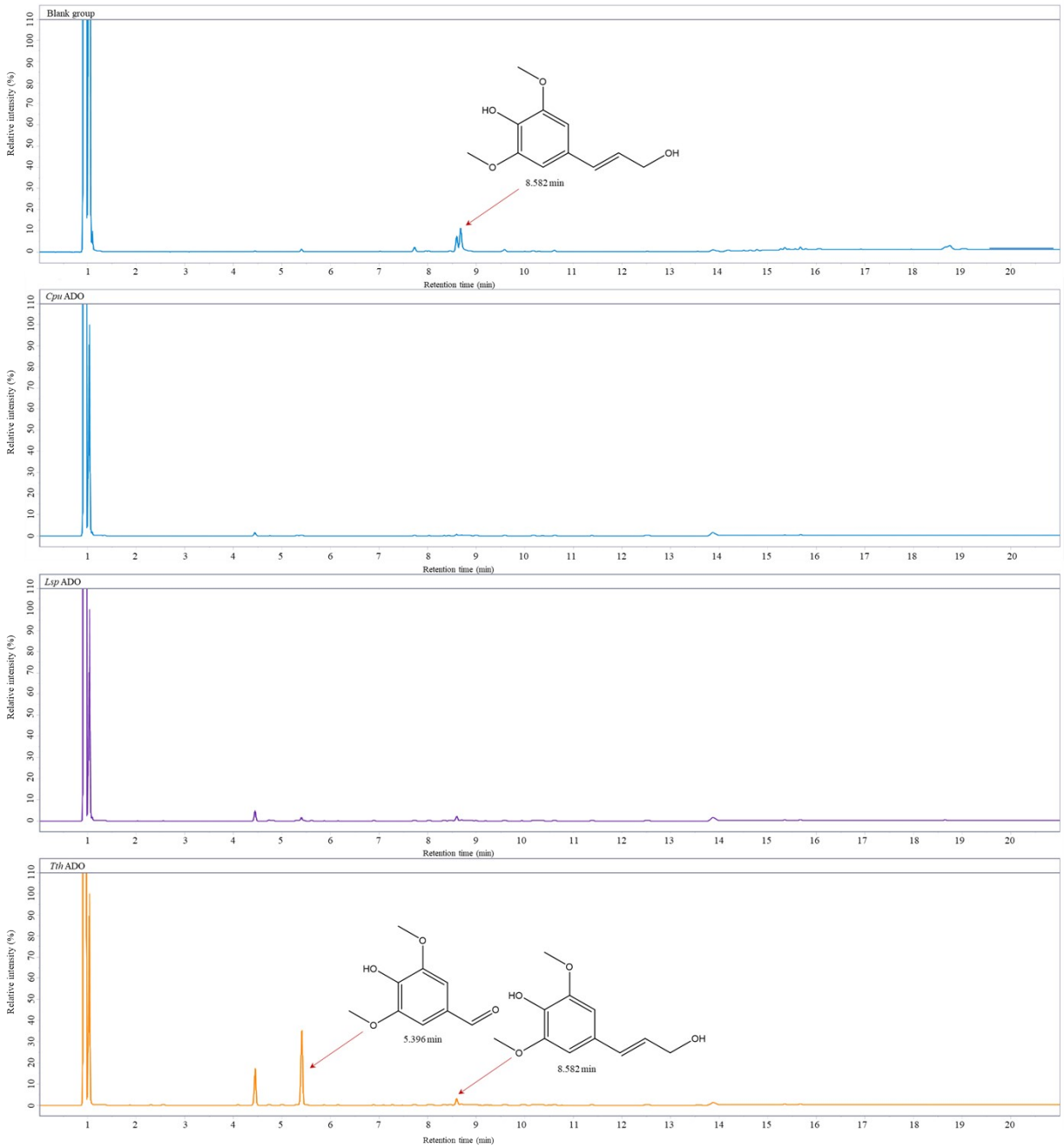

Figure S24-11. Gas chromatography results of the blank control group and different ADOs using sinapyl alcohol as substrate

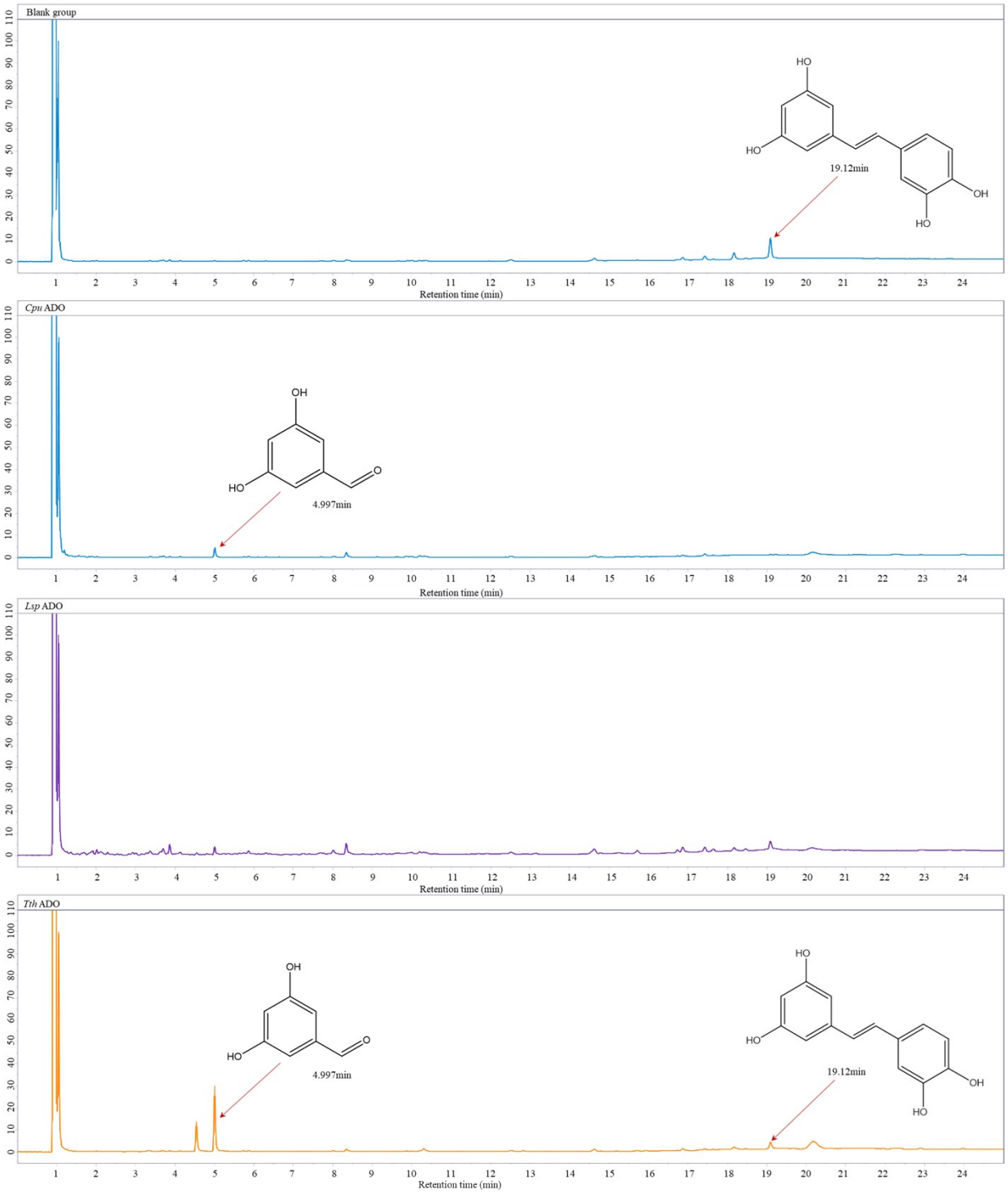

304

305 **Figure S24**-12. Gas chromatography results of the blank control group and different ADOs using piceatannol as

306 substrate

307

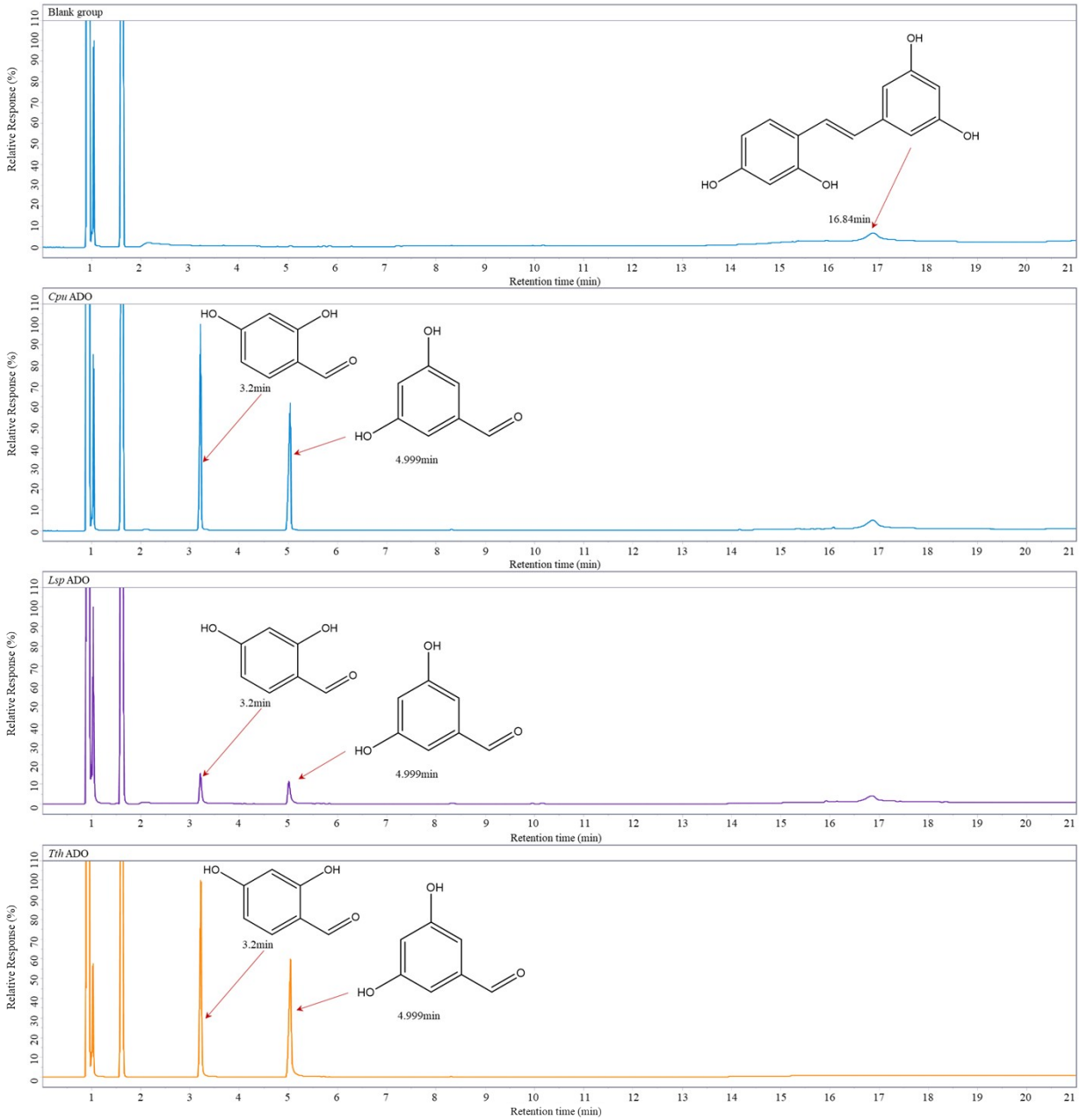

Figure S24-13. Gas chromatography results of the blank control group and different ADOs using Oxyresveratrol as substrate

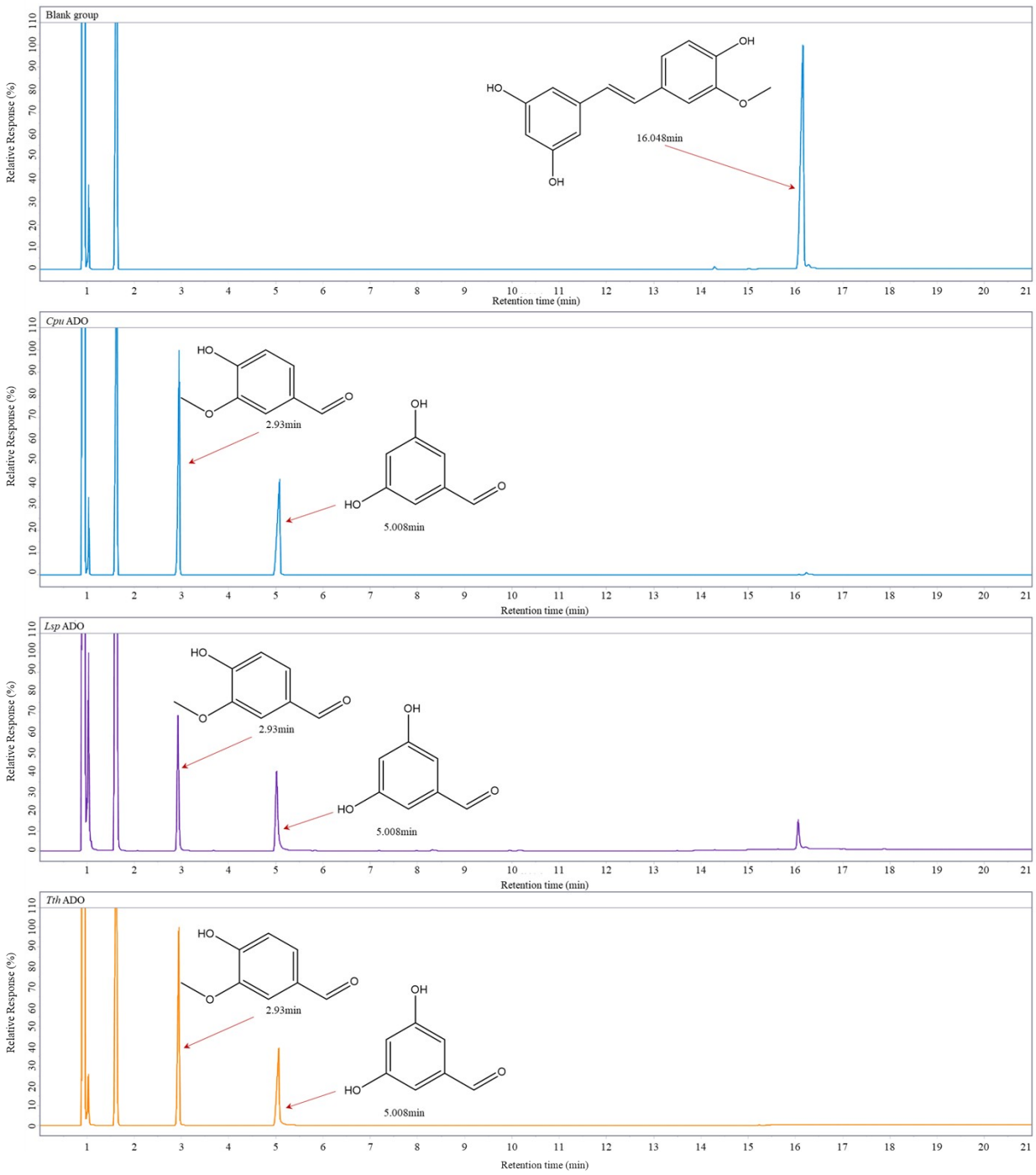

312

313 Figure **S24**-14. Gas chromatography results of the blank control group and different ADOs using Isorhapontigenin as

314 substrate

315

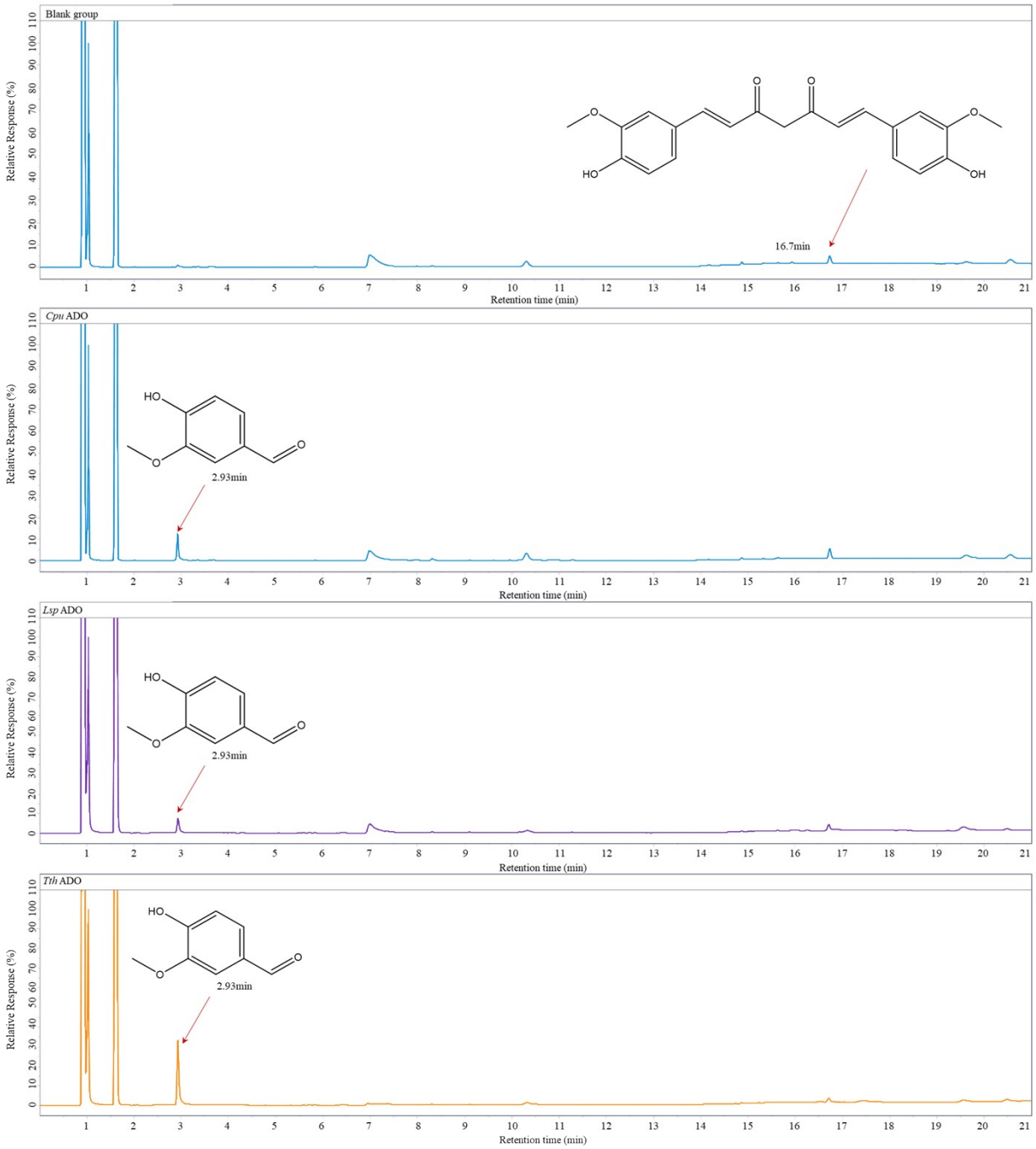

Figure **S24**-15. Gas chromatography results of the blank control group and different ADOs using Curcumin as substrate

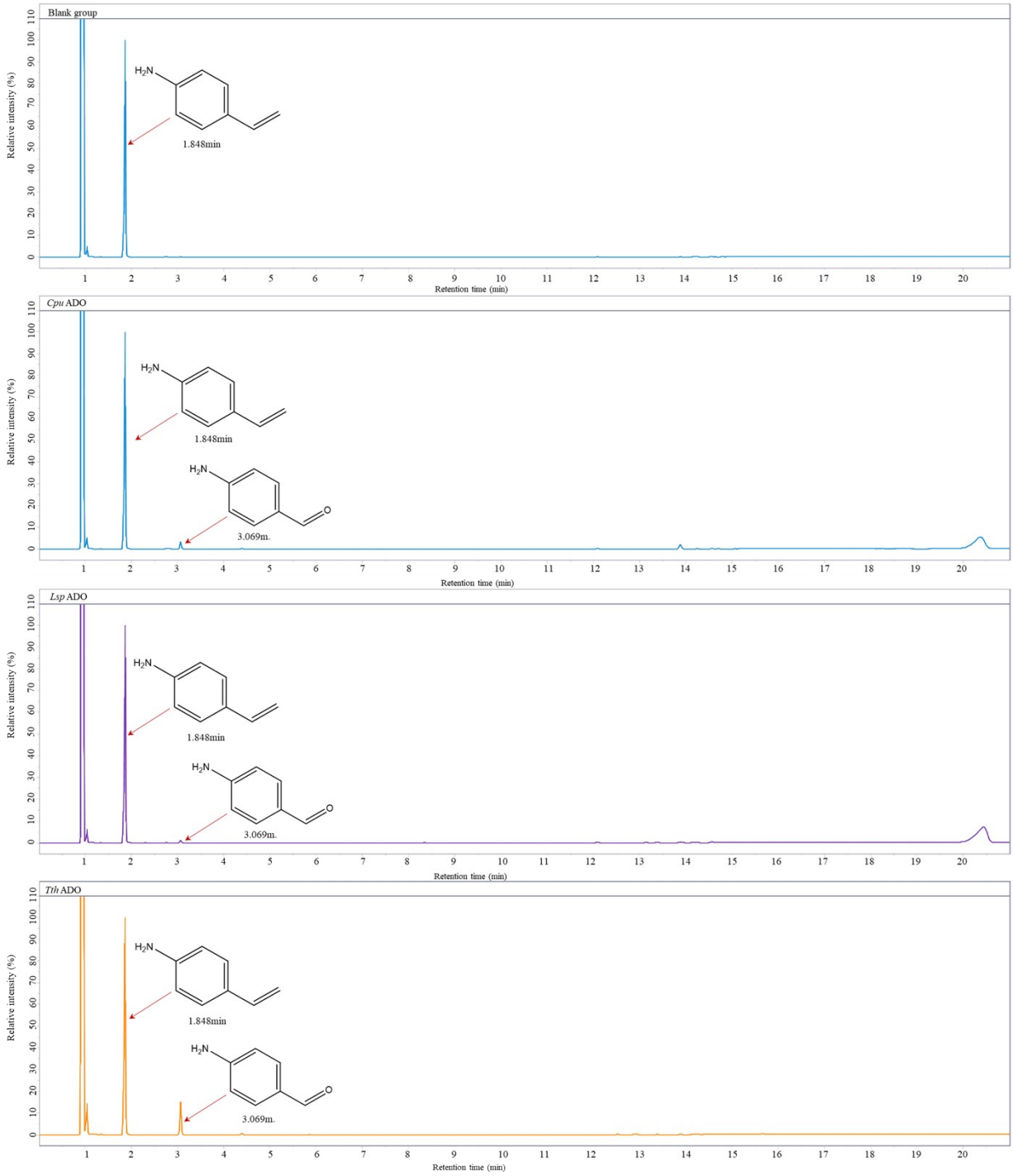

Figure S24-16. Gas chromatography results of the blank control group and different ADOs using 4-vinylaniline as substrate

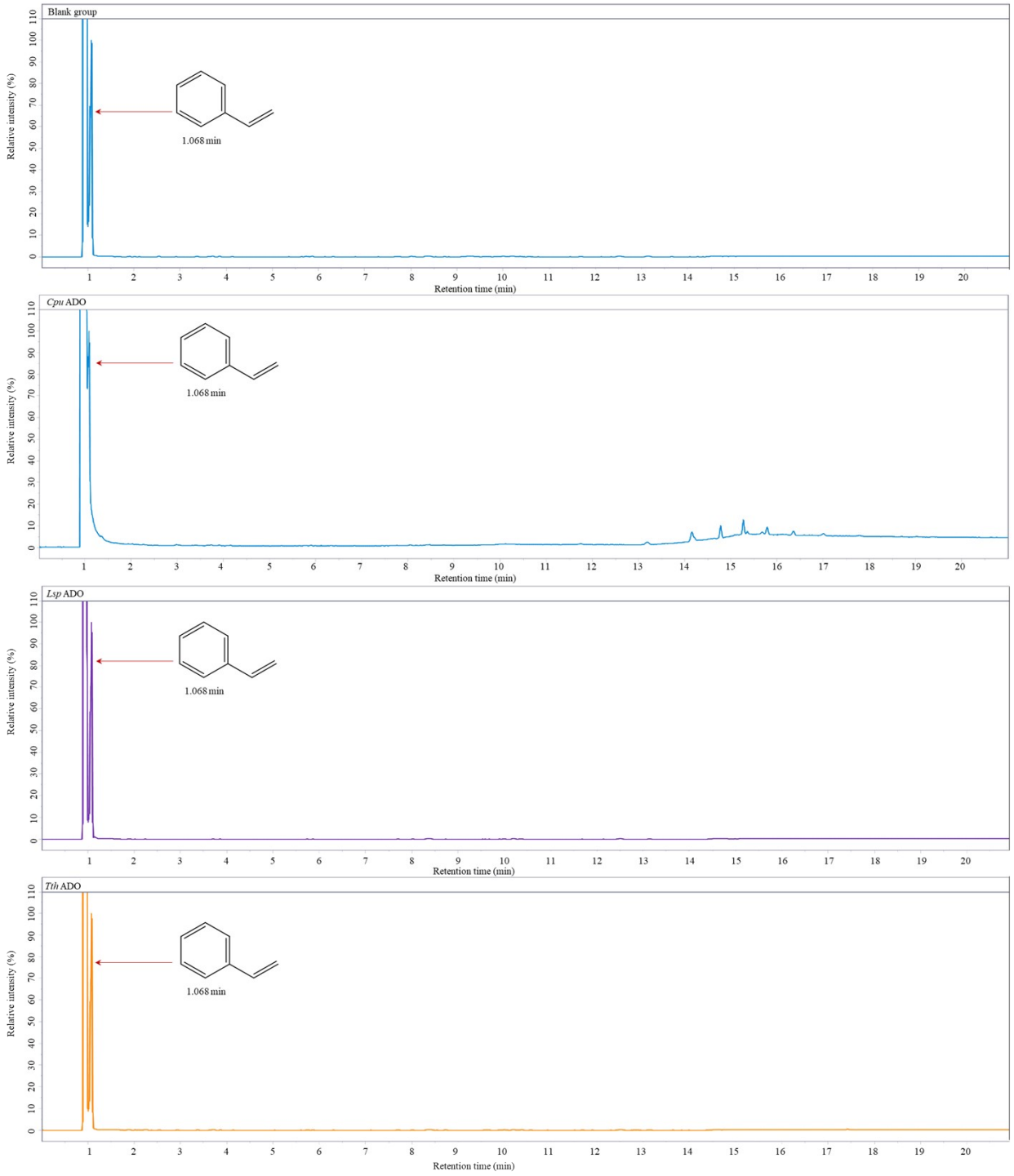

Figure S24-17. Gas chromatography results of the blank control group and different ADOs using styrene as substrate

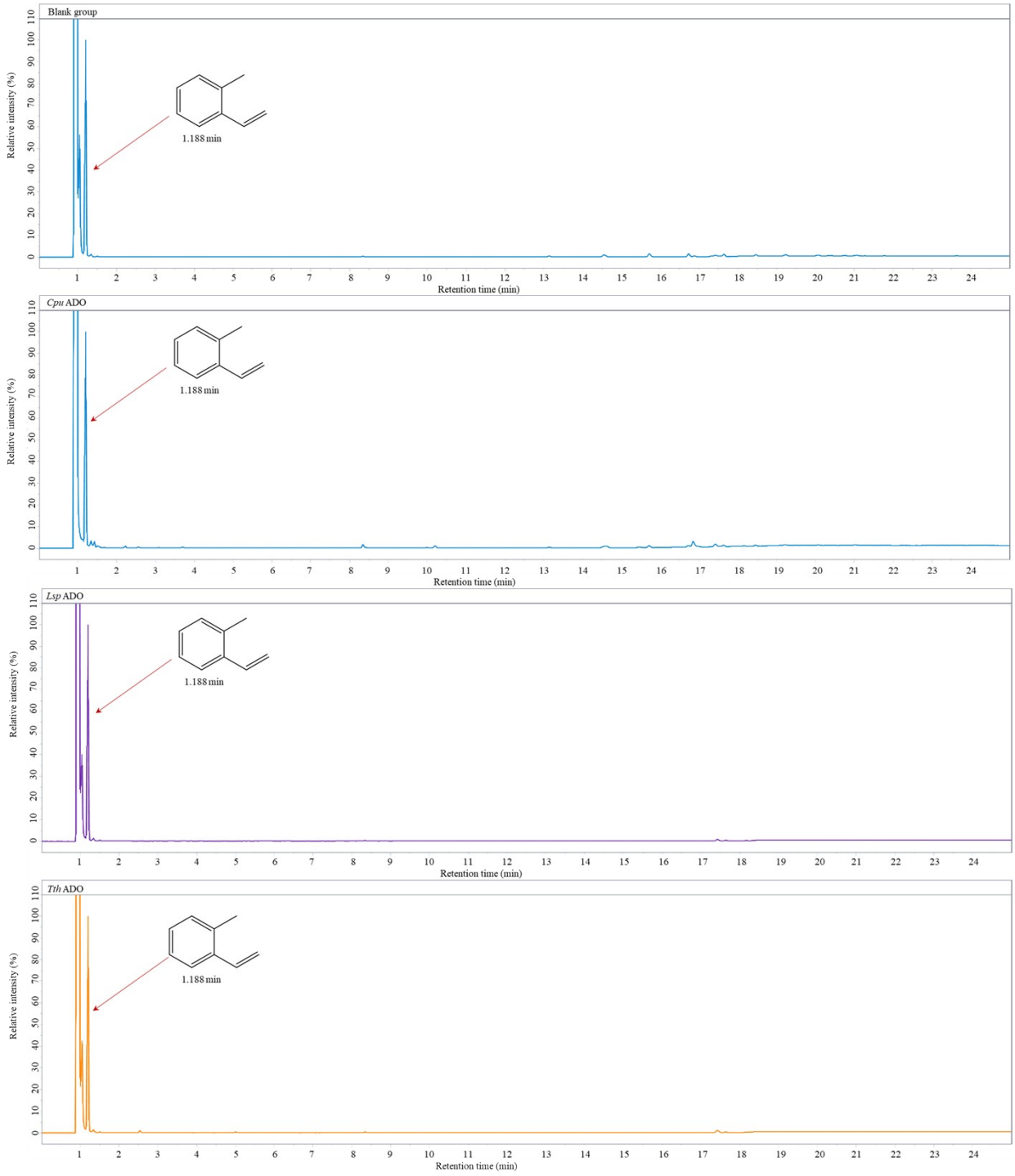

Figure S24-18. Gas chromatography results of the blank control group and different ADOs using 2-methylstyrene as substrate

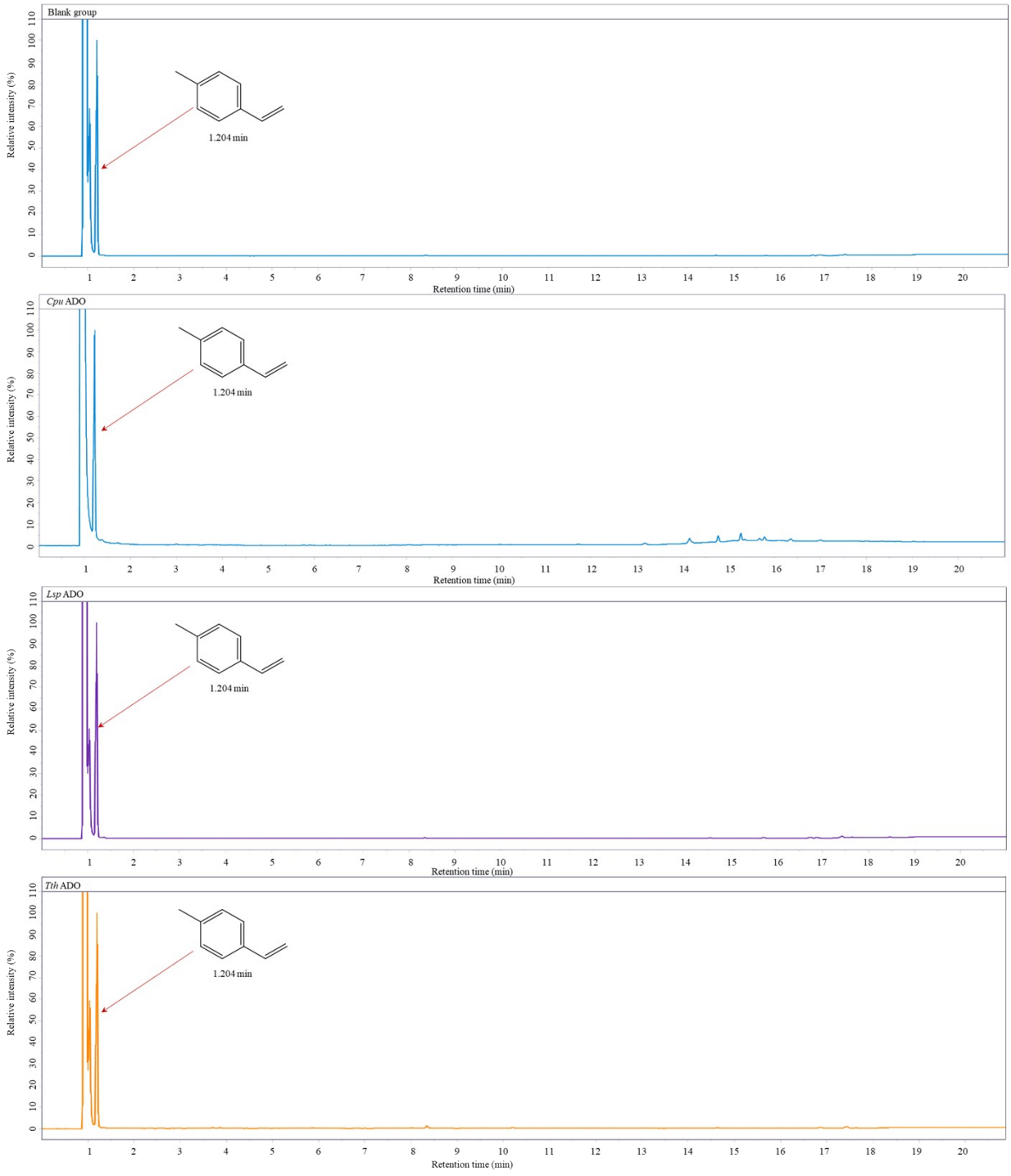

Figure S24-19. Gas chromatography results of the blank control group and different ADOs using 4-methylstyrene as substrate

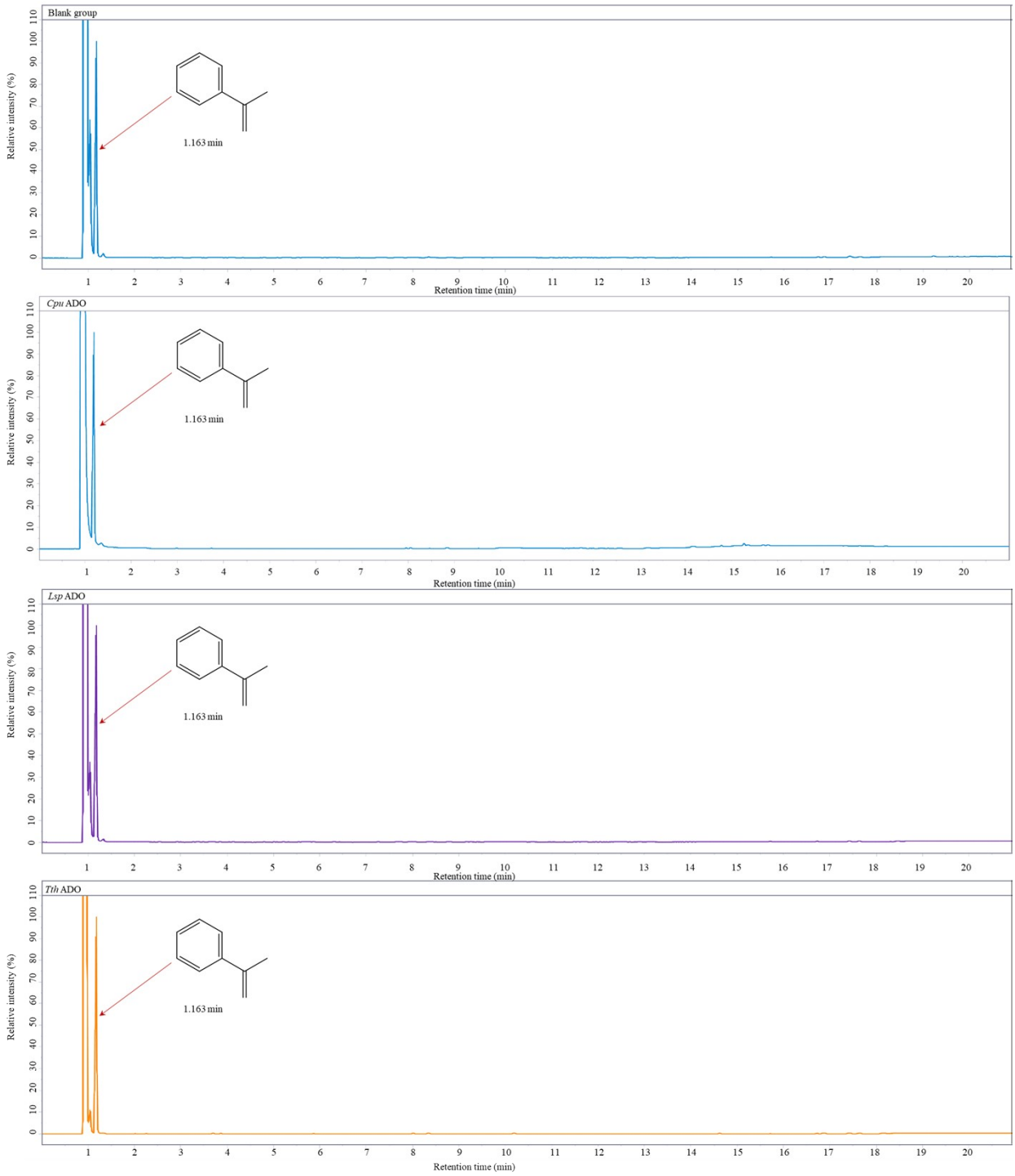

Figure S24-20. Gas chromatography results of the blank control group and different ADOs using 2-phenylpropene as substrate

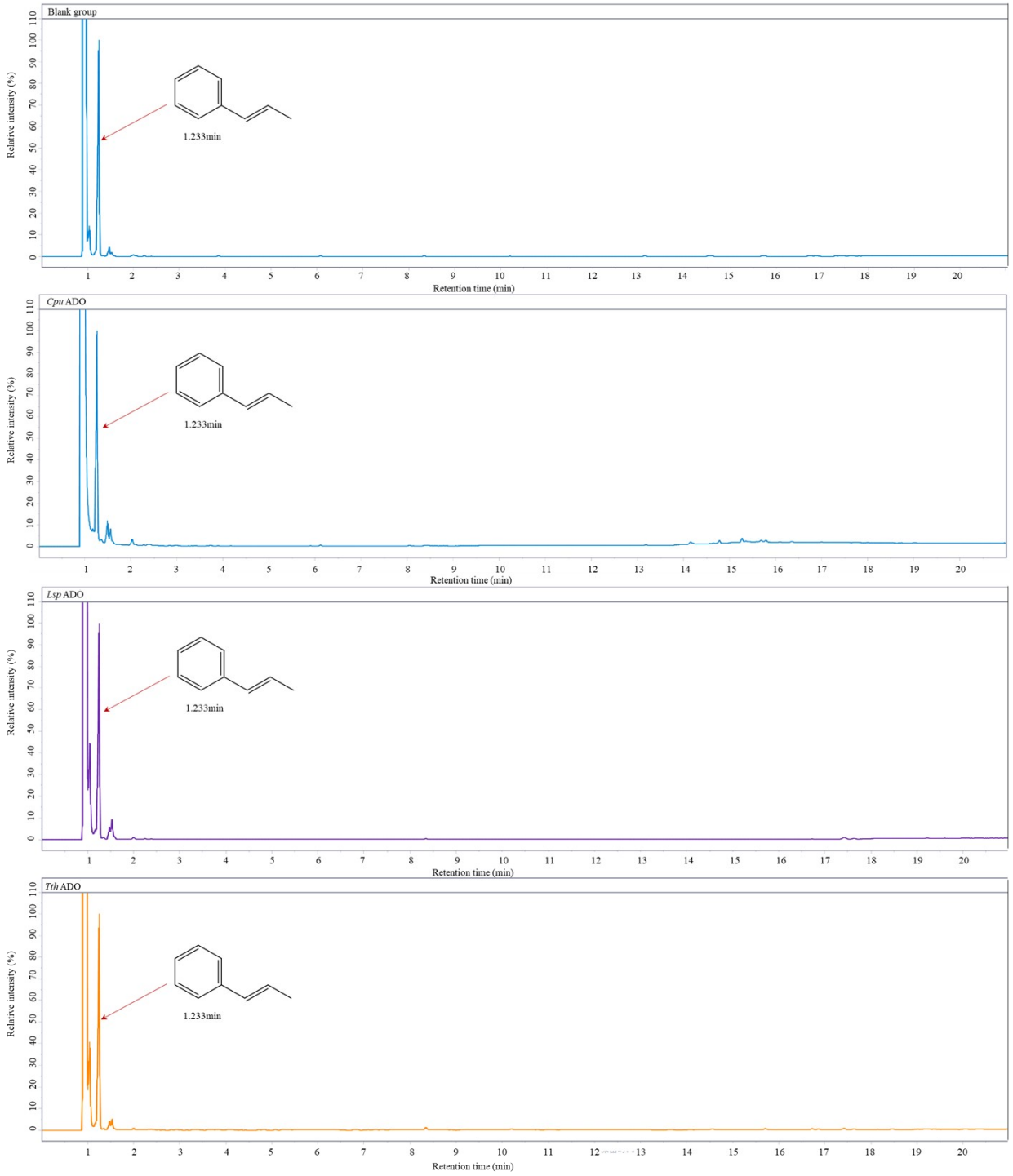

346

Figure S24-21. Gas chromatography results of the blank control group and different ADOs using 1-phenylpropene as substrate

347

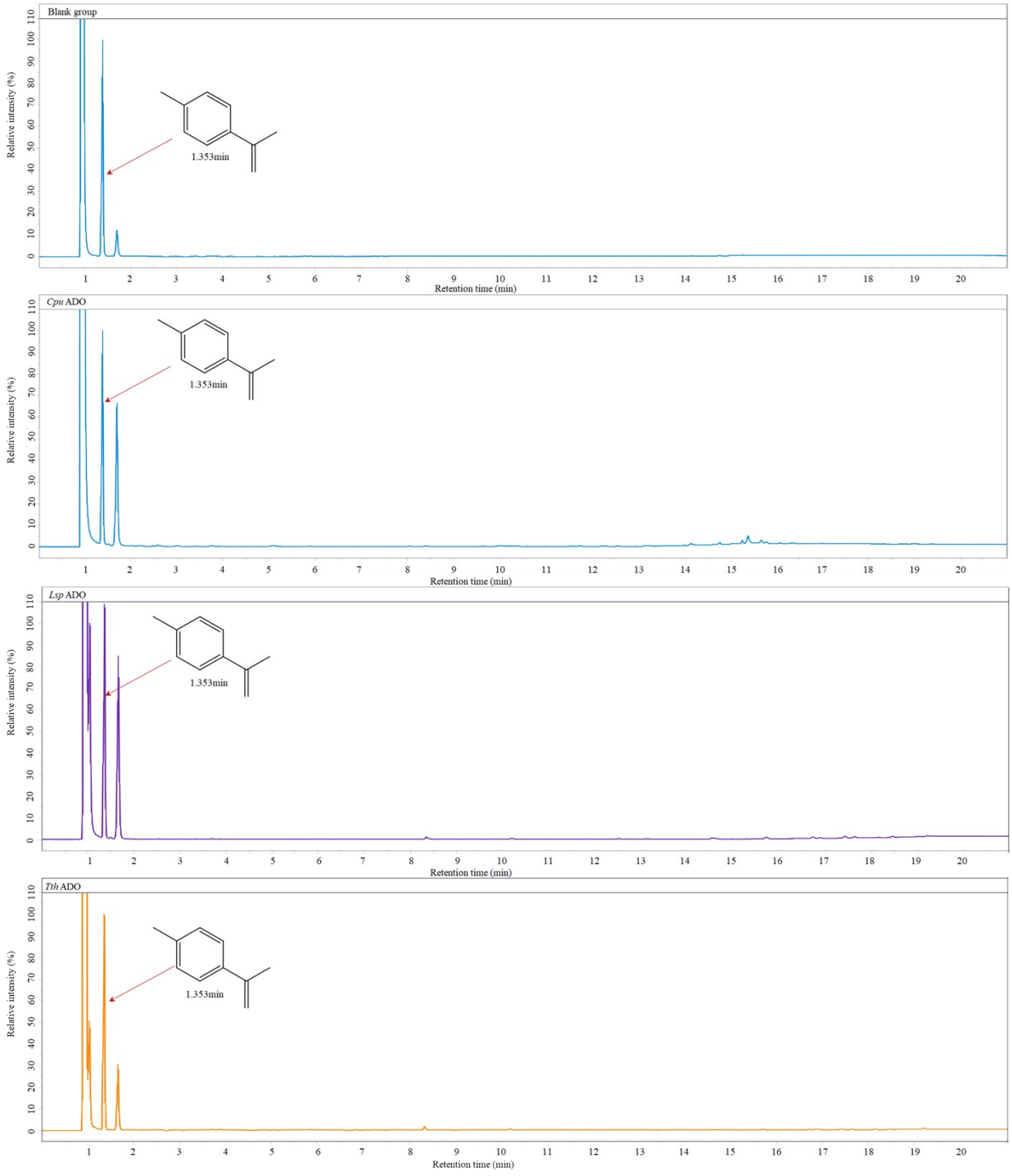

Figure S24-22. Gas chromatography results of the blank control group and different ADOs using 4-isopropenyltoluene as substrate

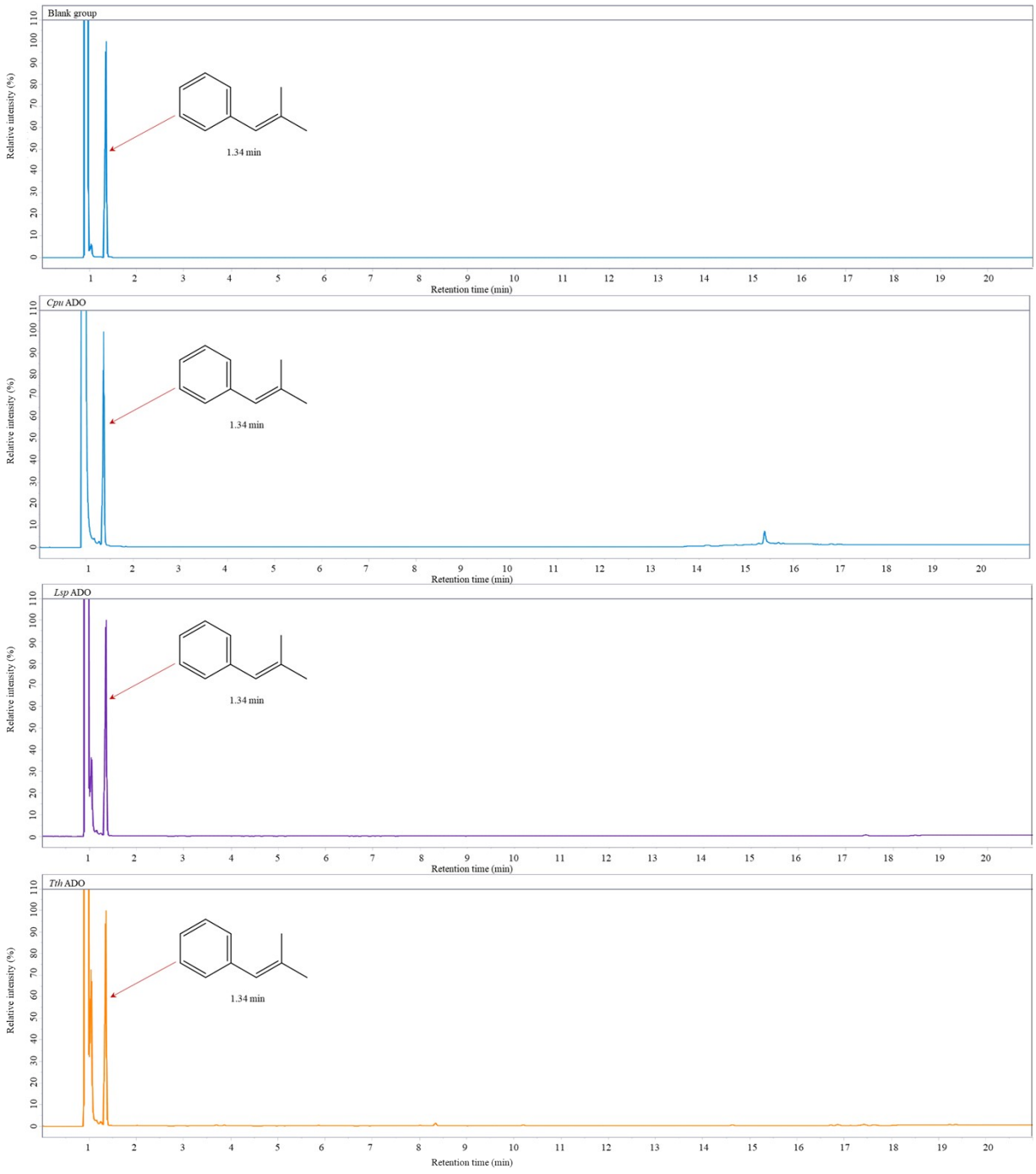

352

Figure S24-23. Gas chromatography results of the blank control group and different ADOs using 2-methyl-1-phenylpropene as substrate

353

354

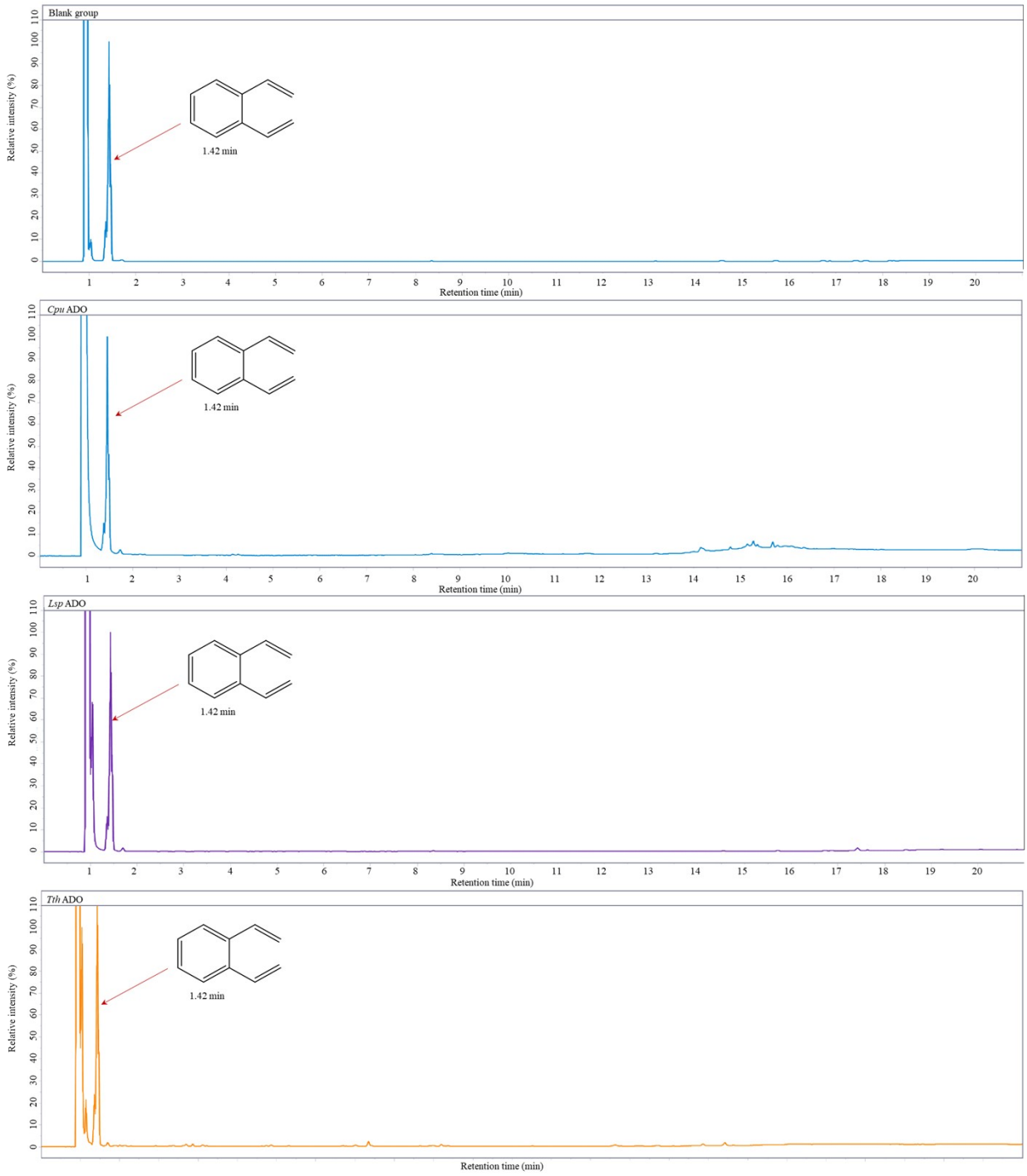

355

Figure S24-24. Gas chromatography results of the blank control group and different ADOs using 1,2-divinylbenzene as substrate

356

357

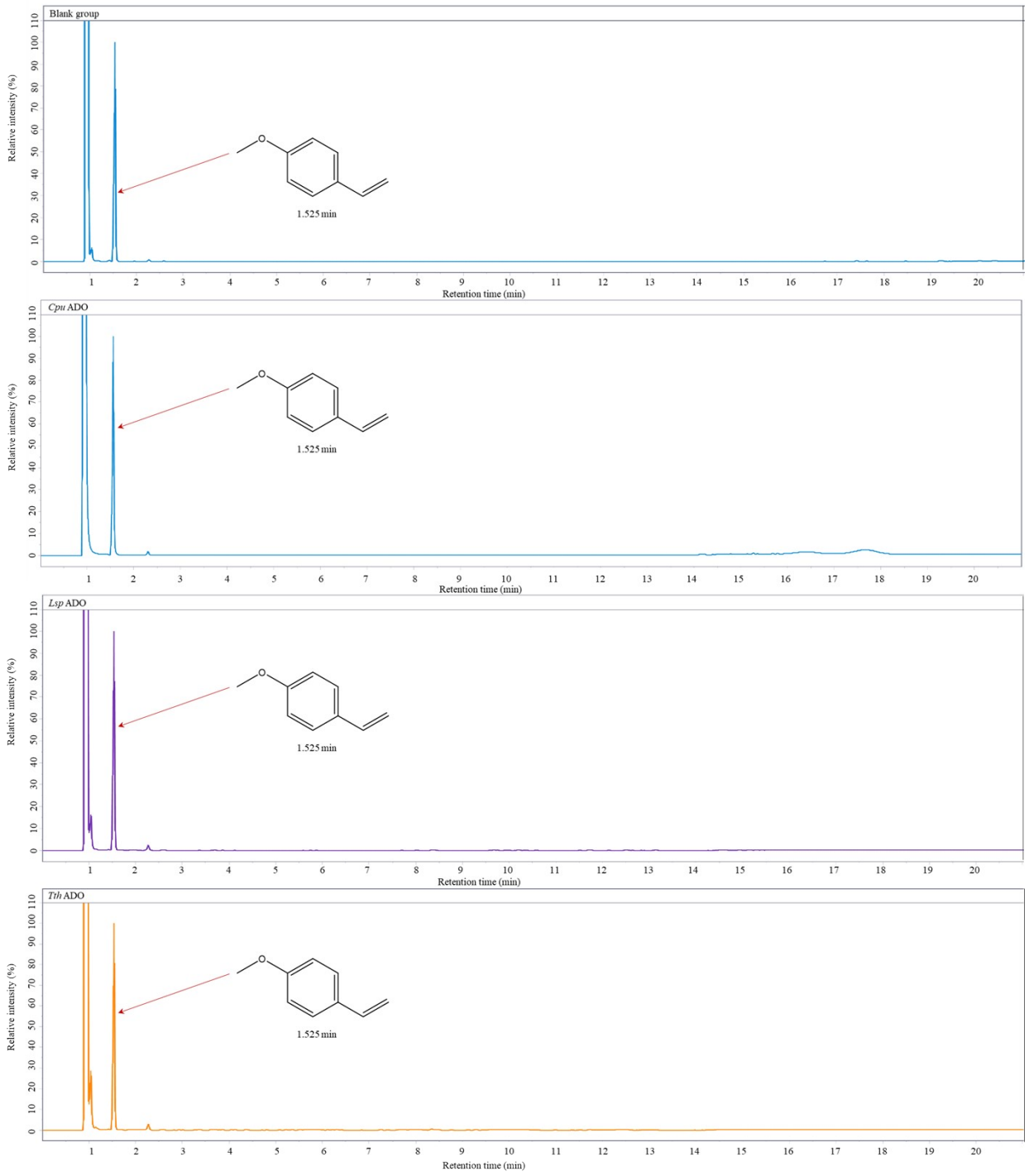

Figure S24-25. Gas chromatography results of the blank control group and different ADOs using 4-methoxystyrene as substrate

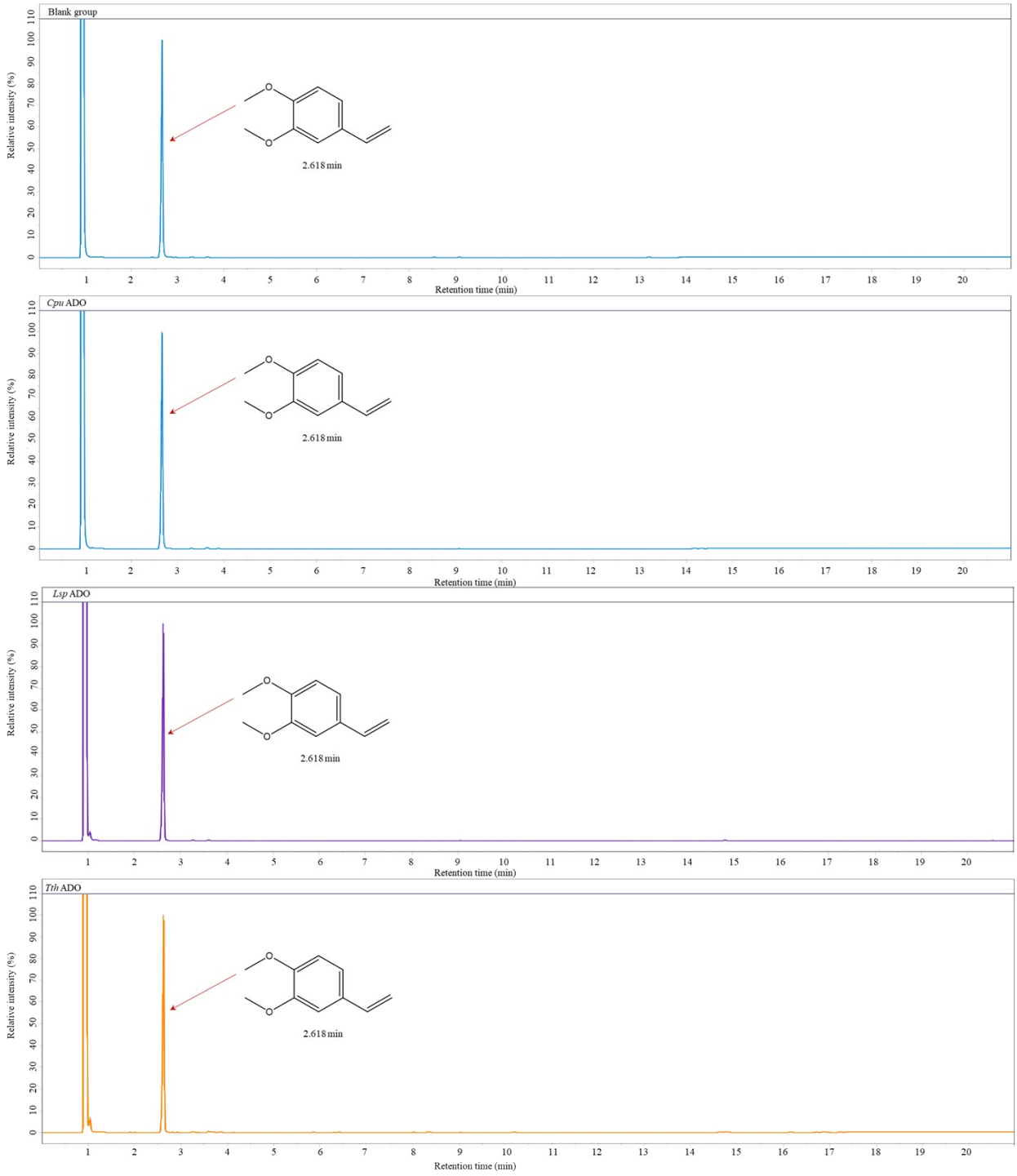

Figure S24-26. Gas chromatography results of the blank control group and different ADOs using 3,4-dimethoxystyrene as substrate

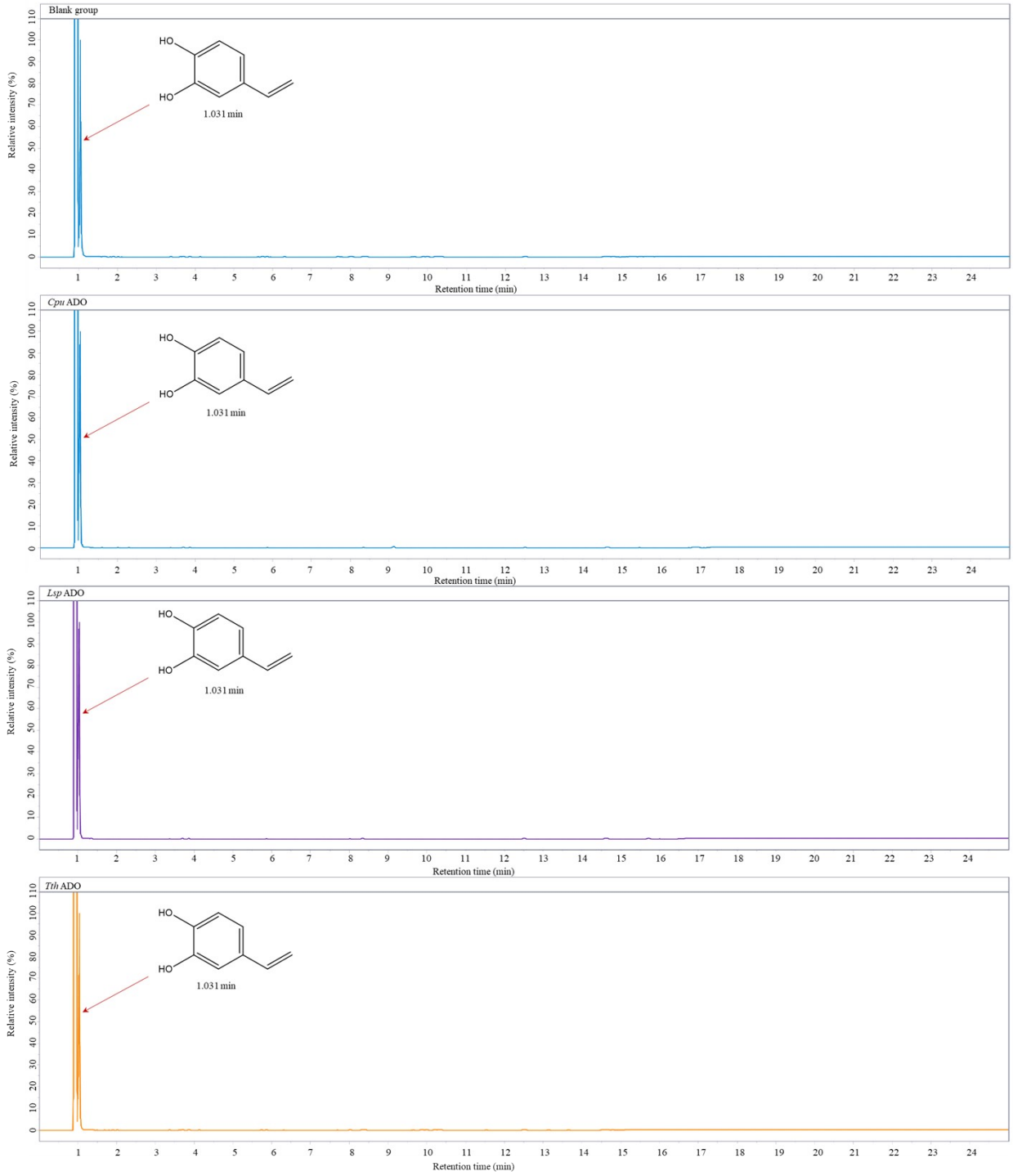

Figure S24-27. Gas chromatography results of the blank control group and different ADOs using 3,4-dihydroxystyrene as substrate

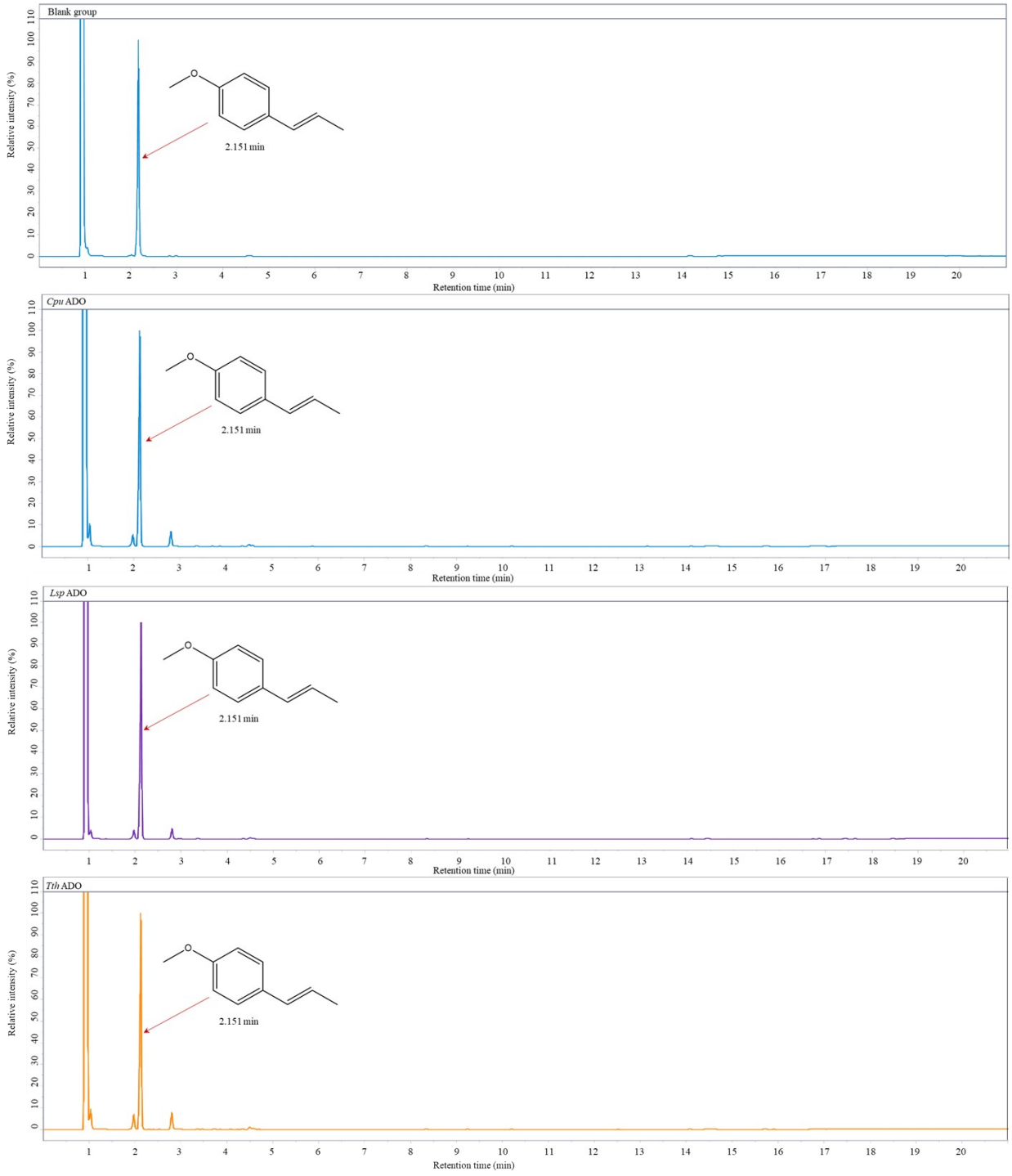

Figure S24-28. Gas chromatography results of the blank control group and different ADOs using trans-anethole as substrate

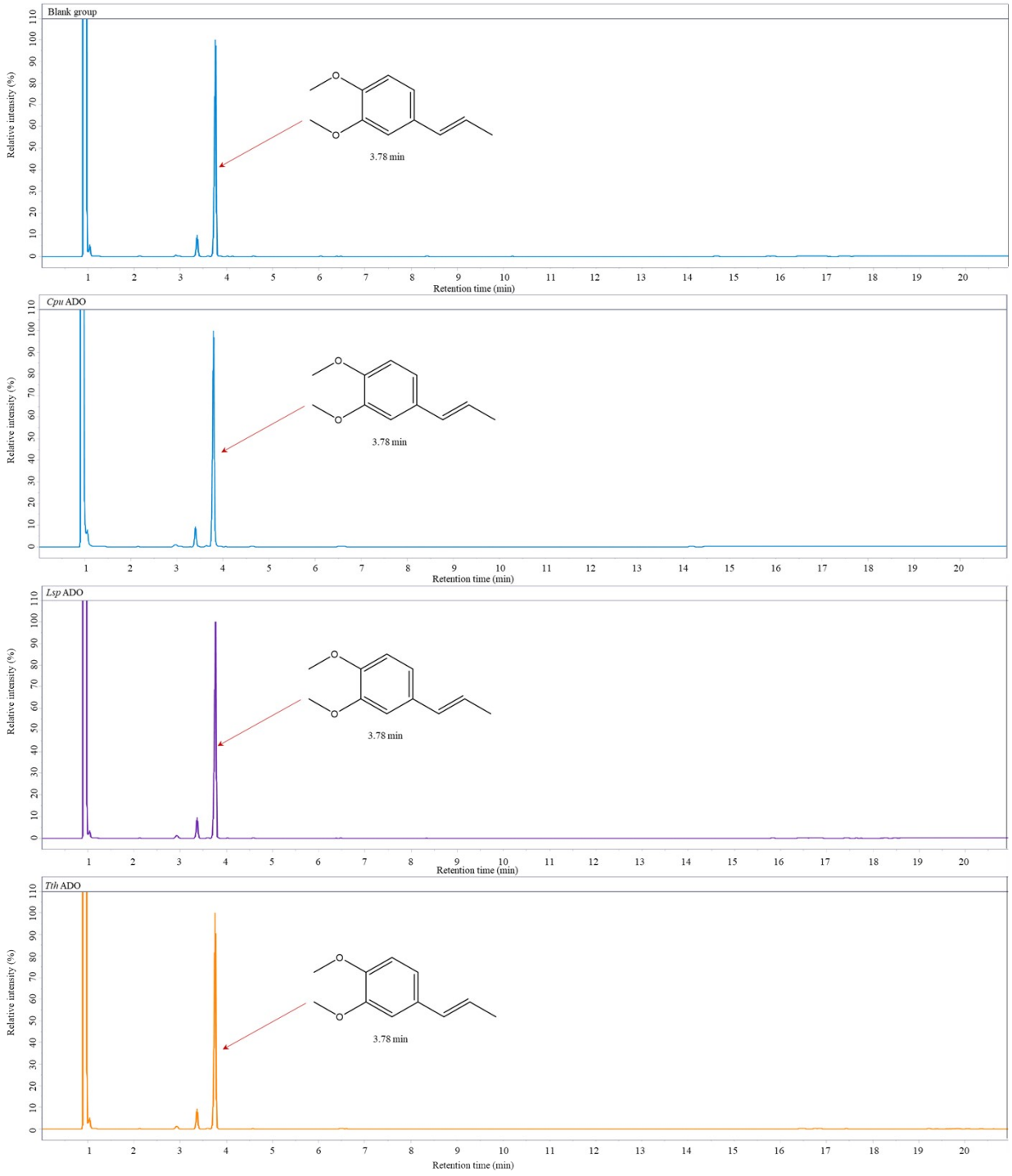

Figure S24-29. Gas chromatography results of the blank control group and different ADOs using methylisoeugenol as substrate

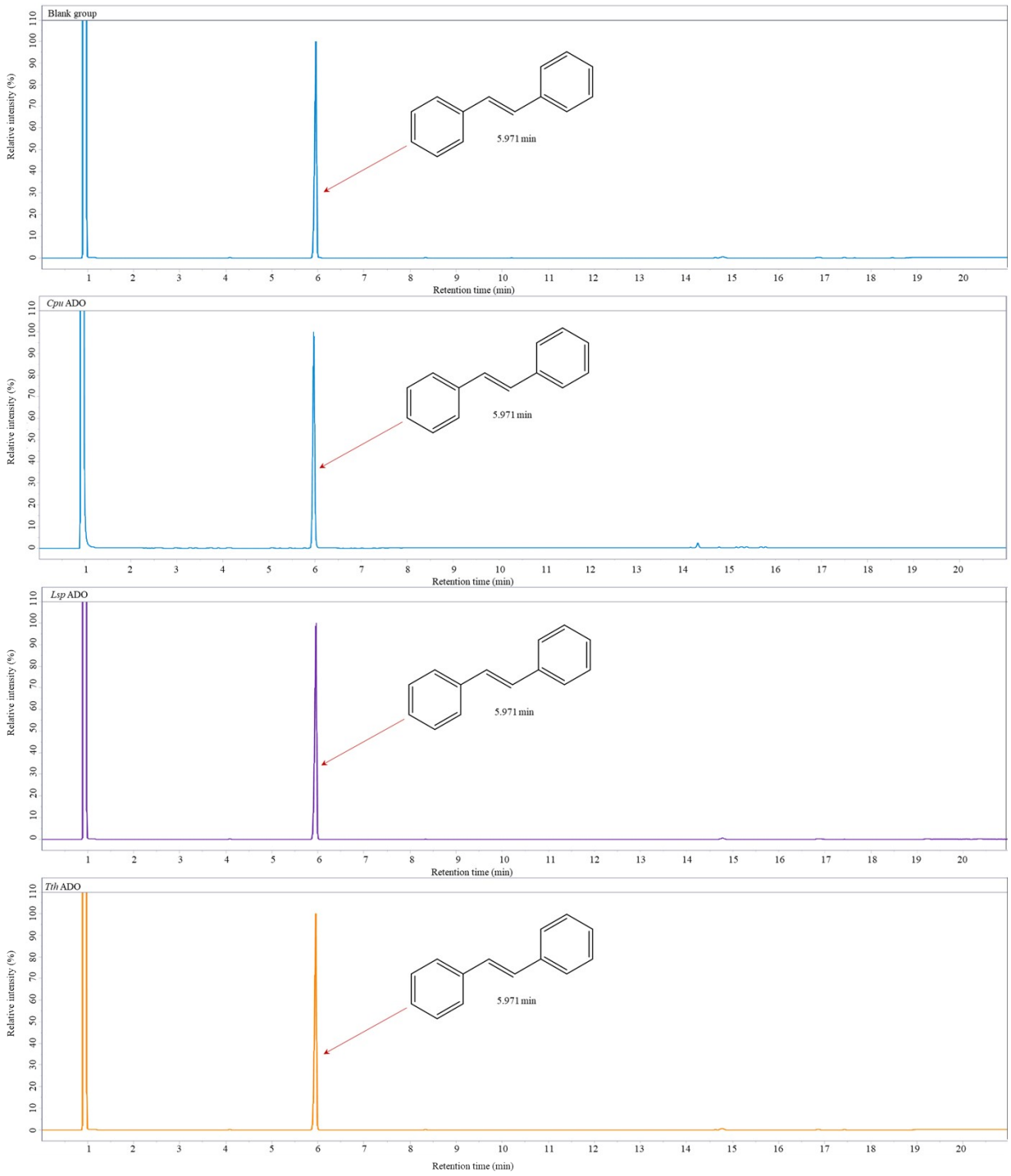

Figure S24-30. Gas chromatography results of the blank control group and different ADOs using trans-stilbene as substrate

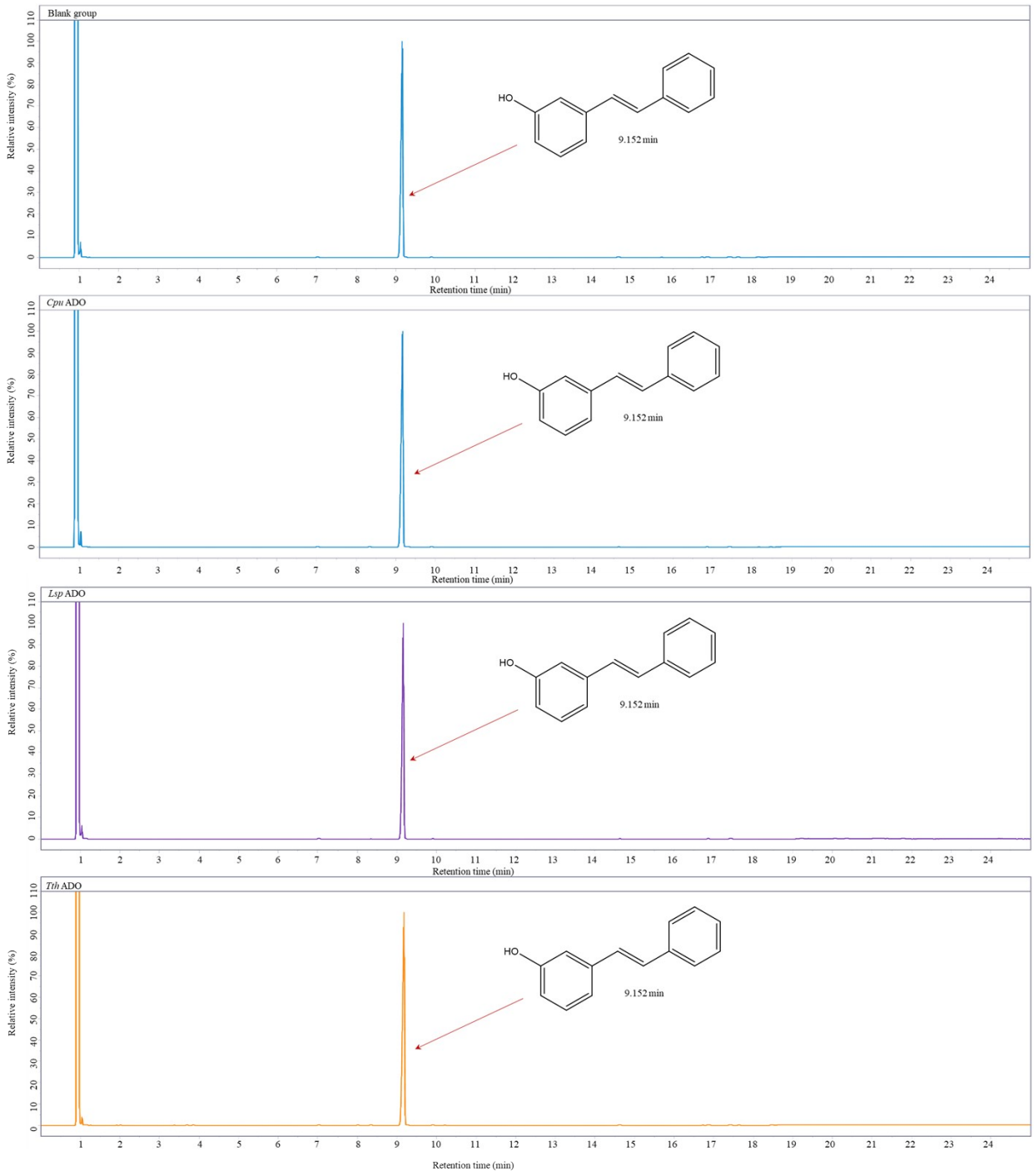

Figure S24-31. Gas chromatography results of the blank control group and different ADOs using 3-[(E)-2-phenylethenyl]phenol as substrate

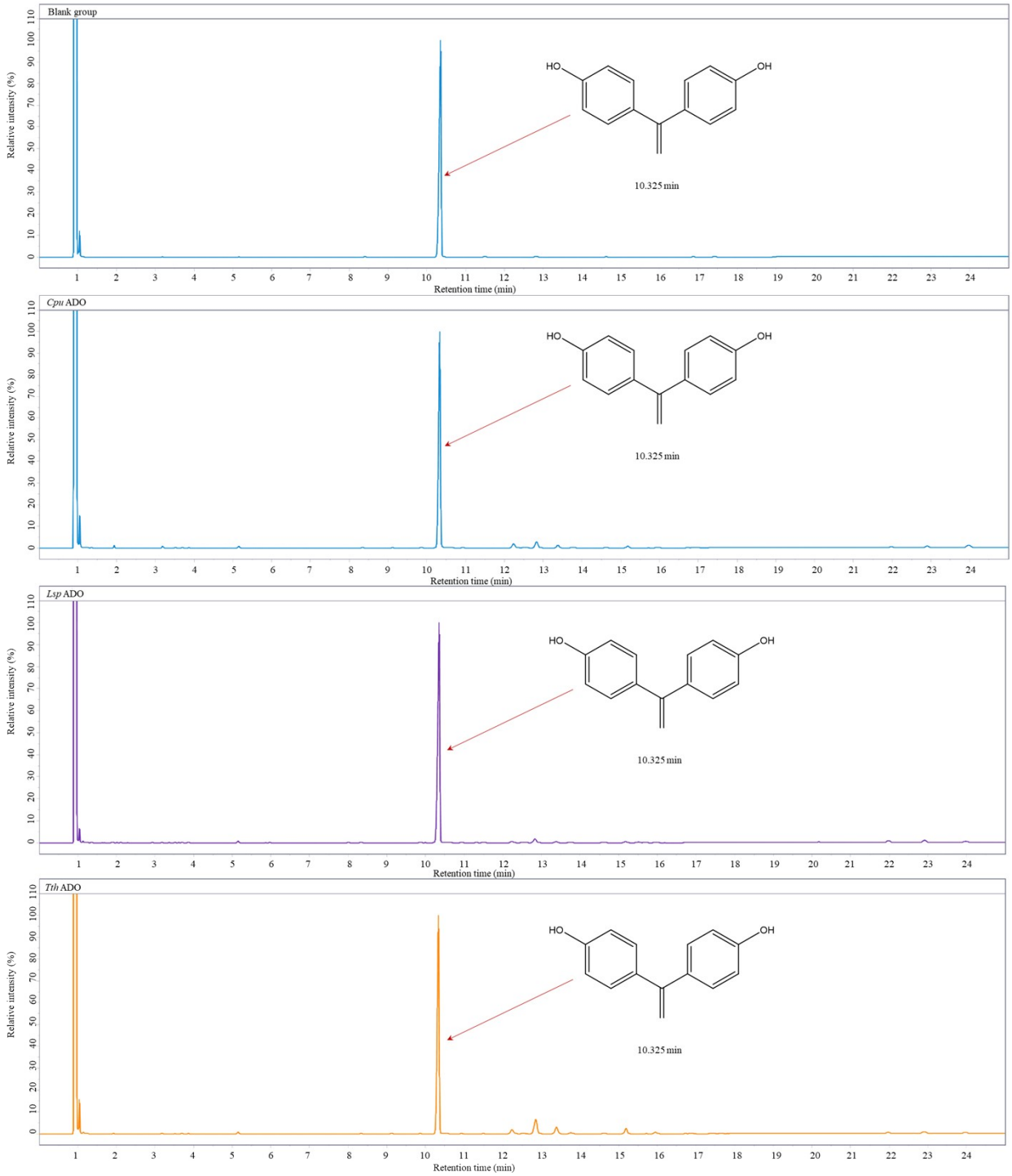

Figure S24-32. Gas chromatography results of the blank control group and different ADOs using 4,4'-vinylidenediphenol as substrate

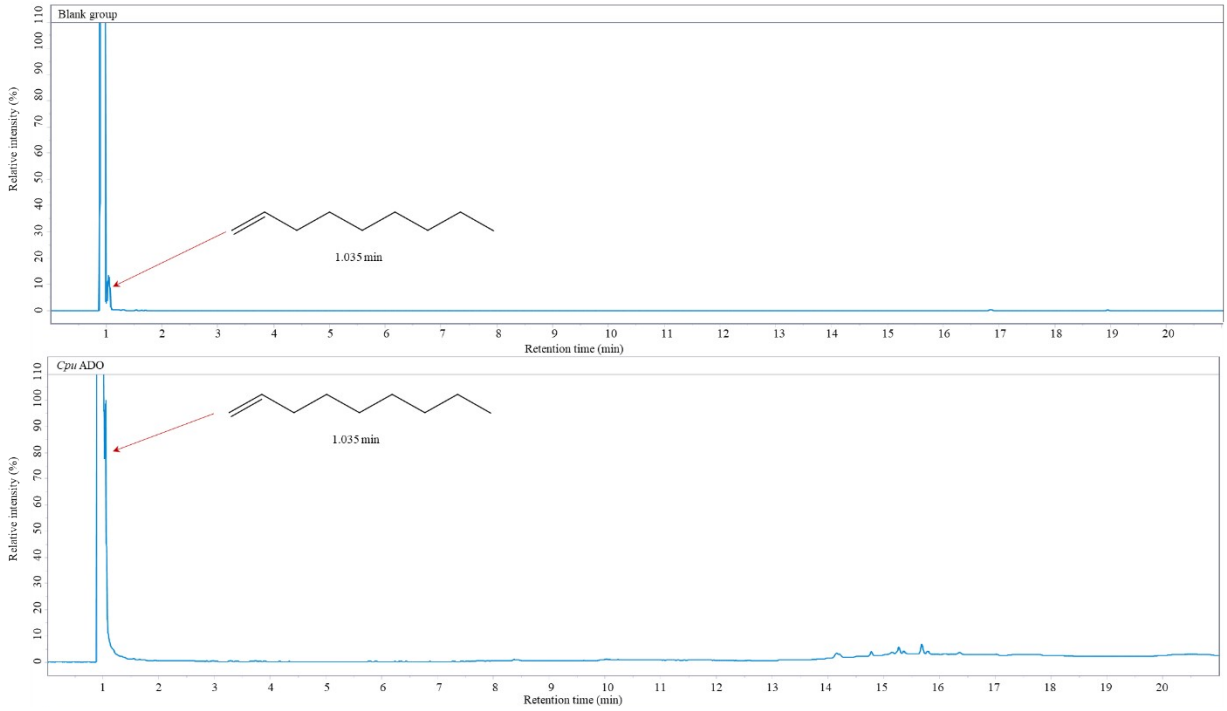

395
396

397 **Figure S24**-33. Gas chromatography results of the blank control group and different ADOs using 1-nonene as
398 substrate

399

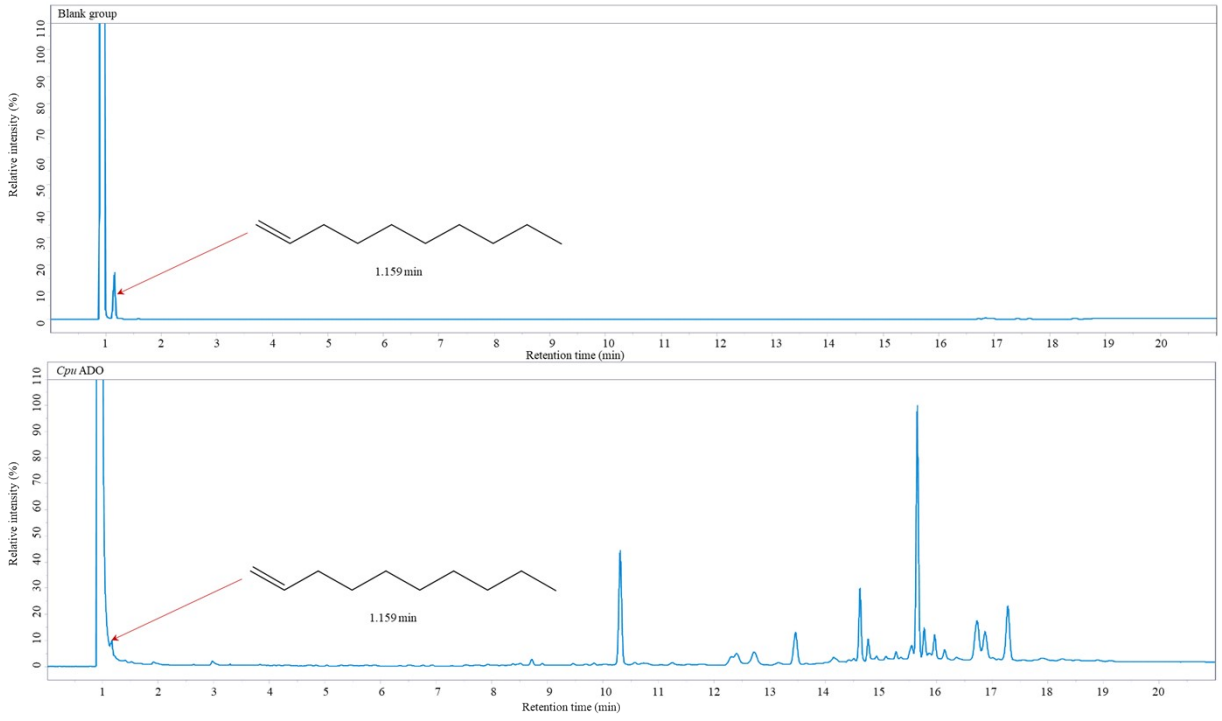

400
401

402 **Figure S24**-34. Gas chromatography results of the blank control group and different ADOs using 1-decene as
403 substrate

404

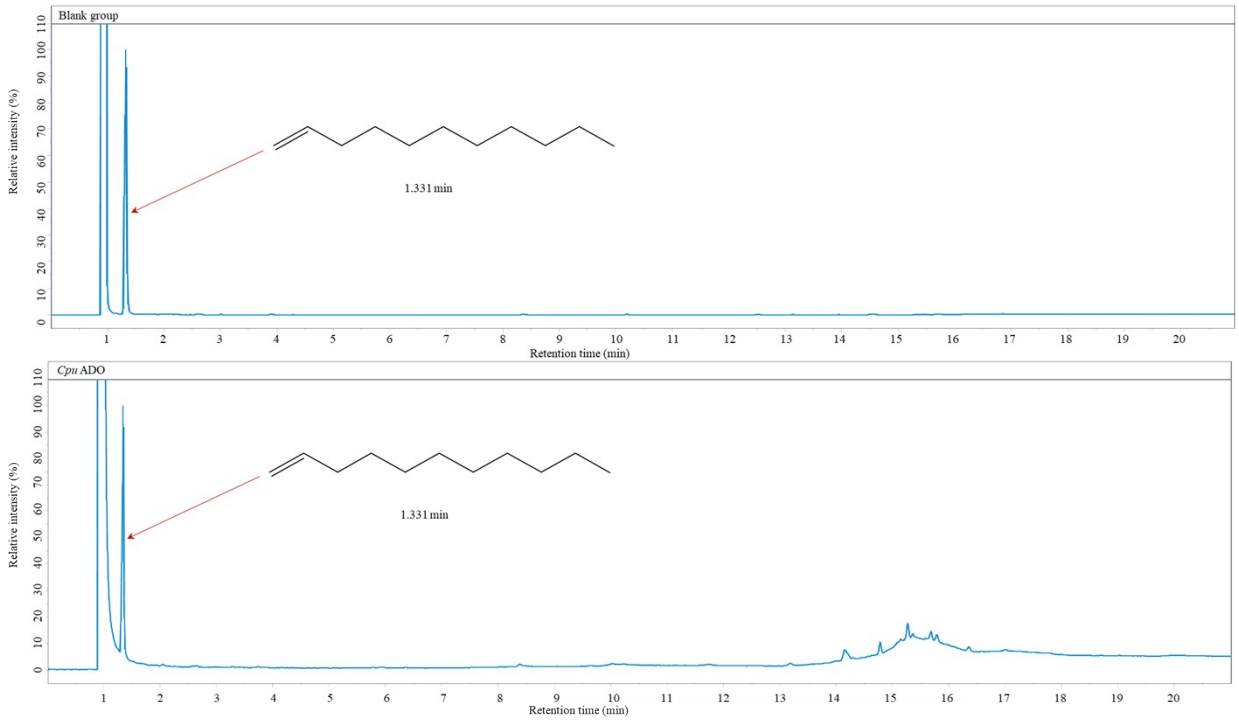

Figure S24-35. Gas chromatography results of the blank control group and different ADOs using 1-undecene as substrate

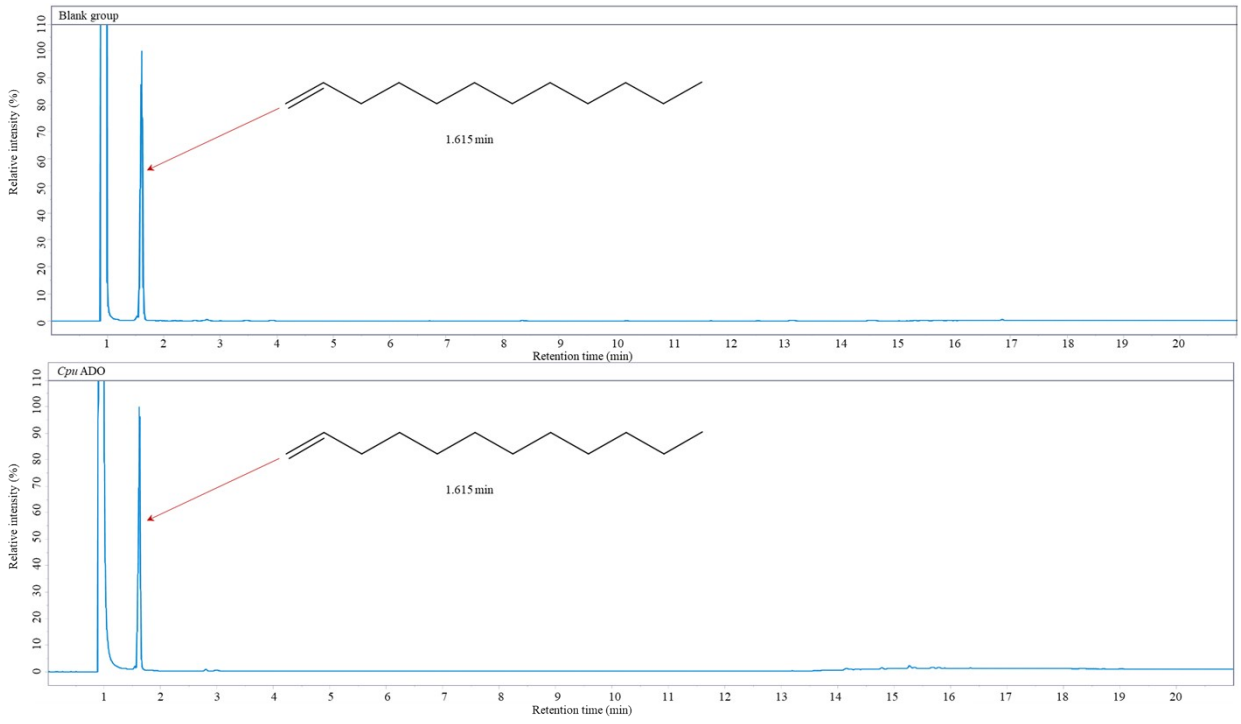

Figure S24-36. Gas chromatography results of the blank control group and different ADOs using 1-dodecene as substrate

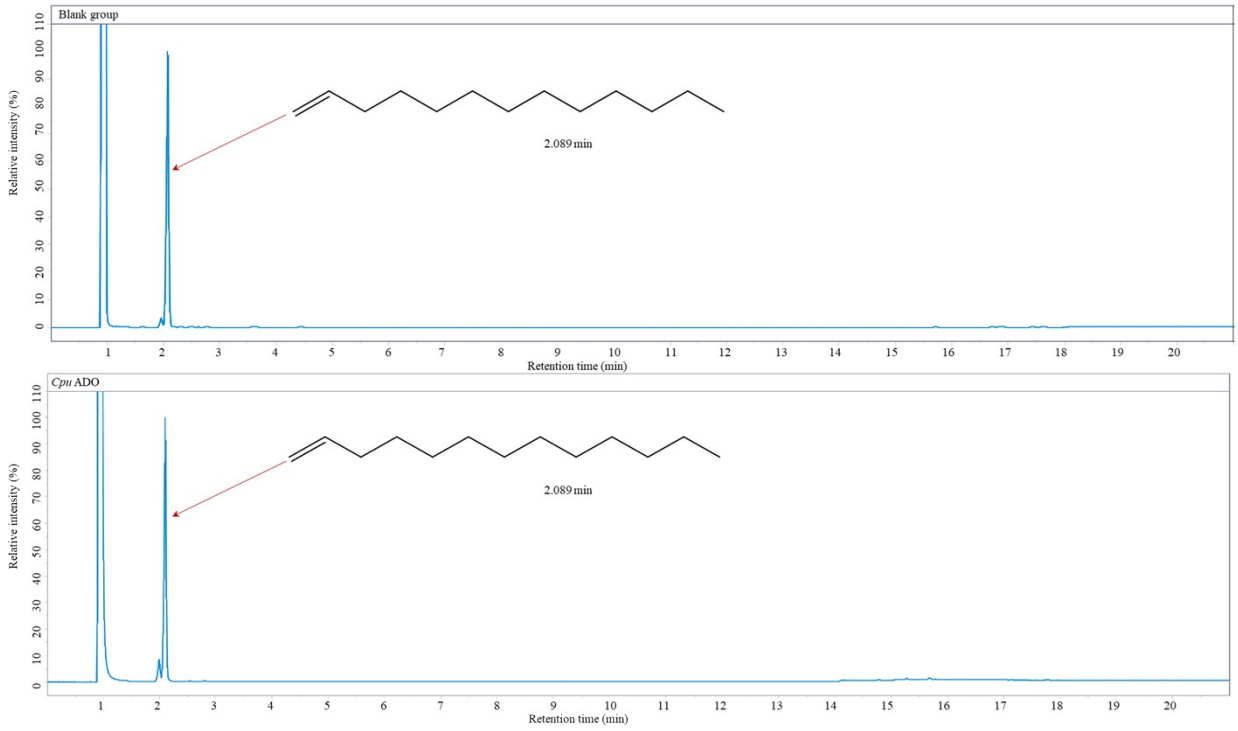

415
416

417 **Figure S24**-37. Gas chromatography results of the blank control group and different ADOs using 1- tridecene as
418 substrate

419

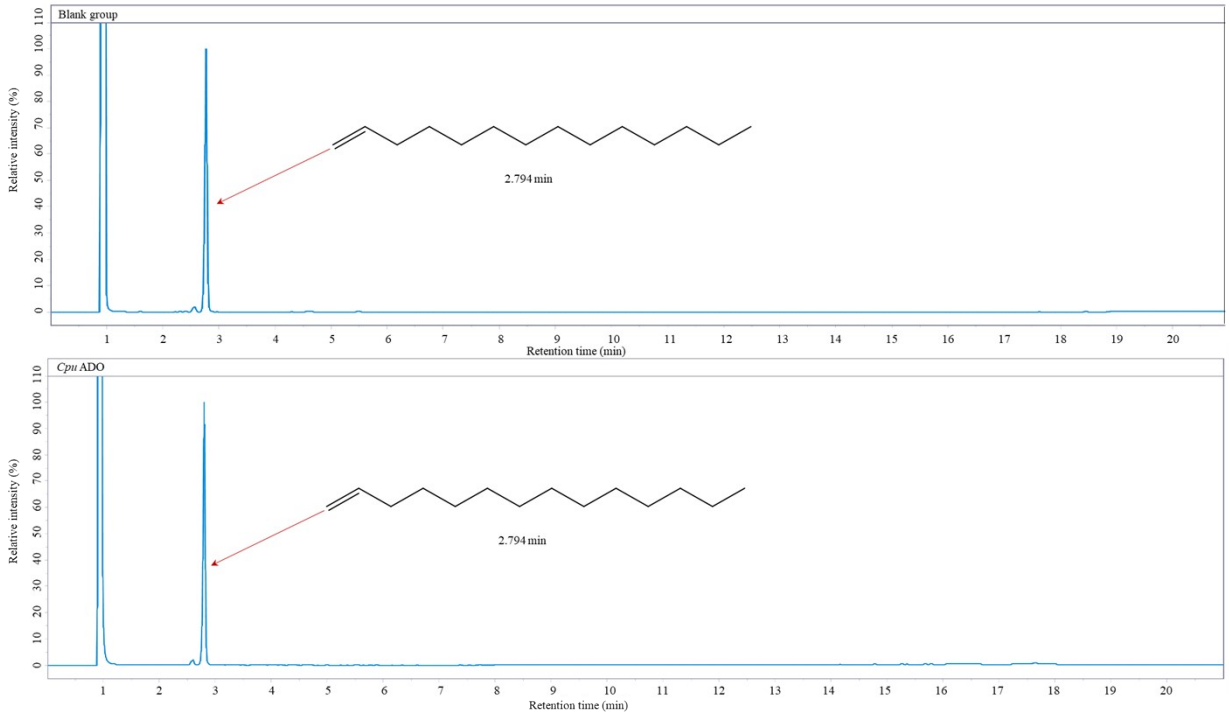

420
421

422 **Figure S24**-38. Gas chromatography results of the blank control group and different ADOs using 1-tetradecene as
423 substrate

424

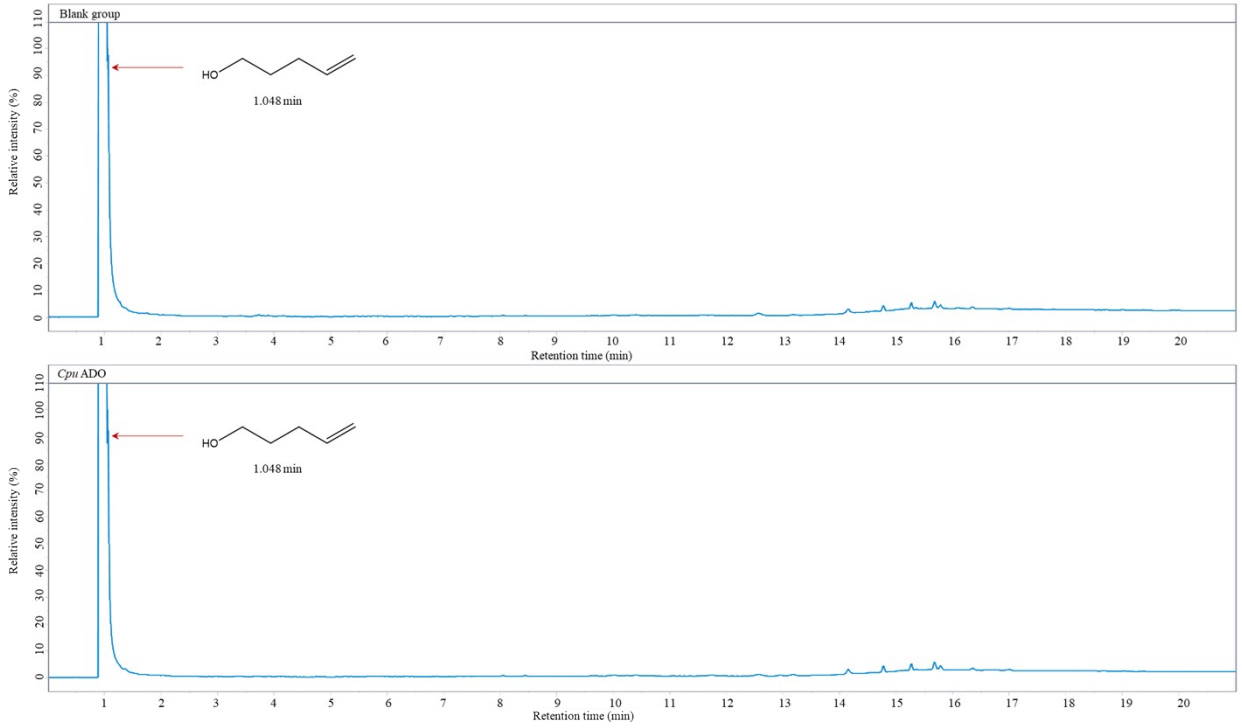

Figure S24-39. Gas chromatography results of the blank control group and different ADOs using 4-penten-1-ol as substrate

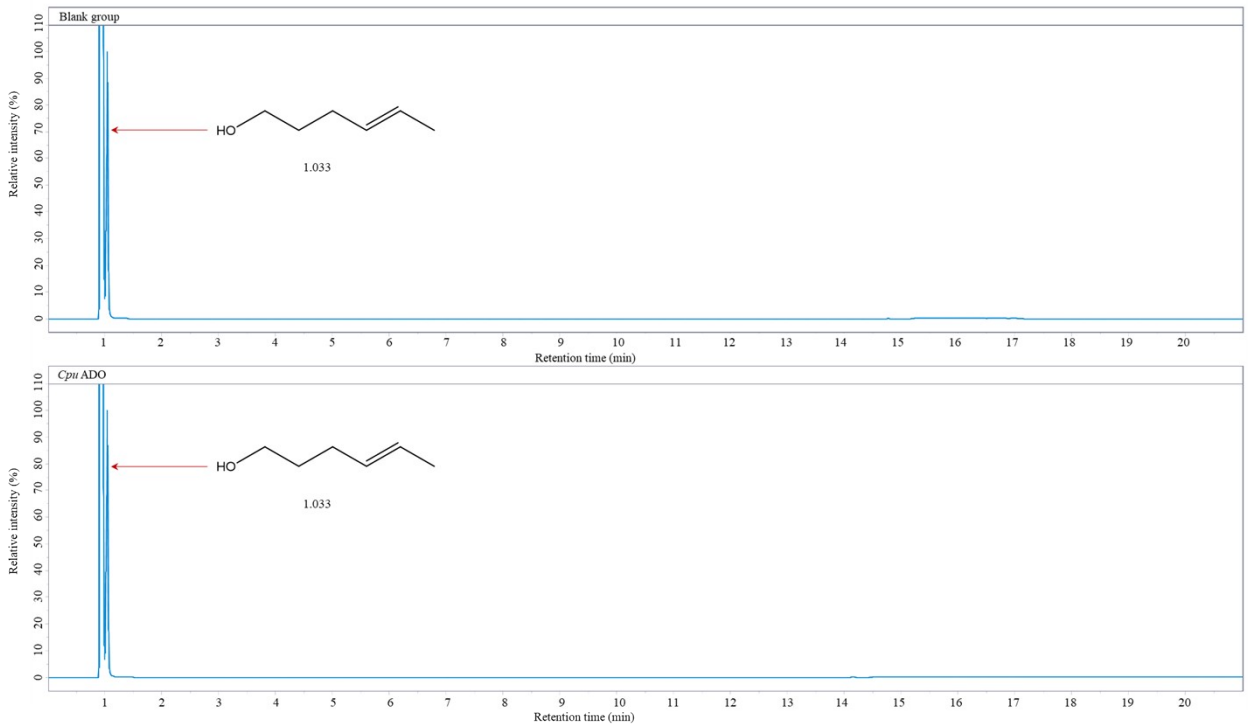

Figure S24-40. Gas chromatography results of the blank control group and different ADOs using 4-hexen-1-ol as substrate

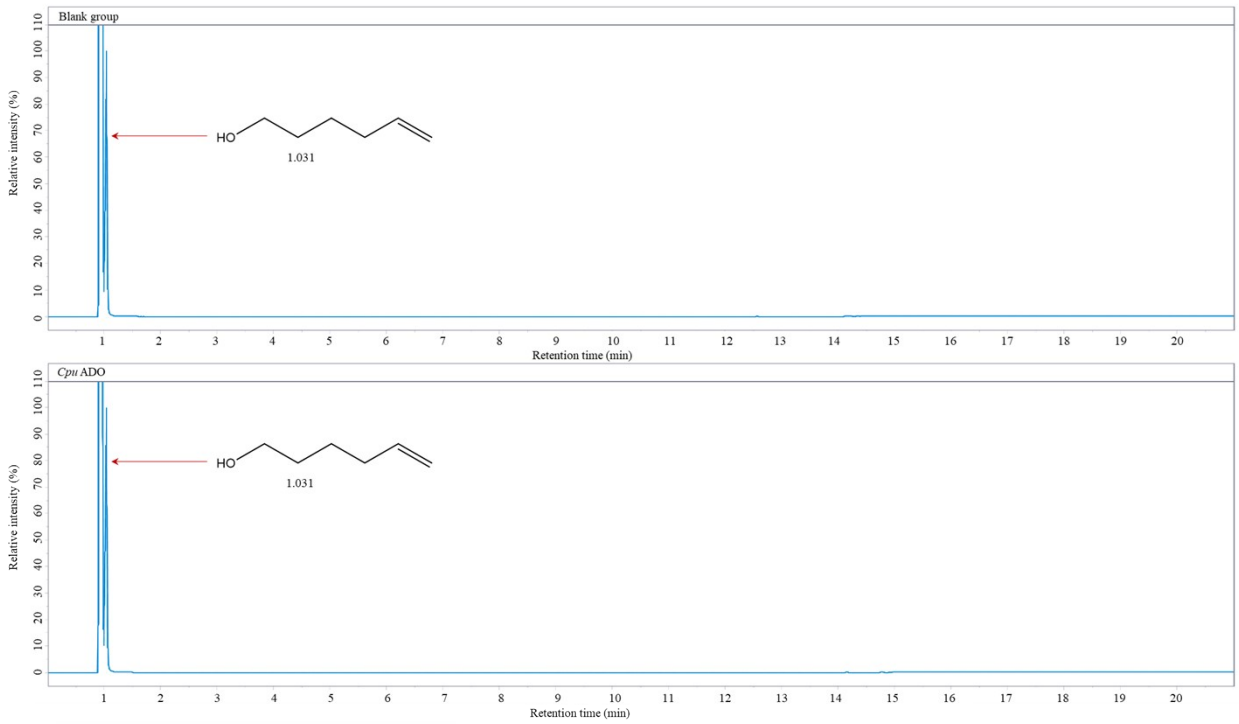

Figure S24-41. Gas chromatography results of the blank control group and different ADOs using 5-hexen-1-ol as substrate

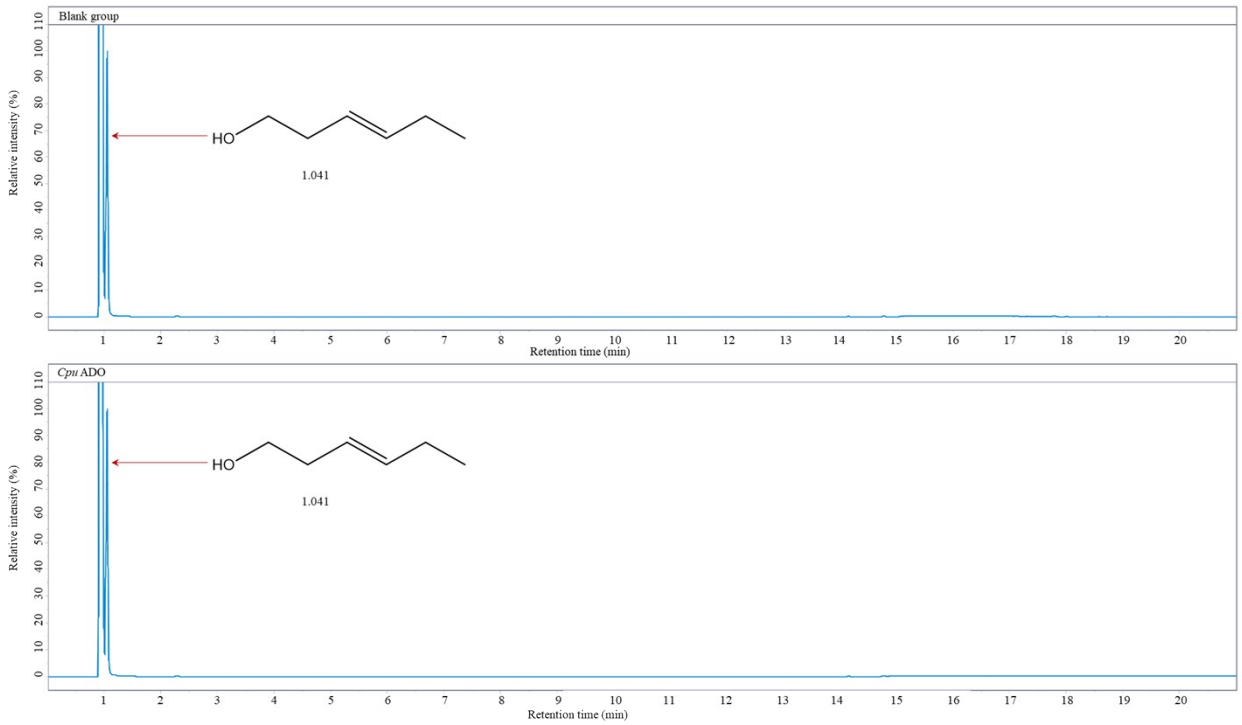

Figure S24-42. Gas chromatography results of the blank control group and different ADOs using trans-3-hexen-1-ol as substrate

Figure S24. Gas chromatograms of reaction products catalyzed by wild-type ADOs with different substrates in substrate scope analysis.